
Tome 11

Février

1973

Numéro 1

う み

La mer

昭和 48 年 2 月

日 仏 海 洋 学 会

La Société franco-japonaise
d'océanographie
Tokyo, Japon

日 仏 海 洋 学 会

編 集 委 員 会

委員長 今村 豊 (東京水産大学)
委員 星野通平 (東海大学) 井上 実 (東京水産大学) 川原田 裕 (気象庁) 森田良美 (東京水産大学) 永田 正 (東京水産大学) 西村 実 (東海大学) 大柴五八郎 (理化学研究所) 杉浦吉雄 (気象研究所) 高木和徳 (東京水産大学) 高野健三 (理化学研究所) 富永政英 (台湾大学) 宇野 寛 (東京水産大学) 渡辺精一 (理化学研究所)

投 稿 規 程

1. 報文の投稿者は原則として本会会員に限る。
2. 原稿は簡潔にわかりやすく書き、図表を含めて印刷ページで12ページ以内を原則とする。原稿は、東京都千代田区神田駿河台 2-3 日仏会館内 日仏海洋学会編集委員会宛に送ること。
3. 編集委員会は、事情により原稿の字句の加除訂正を行なうことがある。
4. 論文 (欧文, 和文とも) には必ず約 200 語の英文 (または仏文) の Abstract (Résumé) をつけること。欧文論文には英文 (または仏文) の Abstract (Résumé) のほかに必ず約 500 字の和文の要旨をつけること。
5. 図および表は必要なものみに限る。図はそのまま版下になるように縮尺を考慮して鮮明に黒インクで書き、論文の図および表には必ず英文 (または仏文) の説明をつけること。
6. 初校は原則として著者が行なう。
7. 報文には 1 編につき 50 部の別刷を無料で著者に進呈する。これ以上の部数に対しては、実費 (送料を含む) を徴収する。

Rédacteur en chef Yutaka IMAMURA (Tokyo University of Fisheries)
Comité de rédaction Michihe HOSHINO (Tokai University) Makoto INOUE (Tokyo University of Fisheries) Yutaka KAWARADA (Meteorological Agency) Yoshimi MORITA (Tokyo University of Fisheries) Tadashi NAGATA (Tokyo University of Fisheries) Minoru NISHIMURA (Tokai University) Gohachiro OSHIBA (Institute of Physical and Chemical Research) Yoshio SUGIURA (Meteorological Research Institute) Kazunori TAKAGI (Tokyo University of Fisheries) Kenzo TAKANO (Institute of Physical and Chemical Research) Masahide TOMINAGA (Taiwan University) Yutaka UNO (Tokyo University of Fisheries) Seichi WATANABE (Institute of Physical and Chemical Research)

RECOMMANDATIONS A L'USAGE DES AUTEURS

1. Les auteurs doivent être, en principe, des Membres de la Société franco-japonaise d'océanographie. Néanmoins, les notes des savants étrangers à la Société seront acceptées, si elles sont présentées par un Membre.
2. Les notes ne peuvent dépasser douze pages. Les manuscrits, dactylographiés sur papier fort, doivent être envoyés au Comité de rédaction de la Société franco-japonaise d'océanographie, c/o Maison franco-japonaise, 2-3 Kanda, Surugadai, Chiyoda-ku, Tokyo.
3. Le Comité de rédaction se réserve le droit d'apporter, le cas échéant, des modifications mineuses aux manuscrits ainsi que de demander aux auteurs de les corriger.
4. Des résumés en langue japonaise ou langue française sont obligatoires.
5. Les figures au trait seront tracées à l'encre de Chine noire sur papier blanc ou sur calque. Les légendes des figures et des tableaux sont indispensables.
6. Les premières épreuves seront corrigées, en principe, par les auteurs.
7. Un tirage à part des articles en cinquante exemplaires est offert gratuitement aux auteurs. Ceux qui en désirent un plus grand nombre peuvent les faire établir à leurs frais.

A Study on Optical Nature in Oceanic Waters*

Kanau MATSUIKE**

Abstract: This paper deals with (1) underwater optical structures and characteristics of oceanic waters, (2) possible and actual insolation amounts attained on the sea surface, and (3) underwater distribution of solar energy, based upon the optical observation data obtained in the North Pacific, the East Indian, and the Antarctic Oceans.

In the observation in each ocean, the upward and downward irradiances from the surface to the depth of 140 m were measured with an underwater irradiance meter to which a collector and filters of blue, green and amber were attached. On the other hand, insolation amounts attained on the sea surface were measured every day with the Eppley actinograph. Also, forms and quantities of clouds were observed every hour in accordance with the WMO Regulation for the entire period of each survey including navigation days to and from objective surveyed oceans.

Attenuation coefficients, relative irradiances and reflectances are calculated based on those observation data. Using the results of these calculations, transmittances of different spectral lights and intensity ratios among lights with different wave lengths in the surveyed oceans are discussed. As a result, it was revealed that, in the East Indian Ocean, each oceanic area distributed with water having an identical light transmittance is almost consistent with each area distributed with each ocean current such as the Equatorial Current and Equatorial Convergence Current; that, in the North Pacific Ocean, a remarkable increase of reflectance is seen particularly for blue light in the upwelling region, and the boundaries between different waters or the border line of the upwelling region can be traced from the optical view points in the Kuroshio and its south; that, in the Antarctic Ocean, especially distinguished differences in optical characteristics among water-masses of the Sub-Antarctic, the Antarctic and the Antarctic Convergence Water were recognized. Furthermore, optical structures and characteristics in each ocean are compared one another and it is revealed that each ocean has a specific characteristics in optical transmittance, reflectance and intensity ratios among lights with different wave lengths.

Referring solar insolation amounts attained on the sea surface, it was found that practical data obtained by the surveys did not coincide with the results which were induced through the calculation formulae that were led from data mainly obtained on land. In consequence, an equation to calculate the possible insolation amounts in consideration of changes of light transmittance in air according to the sun's altitude is introduced in this paper, and using the equation, the daily possible insulations distributed over the oceanic water in both hemispheres in each month are calculated. Furthermore, the actual insulations distributed on the oceanic waters in the Indian Ocean, the North Pacific Ocean and the Antarctic Ocean are calculated, taking relations between cloud amounts and reduction ratio of insolation found from author's observation into consideration. The possible insolation amounts resulted from this study exhibit approximately 10 % smaller than those of UKRAINTSEV (1939) at every latitude, and these results seem to be reasonable values as pointed out by BUDYKO (1956) on this subject. The results introduced herein with regard to the actual insolation amounts attained on the sea surface are consistent with the data observed by ASHBURN (1963) and those exhibited in Soviet Antarctic Expedition (1966).

Finally, the monthly and annual distributions of underwater solar energy flux are calculated in consultation of the reflection amounts at the sea surface introduced by COX and MUNK (1955) and the optical classification of waters by JERLOV (1964). This annual amount of

* Received January 25, 1973

** Tokyo University of Fisheries

underwater solar energy flux at the depth of 10 m is found to be approximately $33.4 \text{ kg}\cdot\text{cal}/\text{cm}^2\cdot\text{year}$ in the equatorial water of the Indian Ocean, and the corresponding amounts are its 54 % in the Kuroshio, 44 % in the Sub-Antarctic Ocean, 13 % in the Antarctic Ocean, and 6 % in the Antarctic Convergence Water. Furthermore, the study also reveals that if the lower limit of the euphotic zone can be assumed as much as $5 \text{ g}\cdot\text{cal}/\text{cm}^2\cdot\text{day}$, the ratio of the water volumes of euphotic zone per unit area of the sea surface accumulated throughout a year among the equatorial water of the Indian Ocean, the Kuroshio area of the North Pacific Ocean, the Sub-Antarctic water, and the water in southern part of the Antarctic Convergence is about 100 : 75 : 50 : 20.

1. Introduction

It is, without doubt, true that solar energy is the most essential element for every creature regardless of whether they live on the land or in the waters of this world. To evaluate the solar energy value delivered to the sea surface and also that penetrating the water is very significant from the aspect not only of the physical study but also the biological and oceanographical aspects. For example, such bio-oceanographical problems as phototaxis, photokinesis, photoperiodism, or primary productivity, etc. can not be resolved without knowledge of underwater irradiance. If oceanic waters can be classified by their different optical structures and characteristics, it will contribute largely to the development of descriptive oceanography; furthermore, if spectral composition of underwater lights in a certain sea for a certain season are disclosed, it can be effectively employed to the applied oceanographical fields such as studies of underwater TV cameras, colours of fishing lines and nets, etc.

A brief history of the optical study of water is worthy of description. FOL and SARASIN (1855) introduced a study of exposures of photographic plates at different depths in the Mediterranean off Cote d'azur at an early stage. Subsequently, SHELFORD and GAIL (1922) published a paper concerning the use of the photo-electric cell for the study of sub-surface-water light. ATKINS and POOLE (1933) wrote a paper on the subject of an application of selenium photocell for observation of underwater light. In Japan, HISHIDA (1954) as well as SASAKI and others (1968) published their works on measurement of submarine solar energy distributed in the sea. Other publications on underwater optical studies were introduced by ATKINS and POOLE (1958), BURT (1958), CLARKE and WERTHEIM

(1956), and TYLER (1958) etc.

The objective waters of these studies mentioned above were generally limited to inlet waters or waters adjacent to land. The optical observation data for oceanic waters were very scarce except that JERLOV (1951) introduced an optical study in respect to the deep sea.

It may be said that opto-oceanographical studies were developed along two directions, firstly the deductive method and secondly the inductive method. For example, the theoretical works of PREISENDORFER (1961) belong to the former category which largely contributed to the progress of new instruments to be used for optical research of waters, while those of JERLOV (1964) are the most representative works which belong to the latter category. JERLOV (1964) published a paper entitled "Optical classification of oceanic waters," in which he said that,

"The distribution of yellow substance and particles is controlled by the dynamical processes in the sea. Furthermore the particle characteristics, judging from data so far collected, show no drastic changes from one oceanic area to another. These circumstances make possible an optical classification of waters."

All the works introduced above were conducted on the basis of relative values divided by surface values extrapolated from underwater observation data to explain underwater optical phenomena. It is, desirable and useful to obtain absolute values instead of such relative values. To satisfy this requirement, it is indispensable to know both the possible and the actual insolation amounts delivered to the sea surface. However, such studies are not sufficient, particularly since those based on observation data obtained on the sea are very scarce.

Such scientists as ANGSTRÖM, KIMBALL, MOSBY, UKRAINTSEV, KUZMIN, MATEER, BUDYKO, ASHBURN, and GAVRILOVA can be listed as the representative pioneer researchers in this field. Among them, ANGSTRÖM (1924), KIMBALL (1928), MOSBY (1936), and KUZMIN (1950) as well as ASHBURN (1963) presented calculation formulae to evaluate actual insolation amount delivered to the earth, while UKRAINTSEV (1939) and GAVRILOVA (1958, 1963) calculated the possible insolation amount through the data obtained from observation stations distributed in the northern regions of the Northern Hemisphere land mass. KIMBALL (1928) and BUDYKO (1956) presented actual insolation amount resulted from surveys both on the land and the sea. For example, BUDYKO (1956) published a distribution chart of actual insolation amount in different regions of the earth based on data collected from 1,060 positions on the land distributed mainly in the northern regions of the Northern Hemisphere and 350 positions on the sea located near the Arctic Ocean.

ASHBURN (1963) and TABATA (1964) endeavored to examine various formulae introduced by the above-mentioned researchers, and reported that each formula produced differing results. BUDYKO (1956) pointed out that the value of possible insolation presented by UKRAINTSEV (1939) were too large and gave his reason for this criticism.

It may not be reasonable to use the formula induced from the data obtained at observation stations on the land for evaluating the values on the sea, due to the fact that there may be a considerable difference in formation and development of clouds between the land and the sea.

Under circumstances of optical studies mentioned above, the author has had the opportunity to take part in the three Expeditions* and has conducted a series of surveys to collect data of upward and downward irradiances of

blue, green and amber lights in water and also insolation delivered to the sea surface as well as cloud conditions. Major subjects dealt with here can be summarized under the following:

1. Underwater optical structures and characteristics in the different oceans
2. The possible and actual insolation amounts delivered to the sea surface
3. Underwater distribution of solar energy

The author hopes that the subject of this paper will be supplemented by accumulation of data through further optical observations which are systematically planned, so that seasonal change of underwater optical structure in each oceanic zone as well as its relation with suspended and dissolved matters may be distinctly clarified.

2. Instrument, observation method and data processing

1. Instruments

1) Underwater irradiance meter

The sensing unit of this irradiance meter consists of a collector with four filters of blue (460 nm at maximum transmittance), green (540 nm at maximum transmittance), amber (Sharpcut, VO-57), and opal (Kenko-ND with 20 % transmittance), each being combined with a corresponding selenium photocell. Such a sensing unit was employed for the survey in combination with EPR 2T type high sensitive recorder (referred to sub-paragraph 3)). The main assembly of this sensing unit was manufactured by Murayama Denki Co., Ltd. while the filters were made by Tōshiba Denki Co., Ltd. The bottom inside of this instrument was purposely filled with adsorber (*i.e.* Silicagel) in order to avoid condensation of vapour or moisture which might be generated inside the equipment.

The specification of this sensing unit is as follows:

- (a) The angular response is approximated to a cosine curve both in air and in water as shown in Fig. 1. Data used for this graph were obtained by experiments in a dark room such that a series of parallel light flux from an artificial light source were directed to the collector from every angle.
- (b) The immersion effect, which means a

* The three Expeditions refer to International Indian Ocean Expedition from November 21st, 1963 to January 22nd, 1964, Antarctic Expedition from December 1st, 1964 to February 10th, 1965 and International Kuroshio Expedition in August, 1965, operated by M/V Umitaka-maru.

ratio of the response in water to that in air, is specified as shown in Fig. 2. This phenomenon is caused by differences between reflection in air and in water occurred on both internal and external surfaces of the sensing unit. Data used for this graph were obtained by experiments in a water basin placed in a dark room and using an artificial light source.

(c) The spectral sensitivity of the photocell with filters, which means a combination of spectral transmittance for each filter such as blue, green and amber and spectral sensitivity of the selenium detector, is as shown in Fig. 3. The gravity centres for filters of blue, green and amber combined with the detector are 473 nm, 545 nm and 608 nm, respectively.

(d) The calibration characteristics by different filters are specified as shown in Fig. 4. Data used for these graphs were obtained by experiments which were conducted when the sky was clear and the sun's altitude was relatively high. Eppley actinograph (see sub-paragraph 2)) was used to measure the attained caloric values in consideration of the linearity of its output against attained solar energy. Tōshiba's No. 5-type illuminometer (see sub-paragraph 4)) was used an aid, with various neutral filters.

(e) The shifting of gravity centres in water for different filters are listed below.

	Depth		
	1 m	10 m	100 m
Blue (nm)	479	475	464
Green (nm)	542	537	514
Amber (nm)	606	588	565

The above values were taken from the formula introduced by JOSEPH (1949b).

$$\lambda_{0(x)} = \frac{\int \lambda J_0(\lambda) \cdot D(\lambda x) \cdot M(\lambda) d\lambda}{\int J_0(\lambda) \cdot D(\lambda x) \cdot M(\lambda) d\lambda}$$

Where

λ : wave length

x : depth

J_0 : spectral distribution of insolation at the water surface

$D(\lambda x)$: transmittance in water

$M(\lambda)$: spectral sensitivity of photocell with coloured filter

$M(\lambda) = T(\lambda) \cdot S(\lambda)$

where $S(\lambda)$: sensitivity of detector

$T(\lambda)$: transmittance of filter

in which general spectral distribution $J_0(\lambda)$ introduced by MOON (1940) and mean spectral transmittance of the Kuroshio which corresponds to I_B optical water type introduced by JERLOV (1964) are used.

2) Eppley actinograph

This instrument is manufactured by Eiko Seiki Sangyo Co., Ltd. The rated solar constant of this actinograph authorized by the Meteorological Agency of the Japanese Government is $14.0 \text{ mV/g} \cdot \text{cal cm}^{-2}, \text{ min}^{-1}$.

3) EPR 2T type high sensitive recorder

A sensitive recorder manufactured by Tōa Denpa Kōgyō Co., Ltd. is applied to with an attachment of resistance box connected to the recorder.

4) No. 5-type illuminometer

A selenium photocell illuminometer manufactured by Tōshiba Denki Co., Ltd. is employed.

5) Net-sonde

A supersonic FM (frequency modulation) system net-sonde manufactured by Furuno Denki Co., Ltd. is employed for the survey work. Its operating distance is 1,000 m with an accuracy of $\pm 0.5 \text{ m}$ and the receivable angle is of 45 degrees. The indicator of this instrument is installed on the stern bridge.

2. Observation method

1) Insolation and cloud

The Eppley actinograph was used to measure the reached insolation on the sea surface, being mounted on the top of the stern bridge and supported firmly by a gimbal so that its posture might always keep horizontal against vibrations on board. By means of connecting this actinograph to the EPR 2T type high sensitive recorder, the insolation was continuously recorded throughout daylight hours during the survey. The survey of cloud form, quantity and cloud form which covered the sun, was performed at one hour intervals depending on the regulation stipulated by WMO (World Meteorological Organization).

2) Submarine irradiance

The upward and downward irradiances of submarine light were surveyed using the underwater irradiance meter with four filters of

blue, green, amber and opal at each measuring point of every observation position. The observations were performed by setting the irradiance meter on the hanging wire with a pendant at the 14 measuring points of 0 (near surface), 5, 10, 20, 30, 40, 50, 60, 70, 80, 90, 100, 120 and 140 m deep. The EPR 2T type high sensitive recorder was used as the indicator, the resistance box being connected in order to measure the values of electric current induced from selenium photocell. The current ranges of the resistance box more than that of 10^{-7} ampere order were usually used because the measured value could not be deprived off linearity by multiplication. When the resistance box had its current range of less than 10^{-7} order, the measured values were converted into the correct current value using the calculated coefficients shown in the following table.

Range	R	$(Rx+R)/R=K$
10^{-7}	10 k Ω	2.0
10^{-8}	100 k Ω	11.
10^{-9}	1000 k Ω	101.

where Rx stands for the internal resistance of the photocell while R indicates the input resistance of the resistance box.

Simultaneously with the measurement of underwater irradiance at each water-layer, solar energy attained on the sea surface was also measured. Each depth of the underwater irradiance meter was determined by the net-sonde placed constantly at 3.5 m above the instrument. A plumb of 5 kg was hung down at the position of 1.5 m under the photocell.

3. Data processing

The relative irradiance has been calculated through the following processes.

1) Using Fig. 4 the current values generated through different filters of the underwater irradiance meter are converted into the caloric values.

2) These caloric values are divided by the corresponding solar energy values attained on the sea surface.

3) The values of underwater irradiance at the water surface were obtained by means of extrapolation from several observed values near the surface in order to eliminate the immersion

effect.

4) As an approach to exhibit the light transmission in water, the values of attenuation per unit optical length was adopted. The following formula was used for the calculations.

$$K = \frac{2.3026}{(Z_2 - Z_1) \sec \alpha} \log_{10} \frac{I_{Z_2}}{I_{Z_1}},$$

where K , I , α , Z_1 and Z_2 stand for as follows:

K : attenuation coefficient

I : relative irradiance in water

α : refraction angle in degrees in water

Z_1, Z_2 : depths of two measuring points

In general, the vertical attenuation coefficient is adopted to express the irradiance in water. This coefficient, however, is not sufficient for such comparison of water characteristics in different zones as discussed in this paper, because the vertical attenuation coefficient is changeable according to different altitudes of the sun.

Lately, JERLOV and NYGARD (1969) presented an elaborate paper "Influence of solar elevation on attenuation of underwater irradiance," providing the following formula as a result of their study.

$$K_0 = K_i \cos \alpha,$$

where K_0 indicates a coefficient for zenith sun, while α stands for values of refraction angle in degrees.

Their study proved that K_0 values are almost unchangeable with different solar elevations. Furthermore, they found the approximate depth range in which the above formula is justified to be as follows, so far as blue light in the Sargasso Sea and green light in the Baltic Sea concerned.

$$K_0 Z_k = 4,$$

where Z_k : water depth so far as the above formula of $K_0 = K_i \cos \alpha$ is justified.

They also disclosed the relation between Z_k and wave length of light, suggesting that Z_k value is the smallest for blue light and increases toward amber light.

The author's method of adopting the value of attenuation coefficient in water, K , is similar to that of JERLOV and NYGARD. In this paper, however, the attenuation coefficient is adopted up to 140 m in depth throughout all the observation stations. Accordingly, the attenuation coefficient may be slightly smaller than the true value in the water deeper than 100 m. For the data obtained under conditions such that the solar ray direction could not be distinctly observed, owing to cloudy or overcast weather during the survey works, the water surface is regarded as the light source itself and the difference in depth between two measuring points as a light pass distance.

5) The reflectance, R , is obtained from dividing the upward irradiance by the downward irradiance per unit insolation for each filter and each observed layer.

Climates have an effect on reflectance in water. TYLER (1960) introduced data of underwater radiance distribution under a clear sky (the sun's altitude was 56.6°) and an overcast sky (the sun's altitude was 40.0°). By using his radiance distribution data, the submarine irradiance value under a clear sky and that of an overcast sky are calculated by means of the following equation.

$$H = \sum \sum N \cos \theta \sin \theta d\theta d\phi,$$

where H : irradiance

N : radiance

θ : tilt angle $0^\circ < \theta < 180^\circ$

ϕ : azimuth angle $0^\circ < \phi < 180^\circ$

As a result, it is clear that the maximum of the discrepancy between the reflectance value under clear sky and that of overcast sky is about 20%. Therefore, when optical structures or characteristics in water of a certain oceanic zone are discussed, allowance of about 20% evaluating the reflectance values must be taken into consideration under different climates.

3. Optical structure of the East Indian Ocean

During the period of the International Indian Ocean Expedition (IIOE), the author carried out the survey work on board the M/V Umitaka-maru, Training and Research Vessel of Tokyo University of Fisheries, from November

21st, 1963 to January 22nd, 1964 to explore optical characteristics of the East Indian Ocean. The data was gathered from the surveys at thirty observation positions.

In this section, an optical structure in the East Indian Ocean is discussed from the viewpoint of relative irradiance, I , attenuation coefficient, K , reflectance, R , and intensity ratios among lights with different wave lengths for filter of blue, green and amber. The results are collated with such data as seston and chlorophyll- a quantities and water temperature distributions obtained at the same time and position.

As shown in Fig. 5, the observation positions are allocated in such way that they are distributed from north to south on the lines of 100, 106, 113, and 120 degrees of East Longitude in the Ocean. To facilitate discussions in this paper, the author refers to the cross-section along each longitude line mentioned above as follows:

Section A: The vertical section along the 100° East Long., where the observation positions from UM-23 to UM-28 are involved.

Section B: The vertical section along the 106° East Long., where the observation positions from UM-14 to UM-22 are allocated.

Section C: The vertical section along the 113° East Long., where the observation positions from UM-6 to UM-13 are distributed.

Section D: The vertical section along the 120° East Long., where the observation positions from UM-1 to UM-5 are included.

Since the ocean currents around this zone are fairly distinct one from another, the zone is discriminated into three different areas, (1) the equatorial countercurrent area where an ocean current streams in the east direction along the islands located in the north of this zone, (2) the southern equatorial current area where a current flows towards the west, and (3) the area sandwiched by the above two currents. Attention was directed to the allocation of the observation positions so that they

were distributed across these three areas.

The diagrams of distribution of relative irradiance for Sections A and B are exhibited in Fig. 6-(1) (Blue, Green and Amber), and Fig. 6-(2) (Blue, Green and Amber). The numbers, 2, 4, 6... in the diagrams correspond to 50 %, 25 %, 12.5 %... of relative irradiance and so on, respectively. In the diagrams, the wider distance between lines indicates less attenuation in relative irradiance. It may be seen from these diagrams that, even in the same ocean the light transmission distinctly varies with the location. The difference is most distinct in blue light.

Subsequently, Fig. 7-(1) (Blue, Green and Amber), and Fig. 7-(2) (Blue, Green and Amber) are presented for study from the viewpoint of the attenuation coefficient. The numerical figures in these diagrams indicate the average values of the attenuation coefficient multiplied by 10^3 . The larger figures show the greater attenuation.

These diagrams show an interesting feature of underwater light which varies with colours such as blue, green or amber. As seen in Section A, a particular water mass which has an excellent light transmission for all colours and a fine optical uniformity in spectral light transmission is vertically extended from the surface to the layer of 50 m deep. A water mass which has a quite similar spectral light transmission is seen from the surface to 60 m deep between Lat. 10° to 15°S in Section B and also from 10 m to 50 m deep between Lat. 13° and 16°S in Section C. The author refers to this as Water-mass A. It can be plainly observed that this Water-mass A is distributed from east to west centring the area of the eastward current. Therefore, it may be hypothetically admitted that spectral light transmission of Water-mass A is that of the equatorial counter convergence current. Underneath Water-mass A, there is a water layer between 70 and 80 m in depth where underwater light greatly attenuates.

Further, the observed result reveals that there is another water mass, which has a quite excellent light transmission, in the layer from the surface to 60 m deep between Lat. 19°S and

23°S in Section B, and also between Lat. 18°S and 25°S in Section C. The author names this as Water-mass B. Although no data beyond the latitude line of 25°S is available, judging from the geographical location of Water-mass B, it can be understood that Water-mass B corresponds to the major part of the south equatorial current which streams northward along the Australian west coast and directs north-westward at about Lat. 20°S . Therefore, it may be admitted that spectral light transmission of Water-mass B is that of the south equatorial current water. Underneath Water-mass B, there is also a water layer between 70 and 80 m deep where the underwater light greatly attenuates.

Furthermore, an optically different water-mass, which is comparatively turbid, is recognized in the sea area where Water-mass A comes in touch with Water-mass B. Similar water-mass is also found in the area between Australia and the Java Island. It is probable that this water is brought from Water-masses A and B. The author refers to it as Water-mass C. Also, there is a layer having a drastic attenuation coefficient underneath Water-mass C. The location of this layer tends to be shallower in the area between Australia and the Java Island and it appears in the water between 30 and 40 m deep.

The distribution of three water masses on the sea surface is shown in Fig. 8.

The mean values of irradiance transmittance for each spectral light in the water between the surface and 10 m deep in respect of Water-masses A, B and C are listed below.

	Blue	Green	Amber
Water-mass A	87 %	63 %	48 %
Water-mass B	87	59	48
Water-mass C	68	40	33

As a result, the gaps in spectral light transmittance between Water-masses A and B are almost negligible but those between Water-masses A and C are fairly large.

Fig. 9 shows vertical distributions of the reflectance, R , for each blue, green and amber light in Section A. For the blue light, the largest reflectance value appears in the upper

layer and its value decreases gradually with depth and its iso-lines run almost horizontal. For the amber light, the trend is quite opposite; namely, the smallest reflectance value indicates in the top layer and it increases gradually with depth. For the green light, the reflectance value scarcely change with depth. In the layer of 70 to 80 m deep where drastic attenuation occurs as mentioned above, the reflectance value for blue light becomes smallest, but, in contrast, the reflectance value for amber light shows largest. This seems to merit special attention.

The intensity ratios among lights with different wave lengths are observed from a viewpoint of vertically sectioned profile. Fig. 10-(1) and (2) exhibit vertical distributions of both the ratios between relative irradiance of blue and green light, I_B/I_G , and those of amber and green light, I_A/I_G , for each Section A and B. The iso-lines of I_B/I_G direct almost horizontal and their values increase according to depth, and the iso-lines of I_A/I_G show also almost horizontal but their values decrease with depth. Both the largest value for I_B/I_G and the smallest value of I_A/I_G appear in the specific layer where the drastic attenuation takes place as pointed out in the above paragraph.

Vertical distributions of water temperatures in this zone are shown in Fig. 11. A warm layer at about 28° to 29°C locates from the surface to 40 or 50 m deep, below which temperature declines rather drastically up to 130 m deep, and then a gentle inclination appears again in the deeper water below 130 m deep.

An inclusive examination is presented to find a general tendency of optical characteristics of water in the East Indian Ocean. Fig. 12 shows the mean values of I_G in each depth. Fig. 13 shows the relation between I_G and I_B/I_G , and that between I_G and I_A/I_G . The graph shows that the curve of I_B/I_G is almost symmetric with respect to that of I_A/I_G .

Finally, the optical data is collated to seston and chlorophyll-*a* quantities simultaneously obtained from the objective zone at the survey. Fig. 14-(1) and (2) provide vertical distributions of the seston quantity for each Section A and B. Sestons were collected through filters of

millipore AA(0.80 μ ±0.05). Fig. 15(1) and (2) exhibit a vertical distribution of chlorophyll-*a** for each Section A and B.

In comparing the seston distribution diagram with that of optical findings, it is disclosed that the layer showing the intensive attenuation of light generally corresponds to the layer having the small seston quantities of 10 to 30 mg/l. In the graph exhibited in Fig. 16 the plotted points have a wide scatter and thus it is impossible to define a relationship between the attenuation coefficients and the seston quantities. It may be attributed to the reasons that the optical phenomenon in water is affected not only by seston quantity but also their quality (*e.g.* organic and inorganic) and sizes; that seston particles smaller than 0.80 μ are excluded. On the other hand, the layer which has the largest chlorophyll-*a* content almost corresponds to the layer having an intensive attenuation for blue light. This intensive attenuation appears to be primarily due to absorption by phytoplankton, judging from the large value of attenuation coefficient of blue light, K_B , the small value of reflectance of blue light, R_B , and the large quantity of chlorophyll-*a*, in this layer. This, however, requires confirmation by the accumulation of observation data. The total irradiance amount in the largest chlorophyll-*a* concentration layer is calculated and expressed by unit of g·cal/cm²·day. The average amount of insolation delivered to the sea surface for each Water-masses A, B and C are 530, 630 and 550 g·cal/cm²·day. The quantity of light reflected on the surface calculated by COX and MUNK (1955) is deducted from each insolation amount, and then, applied the above-mentioned underwater spectral transmittance to each Water-mass A, B and C, the arrival caloric amount in the largest chlorophyll-*a* concentration layer is resulted in as 6.8, 5.0 and 6.0~1.5 g·cal/cm²·day, respectively.

4. Optical structure of the Kuroshio and its southern area

During the season of the International Kuro-

* The quantitative analysis of chlorophyll-*a* were conducted by Mr. K. TAKESUE (Fisheries College, Shimonoseki, Japan).

shio Expedition (C. S. K.) in August, 1965, the optical observations were conducted on board the M/V Umitaka-maru in the Kuroshio zone including its southern area. Data was obtained from ten positions distributed on each latitude between 20°N and 31°N along a meridian of 142°E except for 22°N and 25°N.

Fig. 17-(1), (2) and (3) show the distribution diagrams of relative irradiance, *I*, for blue, green and amber light from the surface to 140 m deep in this zone. The numbers 1, 2, 3, 4, . . . in the diagrams correspond to 562 ‰, 316 ‰, 178 ‰, 100 ‰, 56 ‰, . . . of *I* values. Three positions of Lat. 30°N, 27°N and 20°N are selected as the typical positions to represent the Kuroshio, its southern area, and the southern area of the North Pacific Ocean, respectively. The depth where *I* value for each light is reduced to 1/10 of the surface value, 1/100, 1/1,000 and so on at these positions is compared in Table 1. In addition, the mean value

of irradiance transmittance for each light in the water between the surface and 10 m deep are listed as follows:

	Blue	Green	Amber
Kuroshio	63 %	51 %	12 %
South of Kuroshio	81	68	20
Southern area of North Pacific Ocean	72	54	13

As seen in the above, irradiance transmittance for every light is best in the south of the Kuroshio and worst in the Kuroshio and the mean value of irradiance transmittance in the entire objective water is 71 % for blue, 56 % for green, and 15 % for amber light, respectively. The diagrams exhibit that the iso-lines of *I* form an exceptional pattern in the layer of 80 m deep at about Lat. 24°N, showing an existence of the heterogeneous water having vastly better light transmittance. In this area, it requires a depth of approximately 100 m for blue, 80 m for green and 60 m for amber light to reduce an irradiance value to 1/10 by attenuation. Referring to the vertical distribution of water temperature in the sea around Lat. 24°N, it is clear that this specific cold water is brought up from the deeper layer by so-called Upwelling phenomenon. (See Fig. 25)

The objective water is also reviewed by the attenuation coefficient, *K*, and exhibited its vertical distribution in Fig. 18-(1), (2) and (3). Figures in these diagrams are expressed by amounts of $K \times 10^3$. Through the *K* diagrams, the corresponding particular patterns of iso-lines to those of *I* iso-lines among the different waters can be distinctly confirmed also. The iso-line configuration forming an eye in the centre substantiates the location of the upwelling water around Lat. 24°N. Intensive attenuations both of blue and green lights occurs in about 90 m deep in the Kuroshio area. This depth correspond to the compensation depth reported by ARUGA and MONSI (1962).

Fig. 19-(1), (2) and (3) show the vertical distributions of reflectances, *R*, for blue, green and amber lights. The *R* iso-lines present an extraordinarily complicated profile especially for blue light. The most intensive *R* is seen in the upwelling area. Its value in the layer

Table 1. The depth where relative irradiance is reduced to 1/10 of the surface value, 1/100, 1/1,000 and so on, in the Kuroshio and its southern area.

Relative irradiance	Area	Kuroshio	Southern	Southern
		area 30°N	area of Kuroshio 27°N	area of N.P. Ocean 20°N
1/10	B	48m	78m	60m
	G	33	44	34
	A	14	17	11
1/100	B	80	112	92
	G	61	82	66
	A	26	29	26
1/1,000	B	98	More than 140	118
	G	86	114	94
	A	41	51	43
1/10,000	G	110	140	130
	A	62	71	62
1/100,000	A	81	90	79
1/1,000,000	A	103	111	98
1/10,000,000	A	136	138	127

Remarks: Signs B, G and A stand for blue, green and amber light.

between 50 to 70 m deep is 12 times for blue light and 6 times for amber light when compared with those in the adjacent waters. The R iso-lines in this area form a special configuration discriminating the water from others. In contrast, the least R is observed in the Kuroshio area. The R_B values in the Kuroshio area are 0.3 to 0.4 time as much as those in the south of the Kuroshio. The R values distributed vertically in the objective water are listed in Table 2.

Fig. 20-(1) and (2), and Fig. 21-(1) and (2) show sectioned profiles of I_B/I_G , I_A/I_G , R_B/R_G and R_A/R_G , respectively. In Fig. 20-(1), the iso-lines of I_B/I_G run almost horizontal in the upper layer, but they show drastic inclinations in the layers deeper than about 70 m. Some of these iso-lines form circles in the centres of contour lines in which the largest I_B/I_G values are exhibited. In Fig. 20-(2), the iso-lines of I_A/I_G direct almost horizontal in water shallower than about 40 m deep, but they drastically decline in the deeper layer of the upwelling and the Kuroshio area. The diagrams in Fig. 21-(1) and (2) indicate that the R_B/R_G values are large in the upper layer and they decrease with depth, but, in contrast, the R_A/R_G values are small in the upper layer and they increase with depth. The iso-lines of both R_B/R_G and R_A/R_G show comparatively gradual inclinations, but their patterns still indicate the boundaries among different waters. Through the diagrams presented in Figs. 32 and 33, it is noted that there are two major optical border lines, one locates at about Lat. 24°N and other at about Lat. 28.5°N . Taking the latter as an instance, the intensity ratios among lights with different

wave lengths on each side of this line are described in the following list.

Comparison among ratios		
Upper layer		
	Southern side of Lat. 28.5°N	Northern side of Lat. 28.5°N
R_B/R_G	High	Low
R_A/R_G	Low	High
Lower layer		
R_B/R_G	Middle	Low
R_A/R_G	Low	High
I_B/I_G	High	Low
I_A/I_G	Low	High

As seen in the above list, optical characteristics are opposite on each side. Throughout the list, it may be admitted that the position of Lat. 28.5°N corresponds to the boundary between the Kuroshio and the south of the Kuroshio.

As an approach to find a general tendency of optical characteristics in the Kuroshio and its southern area, the intensity ratios among lights with different wave lengths are examined through their mean values. Fig. 22-(1), (2) and (3) show the mean value of I_G with depth, the relation between I_G and I_B/I_G , and that between I_G and I_A/I_G . Fig. 23-(1), (2) and (3) show the relation between I_G and R_G , I_G and R_B/R_G , and also I_G and R_A/R_G , respectively. Through these diagrams, it is clearly noted that I_B/I_G and R_A/R_G increase with depth but I_A/I_G and R_B/R_G decrease with depth, that R_G hardly changes with depth. The tendencies of these curves are different from those both in the East Indian Ocean (refer to Section 3) and the Antarctic Ocean (refer to Section 5) as hereinafter described.

Table 2. The reflectance values distributed vertically in the Kuroshio and its southern area.

Depth	Area			Southern area of Kuroshio			Southern area of N.P. Ocean			Upwelling area		
	30°N			27°N			20°N			24°N		
m	Blue	Green	Amber	Blue	Green	Amber	Blue	Green	Amber	Blue	Green	Amber
10	2.5	1.0	0.2	7.0	1.8	0.2	2.8	1.0	0.2	9.0	2.0	0.4
30	1.5	1.0	1.2	4.8	1.2	0.8	2.2	1.0	0.4	12.0	4.0	1.0
60	0.5	1.0	6.0	1.5	1.1	3.7	1.2	1.2	2.6	18.0	14.0	20.0
100	0.2	1.0	27.0	0.7	1.5	17.0	0.3	1.4	18.0	5.5	6.0	20.0
140	0.3	2.0	More than 50.0	0.8	2.6	50.0	0.3	1.6	50.0	1.0	2.0	30.0

As a preliminary attempt to detect any connection between optical characteristics and any other oceanographical elements, such as seston, oxygen, salinity, water temperature and pH, vertical distribution diagrams of these elements whose data was simultaneously obtained from the same water during the survey are presented in Figs. 24, 25, 26, 27 and 28, respectively. These elements are still critical whether or not they are related indirectly to the optical findings. The author describes a brief note as to seston and oxygen quantities as follows. In respect of seston,* the comparatively larger quantity of 0.5 to 0.7 mg/l at around Lat. 20°N tends to decrease as positions shift northwards and its least value of 0.3 mg/l appears in the sea around Lat. 24°N. But, the oxygen content tends to increase towards the north, exhibiting 4.5 ml/l in the water at around Lat. 20°N and its largest value of 5.3 ml/l exists in the water at around Lat. 24°N. On the other hand, the water having a comparatively larger seston quantity of 0.5 mg/l and rather less oxygen content of about 4.6 ml/l locates in the Kuroshio area. In the southern area of the North Pacific Ocean, the K_B values in the layer from the surface to a depth of about 50 m do not vary with position, but, R_B values tend to increase as positions shift northwards and steep contour lines with the largest R_B values appear at the position near the upwelling area. It is considered that scatterings of blue light are increasingly intensified as positions move northwards. In contrast to the above, however, the R_B values are very small, but, K_B values are fairly large in the Kuroshio area. Under circumstances mentioned above, it may be said that the smallest seston quantity but the largest oxygen content is in the upwelling area in which the scattering of blue light is intensive, while the larger seston quantity but the smaller oxygen content is found in the Kuroshio in which absorption of blue light is large.

5. Optical structure of the Antarctic Ocean

During the 1964–1965 Antarctic Expedition

* Particles smaller than 0.80 μ could not be collected owing to millipore filter AA(0.80 $\mu \pm 0.05 \mu$) employed for the survey.

operated by the M/V Umitaka-maru, an optical research of water was carried out in the Antarctic Ocean from Lat. 45°S to Lat. 70°S and from a meridian of 132°E to 149°W for a period of December 1st, 1964 to February 10th, 1965. Data was collected from thirty four positions for the survey. The same method applied to the East Indian Ocean and the Kuroshio zone is employed for the optical analyses in the Antarctic Ocean and results are compared with those of other oceans.

The thirty four observation positions were located on the three sides of a triangle drawn in the objective water (refer to Fig. 30). The three sides are specified as follows:

Side A: Between New Zealand and the east end of the Ross Sea across the water from north to south.

Side B: Between the east end and the west end of the Ross Sea across the water from east to west.

Side C: Between the west end of the Ross Sea to New Zealand across the water from south to northeast.

The optical structure is viewed from an angle of vertically sectioned profile across the Sub-Antarctic, the Antarctic Convergence and the Antarctic area from north to south between the positions of Lat. 50°S, Long. 180° and Lat. 67°S, Long. 149°W (*i. e.* Side A).

Fig. 29-(1), (2) and (3) exhibit vertical profiles of the I_B , I_G and I_A values from the surface to 140 m deep. The numbers 1, 2, 3, 4, 5, 6, 7, 8... indicate the value of 562 ‰, 316 ‰, 178 ‰, 100 ‰, 56 ‰, 32 ‰, 18 ‰, 10 ‰ of I values, respectively. Through the I diagrams, it is clearly noticed that there are three different waters each having a specific optical characteristic. Namely, the iso-lines run almost horizontal with wide intervals up to about Lat. 58°S and then suddenly drop at about Lat. 58°S and exhibit a complicated pattern with narrow intervals up to about Lat. 61°S and then, become stable at about Lat. 61°S showing a horizontal pattern towards south with intermediate intervals.

In consideration of the vertical distributions of water temperature and salinity along Side A, (refer to Figs. 42 and 43), these three waters

must be the Sub-Antarctic (hereinafter called as Water A), the Antarctic Convergence (Water C) and the Antarctic water (Water B). It was reported by ISHINO and NASU (1965) that the Antarctic Convergence locates around the position of Lat. $59^{\circ}11'S$, Long. $167^{\circ}26'W$. With regard to Water A, however, optical data obtained from three positions in Water A along Side C reveal an exceptionally better light transmittance. The water involved in these three positions is discriminated from Water A and named as Water A'. Thus, the objective water is divided into Waters A, A', B and C for convenience of further discussion. Their geographical distribution is exhibited in Fig. 30. The mean values of I_B , I_G and I_A in the Waters A, A', B and C are shown in Fig. 31-(1), (2) and (3). The mean irradiance transmittance in Waters A, A', B and C expressed by percentage/10 m are listed as follows:

	Blue	Green	Amber
A'	65	56	15
A	45	45	10
B	28	29	6.0
C	15	16	4.2

The depth where present decimal decrease of I_B , I_G and I_A are shown in Table 3. The depth where blue light attenuates to 1/10 of its surface value in Water B is 1/2 to 1/3 of the corresponding depth in the Kuroshio and the depth in Water C is 1/4 to 1/5 of that in the Kuroshio.

Fig. 32-(1), (2) and (3) show the vertically sectioned distribution of K_B , K_G and K_A from the surface to 140 m deep along Side A. Distinct differences in optical characteristics among Waters A, B and C are also reviewed through these K distribution diagrams. For example, the values of K_B up to the layer of 50 m to 60 m in Water A is almost the same as those in the Kuroshio, but these values in the Waters B and C are very large and almost 3 times to 4 times of the Kuroshio.

Fig. 33-(1), (2) and (3) show the vertically sectioned distributions of R_B , R_G and R_A from the surface to 140 m deep along Side A. The diagrams reveal that R_B is larger in the upper layer and decreases with depth in Water A,

Table 3. The depth where relative irradiance is reduced to 1/10 of the surface value, 1/100, 1/1,000, and so on, in the Antarctic Ocean.

Relative irradiance	Area				
	A'	A	B	C	
1/10	Blue	61m	37m	22m	12m
	Green	39	33	22	15
	Amber	10	8	7	6
1/100	Blue	118	73	50	30
	Green	77	69	49	35
	Amber	28	26	19	17
1/1,000	Blue		112	79	48
	Green	112	102	78	55
	Amber	46	43	33	29
1/10,000	Blue			111	68
	Green		132	112	85
	Amber	66	61	49	41
1/100,000	Blue			(114)	92
	Green				122
	Amber	86	79	62	55
1/1,000,000	Blue				(126)
	Amber	112	100	79	71
1/10,000,000	Amber	131	120	99	90
1/100,000,000	Amber			120	108

and it scarcely change with depth in Waters B and C, that, in contrast, R_A is smaller in the upper layer and increases with depth in Water A, but it scarcely changes with depth in Waters B and C. The Antarctic Intermediate Warm Water located at around Lat. $67^{\circ}S$ has considerably small R_B and extremely large R_A . The R value distributed vertically in the objective Waters are listed in Table 4.

Fig. 34-(1) and (2), and Fig. 35-(1) and (2) show vertical profiles of I_B/I_G , I_A/I_G , R_B/R_G and R_A/R_G from surface to 140 m deep along Side A, respectively. The I_B/I_G value indicate 1 to 3.5 in Water A, 0.4 to 0.8 in Water B and 0.3 in Water C. The I_B/I_G iso-lines drop almost perpendicularly in Water C. In contrast, the iso-lines in the sectioned diagrams across the Kuroshio from north to south direct almost horizontal and the values greatly vary with depth. In the diagram of the I_A/I_G , the values are become smaller with depth, and the iso-lines run almost horizontal in the north of Lat. $55^{\circ}S$ and also in the south of Lat. $61^{\circ}S$. But,

Table 4. The reflectance value distributed vertically in the Antarctic Ocean.

Area Depth	Sub-Antarctic Lat. 55°S			Antarctic Convergence Lat. 59°S			Antarctic Lat. 64°S		
	Blue	Green	Amber	Blue	Green	Amber	Blue	Green	Amber
10m	13	6	0.6	7	9	1	9	6	1.3
30	10	6	1.5	6	6	2	7	5	1.2
60	11	7	4	4	5	2	6	5	2.5
100	1.5	2	4	1.5	2.5	0.6	8	2.5	1
140	0.7	6	50	1	1	4	10		

the iso-lines abruptly decline in the perpendicular direction in the water between Lat. 55°S and Lat. 61°S. The R_B/R_G values become smaller with depth and their iso-lines run almost horizontal in Water A, but, in Water B, they increase with depth and indicate the small value of 1.0 at upper layers and the large value of 4.0 at deeper layers, and then, in Water C, they are smallest in every layer and exhibit less than 1. The R_A/R_G values in the Antarctic Ocean are generally small comparing them with those in other oceans, in particular, the values around Water C are very small and they do not reach 2 throughout layers, while they are more than 10 at about 60 m and 50 at 140 m deep in the Kuroshio.

Fig. 36-(1) and (2) show the relation between I_G and I_B/I_G , and that between I_G and I_A/I_G in Waters A, A', B and C. The mean values of I_B/I_G in Waters A and A' increase with depth. This tendency is also seen both in the East Indian Ocean and in the Kuroshio. The values of I_B/I_G in Waters A and A', however, are almost 1/2 of the Kuroshio. The mean I_B/I_G values in Water B are almost constant and scarcely change with depth, maintaining the value of 1. The mean I_B/I_G values in Water C are less than 1 and they decrease with depth. The sequence of the mean I_B/I_G values in each Water is expressed as $A' > A > B > C$. The I_A/I_G curve in the Waters A and A' most resembles to that in the Kuroshio. The sequence of mean I_A/I_G values in each Water is reversed as $C >$

$B > A > A'$.

Fig. 37-(1), (2) and (3) show the relation between I_G and R_G , I_G and R_B/R_G , I_G and R_A/R_G , in each Water A, A', B and C, respectively. The mean R_G values are almost constant without relation to depth throughout Waters A, A', B and C, maintaining almost 5‰ which is nearly 3 times as much as that in the Kuroshio. The mean R_B/R_G values in Waters A and A' are large at upper layers and they decrease with depth displaying values of 0.5 to 2.0. The mean R_B/R_G values are between 1.0 and 2.0 in Water B and between 0.5 and 1.0 in Water C throughout every layer, but both tend to increase with depth. The mean R_A/R_G values increase with depth, and this tendency is most distinct in Water A', but the values hardly change with depth in Water C where values are rather small indicating 0.1 to 0.2.

Figs. 38, 39, 40, 41, and Fig. 42-(1) and (2) show each a vertically sectioned distribution of water temperature, salinity, oxygen, seston and colour of seston along Side A. If these diagrams could collate with corresponding diagrams as to the optical characteristics of water, the classification of the different water in the Antarctic Ocean discussed above seems to be confirmed more clearly.

The optical characteristics resulting from a series of vertical distribution analyses together with other oceanographical data in Waters A, B and C in the Antarctic Ocean are summarized as follows:

$K_B \times 10^3$	1. A-Upper	2. A-Deeper	3. B-Upper
$R_B \times 10^3$	Ⓢ 40~70	Ⓛ 150	Ⓛ more than 100
$K_A \times 10^3$	Ⓛ 13	Ⓢ 0.7~1.0	5.0~10
	Ⓛ 100~200	Ⓢ 20	Ⓛ more than 100

$R_A \times 10^3$	Ⓢ less than 1	Ⓛ 50	Ⓢ 1.0~2.0
I_B/I_G	Ⓢ 0.9~1.0	Ⓛ 2.0~2.5	Ⓢ 0.5~1.0
I_A/I_G	1.0~5.0	12~14	1.0~4.0
R_B/R_G	Ⓛ 1.5~2.0	Ⓢ 0.2~0.8	Ⓢ 0.3~1.2
R_A/R_G	Ⓢ 0.1~0.2	Ⓛ 9.0	Ⓢ 0.1~0.2
Temp. °C	8~10	6.5~7.0	0.0~0.3
O ₂ ml/l	Ⓢ 6.4~6.6	Ⓢ 6.3~6.4	Ⓛ 7.8~7.9
S ‰	Ⓢ 34.15~34.25	Ⓛ 34.25~34.30	Ⓢ 34.20
Seston quantity mg/l	Ⓢ 0.5~0.8	Ⓢ 0.5	Ⓛ 1.0~1.2
Seston colour (wet)	79	63	61
Seston colour (dry)	79~93	79~93	77
	4. B-Deeper	5. Water C	6. Antarctic Intermediate Warm Water
$K_B \times 10^3$	Ⓢ 30~50	Ⓛ more than 100	Ⓢ 30
$R_B \times 10^3$	Ⓛ 10	5.0	4.0~5.0
$K_A \times 10^3$	Ⓛ 180	Ⓛ more than 100	Ⓢ 60~80
$R_A \times 10^3$	Ⓢ 0.6~4.0	Ⓢ 0.2 (0~30 m)	Ⓛ more than 100
		1.5 (100~120 m)	110~130 m
I_B/I_G	1.0~1.5	Ⓢ 0.3~0.6	Ⓛ 1.5
I_A/I_G	12~16	change abruptly	14
R_B/R_G	Ⓛ 4.0	Ⓢ 0.6~1.0	Ⓢ 0.2
R_A/R_G	Ⓛ 7.0	Ⓢ 0.3~0.9	Ⓛ 7.0
Temp. °C	-1.5~-1.8	1~6 the iso-lines show vertical mode	-1.0~0.5
O ₂ ml/l	6.5~7.2	7.1~7.8	4.6~6.0
S ‰	Ⓛ 34.30~34.40	Ⓢ 34.00	Ⓛ 34.40
Seston quantity mg/l	Ⓛ 2.0	Ⓛ 1.5~1.8	no data
Seston colour (wet)	79	61	no data
Seston colour (dry)	80~90	80~90	no data

1. A-Upper : Upper layer between 0 and 30 m at around Lat. 55°S in Water A
2. A-Deeper : Deeper layer between 100 m and 140 m at around Lat. 55°S in Water A
3. B-Upper : Upper layer between 0 and 30 m at around Lat. 65°S in Water B
4. B-Deeper : Deeper layer between 100 m and 140 m at around Lat. 65°S in Water B
5. Water C : throughout layers around Lat. 59°S in Water C
6. Antarctic Intermediate Warm Water: Deeper layer more than 120 m deep around Lat. 66°S in Water C

where, Ⓢ or Ⓛ stands for small or large, respectively.

This table gives also clear indications of the differences in optical characteristics among Waters A, B and C.

The discussions presented above concern optical characteristics of each limited area such as A and A', B and C within the Antarctic Ocean. In addition, in order to detect a general tendency in optical characteristics for the ocean-wide waters, the following values of the Antarctic Ocean as a whole are calculated and

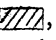
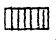
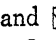
the results are compared with the corresponding values in the Indian and the Pacific Oceans in Figs. 43 and 44.

In Fig. 43

- (1) the mean value of I_G in each depth
- (2) the relation between I_G and I_B/I_G
- (3) the relation between I_G and I_A/I_G

In Fig. 44

- (1) the relation between I_G and R_G
- (2) the relation between I_G and R_B/R_G

(3) the relation between I_G and R_A/R_G . The symbols as ,  and  in these diagrams denote the Antarctic Ocean, the East Indian Ocean and the Kuroshio, respectively, and each solid line indicates the mean value. The space held with two broken lines show the range of distributions: As seen in the diagrams, even if these optical characteristics are reviewed from the ocean-wide waters, there are still prominent differences in their respective optical characteristics exhibiting especially wide gaps in values of I_B/I_G , R_A/R_G and R_G .

6. Possible and actual insolation attained on the sea surface

The optical structures and characteristics of waters were discussed on the basis of relative value of underwater irradiance in the preceding sections. If the absolute value of underwater light were available, it will be easier to clarify the subject of this paper. As a first step to satisfy such a requirement, it is essential to know the distribution of solar energy attained on the sea surface. Unfortunately, reliable information on the systematic study in this field is not sufficient and systematic data of insolation attained on the oceanic water surface is meagre. An approach to find both the possible and the actual insolation amount attained on the sea surface is introduced based on data obtained during the Antarctic Ocean Expedition (from Oct., '64 to Mar., '65), International Indian Expedition (Nov., '63 to Feb., '64) and International Kuroshio Expedition (Aug., '65) in this section.

1. Possible insolation

The Eppley actinograph with the sensing unit covered by a spherical glass was employed for the measurement of solar energy attained on the oceanic water surface.

When the evaluation of solar light in the air is discussed, it is usual to treat the scattered light discriminately from the direct light. In this paper, however, the same concept as applied to the underwater lights in the previous section is adopted for solar light in the air, and both the scattered and direct light are put together into the following formula (*i.e.* direct light equation).

$$I_H = J_0 \frac{r_m^2}{r^2} \sin a e^{-KH \cos a}$$

let e^{-KH} be replaced by q

$$I_H = J_0 \frac{r_m^2}{r^2} \sin a q^{\cos a}, \tag{1}$$

- where I_H : insolation on the horizontal plane
- r : distance between sun and earth
- r_m : mean distance between sun and earth
- H : atmospheric thickness at zenith
- K : extinction coefficient
- J_0 : solar constant
- a : sun's altitude

Accordingly, the quantity q used in the above equation is substantially different from the transmissivity with respect to the direct light.

Note: In the previous paper (1969), the quantity q defined by the equation $I = I_0 q^{\cos a}$ is used, where I_0 stands for the solar constant in relation to seasonal changes. But, the quantity q defined more reasonably by the formula $I_H = J_0 \frac{r_m^2}{r^2} \sin a q^{\cos a}$ is adopted in this paper.

The daily changes of the quantity q in the clear sky above the different oceans are exhibited in Fig. 45. As seen in the graph, each curve which indicates q 's daily changes exhibits a similar configuration without relating to the positions which are widely distributed over the earth. Fig. 46 exhibits variations of the quantity q in accordance with sun's altitudes in the clear sky. The quantity q is almost constant when the sun's altitude is comparatively higher. But, the lower the altitude is, the larger the quantity q , due to the influence of scattered light. It may be basically unreasonable to discuss the whole solar light including both the direct and scattered light by means of Equation (1). However, the fact that the curve drawn with plotted points is very smooth without any large dispersion suggests that probable influence on the quantity q by the difference in vapour or dust content in the air above the ocean may be considered slight, and the quantity q can be treated as only a function of the sun's altitude.

In this sense, the relation between the q and

the sun's altitude may be expressed through the Fourier Formula as follows:

$$q = 1 - 0.233 \sin a - 0.0447 \sin 3a - 0.0225 \sin 5a - 0.0103 \sin 7a - 0.00544 \sin 9a - \dots \quad (2)$$

a : sun's altitude (degrees)

Using the diagram shown in Fig. 46 or Equation (2), the possible insolation of each calendar month is calculated by the following procedure.

- a) Calculate the daily sun's altitude at each latitude for each month.
- b) Read off the value of q at each sun's altitude from the diagram of Fig. 46 or calculate it from Equation (2).
- c) Find the momentary insolation amount I_H from the q , sun's altitude and solar

constant (in relation to seasonal changes) through Equation (1) and integrate it from sunrise to sunset.

The above process can be expressed by the following formula.

$$S_0 = \int_{\text{sunrise}}^{\text{sunset}} J_0 \frac{r_m^2}{r^2} \sin a q^{\cos \epsilon} dt, \quad (3)$$

where $\sin a = \sin l \sin d + \cos l \cos d \cos h$

$$q = 1 - 0.233 \sin a - 0.0447 \sin 3a - 0.0225 \sin 5a - 0.0103 \sin 7a - 0.00544 \sin 9a \dots$$

l : latitude d : declination of the sun

h : hour angle S_0 : possible insolation

The calculated results of possible insolation from Lat. 65°N to Lat. 65°S throughout a year are exhibited in Fig. 47-(1) and (2), and also in Table 5. Contribution of the q in low sun's

Table 5. Possible insolation attained on the sea surface.

The Northern Hemisphere

Month \ Lat.	5°N	15°N	25°N	35°N	45°N	55°N	65°N
Jan.	0.61	0.51	0.41	0.29	0.18	0.09	0.04
Feb.	0.65	0.58	0.49	0.39	0.28	0.17	0.09
Mar.	0.67	0.65	0.59	0.52	0.43	0.33	0.22
Apr.	0.67	0.69	0.67	0.64	0.59	0.51	0.43
May	0.65	0.70	0.71	0.72	0.70	0.66	0.61
Jun.	0.64	0.70	0.73	0.74	0.74	0.72	0.69
Jul.	0.64	0.70	0.73	0.73	0.72	0.70	0.65
Aug.	0.66	0.69	0.69	0.67	0.63	0.57	0.50
Sep.	0.67	0.67	0.62	0.57	0.50	0.40	0.30
Oct.	0.66	0.61	0.54	0.44	0.34	0.23	0.14
Nov.	0.62	0.53	0.45	0.33	0.21	0.11	0.05
Dec.	0.59	0.50	0.39	0.27	0.16	0.07	0.03

kg·cal/cm²·day

The Southern Hemisphere

Month \ Lat.	5°S	15°S	25°S	35°S	45°S	55°S	65°S
Jan.	0.68	0.74	0.77	0.78	0.76	0.73	0.69
Feb.	0.68	0.72	0.72	0.70	0.65	0.59	0.49
Mar.	0.68	0.67	0.63	0.57	0.49	0.39	0.28
Apr.	0.64	0.58	0.51	0.42	0.31	0.21	0.10
May	0.59	0.51	0.41	0.30	0.19	0.11	0.04
Jun.	0.55	0.47	0.36	0.26	0.15	0.07	0.03
Jul.	0.56	0.48	0.38	0.27	0.17	0.08	0.03
Aug.	0.61	0.55	0.46	0.36	0.25	0.16	0.08
Sep.	0.66	0.62	0.58	0.50	0.41	0.30	0.21
Oct.	0.68	0.69	0.68	0.64	0.58	0.50	0.40
Nov.	0.68	0.73	0.75	0.75	0.74	0.68	0.63
Dec.	0.68	0.74	0.77	0.79	0.79	0.77	0.75

kg·cal/cm²·day

altitude on the total insolation amount is very slight.

UKRAINTSEV (1939) calculated the values of the possible insolation in the Northern Hemisphere throughout a year by using the following formula.

$$(Q+q)=m \sum s+n$$

$\sum s$: total hours of daylight

m, n : coefficient related to year and latitude

His formula was induced based on data obtained from the observation stations distributed from Lat. 35°N to 70°N on Europe and Asia Continents. BUDYKO (1956) pointed out that the value of the possible insolation presented by UKRAINTSEV (1939) were too large and gave his reason for this criticism that those rather large values were caused by the proto-type instrument at the initial stage and UKRAINTSEV provided the possible insolation in very transparent air regardless of mean transmittance.

In comparing the Ukraintsev's values of possible insolation with those listed in Table 5, his values are larger by about 10 % than those in Table 5.

MATEER (1955) and GAVRILOVA (1963) introduced independently the values of possible insolation in the area locating north of Lat. 50°N centring the Arctic Zone using a method similar to Ukraintsev's. In comparing their values with those listed in Table 6, some of their values coincide with corresponding values in Table 6 and some are 2 % to 3 % larger than corresponding ones in the Table.

ASHBURN (1963) presented the data of the solar insolation at the ocean station PAPA (Lat. 50°N, Long. 145°W) during years of 1960 and 1961. In comparing his mean values in the clear sky with that of Lat. 50°N in this paper, both values are almost coincident.

2. Actual insolation

The relation between the q and the sun's altitude in each cloud form veiling the sun is exhibited by way of mean values in Fig. 48. A rather large dispersion is noticed while drawing curves of this graph due to possible differences in light transmittance through different thicknesses of cloud even though there is no difference in cloud form.

HAURWITZ (1948) introduced a diagram in

Table 6. Distribution of weathers in the Antarctic Ocean in summer of 1964-1965.

Month	Weather	b	bc	c	o	r	d	s	f	Total
Dec.	Frequency	49	59	57	224	14	34	36	23	496
	%	9.9	11.9	11.5	45.2	2.8	6.9	7.3	4.6	100.1
Jan.	Frequency	46	64	64	276	9	13	49	45	566
	%	8.1	11.3	11.3	48.8	1.6	2.3	8.7	8.0	100.1
Feb.	Frequency	1	20	23	90	10	6	17	3	170
	%	0.6	11.8	13.1	52.9	5.9	3.5	1.0	1.8	99.6
Total	Frequency	96	143	144	590	33	53	102	71	1232
	%	7.8	11.6	11.7	47.9	2.7	4.3	8.3	5.8	100

Table 7. Distribution of sea conditions in the Antarctic Ocean in summer of 1964-1965.

Month	Sea condition	0	1	2	3	4	5	6	7	8	9	Total
Dec.	Frequency	0	28	111	138	154	22	28	15	0	0	496
	%	0	5.6	22.4	27.8	31.0	4.4	5.6	3.0	0	0	100
Jan.	Frequency	0	0	73	155	190	132	3	12	1	0	566
	%	0	0	12.9	27.4	33.6	23.3	0.5	2.1	0.2	0	100
Feb.	Frequency	0	0	7	32	46	39	30	16	0	0	170
	%	0	0	4.1	18.1	27.1	22.9	17.6	9.4	0	0	100
Total	Frequency	0	28	191	325	390	193	61	43	1	0	1232
	%	0	2.3	15.5	26.4	31.7	15.7	5.0	3.5	0.1	0	100.2

Remarks: Numerical letters stand for sea condition by Bufort classifications.

which the relation between insolation and light path length in each cloud form is exhibited. Taking advantage of his diagram, the quantity q is calculated and the result is compared with the quantity q obtained through the diagrams in Fig. 48. As a result, the quantity q of the former is found just identical with that of the latter for the blue sky and sky with Ci and Cs cloud. Besides, the quantity q of the former is larger by 0.02 to 0.03 than that of latter under sky conditions of As, Ac, St, Sc and Ns cloud.

Although occasions that the sky has only one form of cloud are very few, daily insolation for each cloud form is calculated through the graph in Fig. 48 for the summer of the Antarctic Ocean and listed as follows:

	Cloud form			
	CiCs	AcAs	StSc	Ns
Antarctic Ocean Lat. 55°S	600	390	250	160

Subsequently, the relation between the cloud amount and such reduction ratio as

$$\frac{\text{possible insolation} - \text{actual insolation}}{\text{possible insolation}}$$

is exhibited by the graph in Fig. 49 and also expressed by the following equation.

$$Q \doteq Q_0(1 - 0.026C^{1.3}), \quad (4)$$

where Q : actual insolation

Q_0 : possible insolation

C : cloud amount (0, 1, 2, 3, ... 10)

Concerning the calculation formula to evaluate the actual insolation amount, such scientists as ANGSTÖM (1924), KIMBALL (1928), MOSBY (1936) and KUZMIN (1950) as well as ASHBURN (1963) can be listed as the representative researchers. Among them, KIMBALL (1928) introduced the following formula.

$$Q = Q_0(1 - 0.068C),$$

where Q : actual insolation

Q_0 : possible insolation

C : cloud amount (0, 1, 2, 3, ... 10)

A different type of formula to determine the insolation amount was introduced by KUZMIN

(1950). He put two coefficients of cloud amount to the formula as follows:

$$\frac{Q}{Q_0} = 1 - 0.14(n_0 - n_H) - 0.67n_H,$$

where n_0 : total cloud amount

n_H : cloud amount in lower layer

ASHBURN (1963) and TABATA (1964) endeavoured to examine various formulae introduced by the above-mentioned researchers and reported that such formula produced differing results.

The actual insolation amount on the sea surface is calculated using Equation (4) in the wider oceanic waters, such as A to H zone in the Indian Ocean, I to L zones in the North Pacific Ocean, and M to P zone in the Antarctic Oceans as shown in Fig. 50. Cloud amount data in each zone of each ocean are cited from U. S. Navy Marine Climatic Atlas of the World, which are statistically compiled from observation data for 50 to 90 years in Vol. II for the North Pacific Ocean and Vol. III for the Indian Ocean, and for 10 years in Vol. VII for the Antarctic Ocean. Fig. 51 shows the calculated results of the actual insolation amount in each zone. Seasonal fluctuations of insolation for the zones facing to the land mass such as A, B and C exhibit rather complicated patterns comparing these in the midst of the ocean. The monthly insolation amount in summer of the Antarctic Ocean (Dec., Jan. and Feb.), the East Indian Ocean (Dec. and Jan.) and the Kuroshio (Aug.) are about 12,000, 17,000 and 15,000 g·cal/cm²·month, respectively.

There is information as to the insolation amount around the water from Long. 72°E to Long. 171°E along a latitude of 10°S presented by KIMBALL (1928). When comparing his amount with that introduced in this paper for the same water, Kimball's is a little larger in August and September, but smaller in the other months except during July in which both are almost identical. The gaps between both amounts are less than 10%. The results for the latter are consistent with the data introduced by ASHBURN (1963) for the position of Lat. 50°N, Long. 145°W and those exhibited in Soviet Antarctic Expedition (1966) for the oceanic water from Lat. 45°S to Lat. 70°S and

from Long. 132°E to Long. 149°W.

7. Distribution of underwater solar energy

Underwater solar energy and its seasonal distributions in the different waters will be discussed in this section. Before dealing in detail with the subject, it is, however, necessary to evaluate the reflected amounts of solar energy on the sea surface. Fortunately, there are several references with regard to solar energy reflection on the sea surface such as those by POWELL and CLARKE (1936), NEIBURGER (1948), BURT (1954), ANDERSON (1954), COX and MUNK (1956), and NEUMANN and HOLLMAN (1961), etc. Among these references, taking advantage of information introduced by COX and MUNK (1956) the reflected amounts of solar energy on the sea surface are calculated with reference to weather and sea condition data.

To begin with, selecting the Antarctic Ocean in summer, the subject is discussed based on data on three parameters... insolation, weather and sea conditions (provided in Tables 6 and 7, respectively), and underwater spectral light transmittance. Firstly, an approximate insolation amount reflected on the sea surface in summer of the Antarctic Ocean is evaluated as 550~600 g·cal/cm²·month; secondly, monthly amount of solar energy penetrated into the surface water of the Antarctic Ocean in summer is estimated at about 11,500 g·cal/cm²·month; thirdly, underwater distribution of solar energy in each area of the Antarctic Ocean in summer is estimated as follows:

		Unit: g·cal/cm ² ·month			
Area	Layer	A'	A	B	C
	0m	11,500	11,500	11,500	11,500
	1	4,900	4,800	4,300	3,800
	2	4,100	4,000	3,100	2,600
	5	3,000	2,700	1,600	1,100
	10	1,900	1,600	680	310
	20			150	33
	25	850	480		
	50	210	81	25	
	75	48	14		
	100	12	2.6		
	150		0.092		

The estimate of underwater solar energy is achieved in consultation with JERLOV (1964) in which he calculated the decreasing percentage of total irradiance (of which wave lengths were from 300 to 2,500 nm) in accordance with depth of water based on spectral transmittance of the surface layer. It is clear that the underwater solar energy distribution differs very much with different waters even if their localities are close one to another; for example, the mean amount in depth of 10 m in the Antarctic Convergence area is equal to 1/6 as much as the corresponding amount in the Sub-Antarctic area.

Subsequently, extending the aforementioned calculation process to the wider waters such as A to P areas classified in Fig. 51, the distribution of underwater solar energy in those areas in every month are evaluated. Fig. 52-(1)~(8) show the distribution of underwater solar energy in 8 areas selected from the Indian Ocean, the North Pacific Ocean and the Antarctic Ocean. Weather and sea condition data on corresponding waters are quoted from U. S. Navy Marine Climatic Atlas of the World.

The total annual amounts of underwater solar energy in different areas are obtained by means of accumulating individual amounts in each layer and are exhibited in Fig. 53. A comparison of the annual amounts of underwater solar energy in each depth, expressed by ratios between the equatorial water in the Indian Ocean and other waters, are listed in Table 8. The discrepancies in the annual amounts among different waters are very large; for example, the annual amount in the depth of 10 m of the Antarctic Convergence area correspond to 1/17 as much as that of the equatorial water in the Indian Ocean and 1/9 of the amount in the Kuroshio.

Furthermore, if the lowest limit of solar energy for the euphotic zone can be assumed as 5 g·cal/cm²·day, the total water volumes of the euphotic zone per unit sea surface area accumulated for a year among different areas are compared, resulting in the following ratios.

$$I_E : K : S_A : A_C = 100 : 75 : 50 : 20,$$

where I_E : the equatorial area of the Indian Ocean

K : the Kuroshio area

Table 8. Annual amount of underwater solar energy.

Depth	Area	Indian Ocean		Kuroshio area		Sub-Ant. Ocean	Ant. Ocean Lat. 55~60°S	
		Total	Lat. 0°	Lat. 35°N	Lat. 45°S		Ant.	Conv.
m		Kg·cal/ cm ² ·year	Ratio	Ratio	Ratio		Ratio	Ratio
0		160.7	100 %	67 %	65 %		46 %	46 %
1		70.9	100	65	62		39	35
5		46.6	100	59	52		23	15
10		33.4	100	54	44		13	8
25		17.8	100	46	25		3	0.5
50		5.3	100	36	14		0.3	
100		0.45	100	24	5			

S_A : the Sub-Antarctic area

A_C : the southern area of the Antarctic Convergence

8. Summary

The subject dealt with in this paper can be classified into three major parts; firstly, underwater optical structures and characteristics in the different oceans; secondly, the possible and actual insolation amounts attained on the sea surface; and thirdly, underwater distribution of solar energy. The important aspects are summarized as follows:

The underwater optical structures and characteristics in the different oceans

(1) The water masses classified, based on spectral light transmittance, are almost consistent with the waters in different ocean currents in the East Indian Ocean such as the South Equatorial Current and the Equatorial Counter Convergence Current.

(2) Underwater optical structures related to spectral light transmittance or attenuation, reflectance and intensity ratios among lights with different wave lengths, vary remarkably with different waters such as Sub-Antarctic, the Antarctic, the Antarctic Convergence, the Kuroshio and its southern area, and the East Indian Ocean. For example, attenuation of blue light is unusually large in the south of the Antarctic Convergence and its values are 3 to 4 times as much as those in the Kuroshio. The I_B/I_0 values in the Sub-Antarctic area are more than

1 and increase with depth, but the corresponding values in the Antarctic area are about 1 exhibiting almost constant at all depths, and they are less than 1 in the Antarctic Convergence area and decrease with depth.

(3) The distinct border lines of the different water masses can be observed through the vertical profiles of relative irradiance, attenuation coefficient and reflectance of spectral light as well as intensity ratio among light with different wave lengths (*i. e.* Antarctic Convergence, Kuroshio and upwelling area). For example, a remarkable reflectance is found, especially for blue light, in the upwelling area where it has values almost 12 times as much as those in each adjacent areas both in the south and the north of the North Pacific Ocean. In addition, the iso-lines for the I_B/I_0 and R_B/R_0 exhibit a horizontal configuration in the East Indian Ocean, the North Pacific Ocean and the Sub-Antarctic area, but corresponding iso-lines in the Antarctic Convergence area indicate a vertical configuration.

The possible and actual insolation amounts attained on the sea surface

(1) An equation to calculate the possible insolation amount is derived. Using the equation, daily possible insulations distributed over the oceanic water in both hemispheres from Lat. 65°N to Lat. 65°S, in each month, are calculated. The results are exhibited in Fig. 47-(1) and (2) or in Table 5. The formula is stated as follows:

$$S_0 = \int_{\text{sunrise}}^{\text{sunset}} J_0 \frac{r_m^2}{r^2} \sin a q^{\cos a} dt,$$

where $\sin a = \sin l \sin d + \cos l \cos d \cos h$
 $q = 1 - 0.233 \sin a - 0.0447 \sin 3a$
 $- 0.0225 \sin 5a - 0.0103 \sin 7a$
 $- 0.00544 \sin 9a \dots$

S_0 : possible insolation
 a : sun's altitude
 r : distance between sun and earth
 l : latitude
 r_m : mean distance between sun and earth
 h : hour angle
 d : declination of the sun
 J_0 : solar constant

The results are approximately 10 % smaller than those of UKRAINTSEV (1939) at every latitude.

(2) An equation to calculate the actual insolation amount is derived. Using the equation, the actual insolutions distributed on the oceanic waters of the Indian Ocean, the North Pacific Ocean and the Antarctic Ocean are calculated. The results are exhibited in Fig. 49. The formula is stated as follows:

$$Q = Q_0(1 - 0.026C^{1.3})$$

C : cloud amount (0, 1, 2, 3, ... 10)
 Q_0 : possible insolation amount
 Q : actual insolation amount

The result are almost consistent with the data in the position of Lat. 50°N, Long. 145°W introduced by ASHBURN (1963) and also those of the oceanic area from Lat. 45°S to 70°S and from Long. 132°E to 149°W exhibited in Soviet Antarctic Expedition (1966).

Underwater distribution of solar energy

(1) The monthly amounts of solar energy distributed in each depth of different areas in the Indian Ocean, the North Pacific Ocean and the Antarctic Ocean are obtained as shown in Fig. 52-(1)~(8). The results show that the underwater distribution of solar energy differs very much with different waters even if their localities are close to one another. For example, their mean amounts in summer at 10 m deep in the Antarctic Convergence area is consistent with 1/6 as much as the corresponding amounts

in the Sub-Antarctic area.

(2) The annual amounts of underwater solar energy distributed in each depth of the different areas are obtained and exhibited in Fig. 53. For example, the annual amount of solar energy in the layer of 10 m deep of the Antarctic Convergence area corresponds to 1/17 as much as that of the equatorial water in the Indian Ocean and 1/9 of the corresponding amount in the Kuroshio.

(3) If the lowest limit of solar energy for the euphotic zone can be assumed as 5 g·cal/cm²·day, the ratio of total water volumes of the euphotic zone per unit sea surface area accumulated for a year among the equatorial water of the Indian Ocean, the Kuroshio area, the Sub-Antarctic area and the southern area of the Antarctic Convergence is about 100:75:50:20, respectively.

Prior to closing this paper, the author suggests that a systematic study of geographical and seasonal fluctuations of solar energy attained on the sea surface and penetrated into water will be developed further in order that its relationship with biological and oceanographical problems, particularly, the organization of oceanic production may be more clearly resolved.

Acknowledgements

The author wishes to express his hearty thanks to Dr. Tadayoshi SASAKI, Professor of the Tokyo University of Fisheries, who have given me valuable guidances and advices with regard to this paper. Also, he is very grateful for kind instructions and encouragements, along the development of his studies, favoured by Mr. Noboru OKAMI, Scientist of Physical Oceanography Laboratory of the Institute of Physical and Chemical Research.

References

- ALBRECHT, F. H. W. (1958): The Australian Radiation Network, United Nations Educational Science and Cultural Organization, Arid Zone Climatol., II, 99-105.
 ANDERSON, E. R. (1954): Energy-budget studies. In: Water Loss Investigations: Lake Hefner Studies. U.S., Geol. Surv., Profess. Papers, 269, 71-117.

- ANGSTRÖM, A. (1924): Solar and Terrestrial Radiation. Roy. Met. Soc., Quart. J., **50**, 121-126.
- ARUGA, Y. and M. MONSI (1962): Primary production in the northwestern part of the Pacific off Honshu, Japan. J. Oceanog. Soc. Japan, **18**(2), 85-94.
- ASHBURN, E. V. (1963): The radiative heat budget at the ocean-atmosphere interface. Deep-Sea Res., **10**, 597-606.
- ATKINS, W. R. G. and H. H. POOLE (1933): The photo-electric measurement of penetration of light of various wave lengths into the sea and the physiological bearing of the results. Phil. Trans. Roy. Soc. London, Ser. B, **222**, 129.
- ATKINS, W. R. G. and H. H. POOLE (1958): Cube photometer measurements of the angular distribution of submarine daylight and the total submarine illumination. J. Conseil, Conseil Perm. Intern. Exploration Mer, **23**, 327-336.
- BIRGE, E. A. and C. JUDAY (1926): Transmission of solar radiation by the waters of inland lakes. Wisconsin Acad. Sci., Arts and Letters, Trans., **24**, 509-590.
- BLACK, J. N. (1956): The distribution of solar radiation over the earth's surface. Archiv Meteorol., Geophys. Bioklimatol. 7, Ser. B, 165-189.
- BUDYKO, M. I. (1956): The heat balance of the earth's surface. Gidrometeorl, Izd, Leningrad, 23-24. (In Japanese)
- BUDYKO, M. I. (1969): The effect of solar radiation variation on the climate of the earth. Tellus, **21**, 5, 611-619.
- BUNT, J. S. and C. C. LEE (1970): Seasonal primary production in Antarctic Sea Ice at McMurdo Sound in 1967. J. Marine Res., **28**, 304-819.
- BURT, W. V. (1954): Albedo over wind roughened water. J. Meteorol., **11**, 283-290.
- BURT, W. V. (1958): Selective transmission of light in tropical Pacific waters. Deep-Sea Res., **5**, 51-61.
- CLARKE, G. L. (1941): Observations on transparency in the south-western section of the north Atlantic Ocean. J. Marine Res., **4**, 221-230.
- CLARKE, G. L. and G. K. WERTHEIM (1956): Measurements of illumination at great depths and at night in the Atlantic Ocean by means of a new bathyphotometer. Deep-Sea Res., **3**, 189-205.
- CLARKE, G. L. and E. J. DENTON (1962): Light and animal life. In: M. N. HILL (General Editor), The Sea, Ideas and Observations on Progress in the Study of the Seas. Interscience, New York, N. Y., **1**, 456-468.
- COX, C. and W. MUNK (1955): Some problems in optical oceanography. J. Marine Res., **14**, 63-78.
- COX, C. and W. MUNK (1956): Slopes of the sea surface deduced from photographs of sun glitter. Bull. Scripps Inst. Oceanog. Univ. Calif., **6**, 401-488.
- DUNTLEY, S. Q. (1963): Light in the sea. J. Opt. Soc. Am., **53**, 214-233.
- FUKUDA, M. (1960): Transparency measurements in the Baltic Sea. Medd. Oceanog. Inst. Göteborg, **27**, 1-18.
- GAVRILOVA, M. K. (1958): Total Radiation in the Soviet and non-Soviet Arctic. Trudy ANII, 217.
- GAVRILOVA, M. K. (1963): Radiation Climate of the Arctic. Gidrometeorl, Izd, Leningrad, 48-57, 144. (In English)
- HANAOKA, T., A. FURUKUWA and K. NOGAMI (1960): Studies on suspended matter in the sea, 4. On the relation between suspension factor, extinction coefficient and turbidity. Bull. Japan. Soc. Sci. Fisheries, **26**, 469-471.
- HAURWITZ, B. (1948): Insolation in relation to cloud type. J. Meteorol., **5**, 110-113.
- HISHIDA, K. (1954): Physical studies on the turbidity in the sea water, with special reference to the relation of the radiant energy. J. Oceanog. Soc. Japan, **9**(3), 143-181.
- HISHIDA, K. and M. KISHINO (1965): On the albedo of radiation of the sea surface. J. Oceanog. Soc. Japan, **21**(4), 148-153.
- HOLMES R. W. (1964): Description and Evaluation of methods of determining incident solar radiation, submarine daylight, chlorophyll A and primary production. Special Scientific report. Fisheries. Scripps Inst. of Oceanography.
- INOUE, N., S. NISHIZAWA and M. FUKUDA (1955): The perfection of a turbidity meter and the photographic study of suspended matter and plankton in the sea using an undersea observation chamber. Proc. U. N. E. S. C. O. Symp. Phys. Oceanog., Tokyo, 1955, pp. 53-58.
- ISHINO, M. and K. NASU (1965): Conditions hydrologiques dans des régions au sud de l'Australie et de la Nouvelle-Zélande et des régions environnant la mer de Ross. La mer, **3**(1), 9-18. (In Japanese)
- IVANOFF, A. (1959): Optical method of investigation of the ocean. The p - β diagram. J. Opt. Soc. Am., **49**, 103-104.
- IVANOFF, A., N. JERLOV and T. H. WATERMAN (1961): A comparative study of irradiance, beam transmittance and scattering in the sea near Bermuda. Limnol. Oceanog., **6**, 129-148.
- JERLOV, N. G. (1951): Optical studies of ocean water. Rept. Swedish Deep-Sea Expedition, **3**,

- 1-59.
- JERLOV, N.G. and M. FUKUDA (1963): Radiance distribution in the upper layers of the sea. *Tellus*, **12**, 348-355.
- JERLOV, N.G. (1964): Optical classification of ocean water. In: *Physical aspects of light in the sea*. Univ. Hawaii Press, Honolulu, Hawaii, 45-49.
- JERLOV, N.G. (1968): *Optical oceanography*. Elsevier Oceanography Series. 5. Elsevier Publishing Co. Amsterdam. 118-123.
- JERLOV, N.G. and K. NYGARD (1969): Influence of solar elevation on attenuation of underwater irradiance. *København Univ. institute for Fysisk Oceanografi Report 4*, 1-9.
- JOSEPH, J. (1949b): Über die Messung des "Vertikalen Extinktions-koeffizienten". *Deut. Hydrograph. Z.*, **2**, 255-267.
- JOSEPH, J. (1955): Extinction measurements to indicate distribution and transport of watermasses. *Proc. U. N. E. S. C. O. Symp. Phys. Oceanog.*, Tokyo, pp. 59-75.
- KIMBALL, H. H. (1924): Records of total solar radiation intensity and their relation to daylight intensity. *Monthly Weather Rev.*, **52**, 475.
- KIMBALL, H. H. (1928): Amount of solar radiation that reaches the surface of the earth on the land and on the sea, and methods by which it is measured. *Monthly Weather Rev.*, **56**, 393-399.
- KONDO, J. (1967): Analysis of solar radiation and downward longwave radiation data in Japan. The science rep. of Tōhoku Univ. Series 5, Geophysics, **18**(3), 91-124.
- KUZMIN, P. P. (1950): Method for determining the maximum intensity of snow melt. *Trudy of the state Hydrological Inst.*, No. 24. 78.
- MANI, A., O. CHACKO and S. HARIHARAN (1969): A study of Angström's turbidity parameters from solar radiation measurements in India. *Tellus*, **21**, 829-843.
- MATEER, C. L. (1955): Average Insolation in Canada during cloudless Day. *Canada. J. Technol.*, **33**, 12-32.
- MATSUIKE, K. (1967): Study on the optical characteristics of the water in the three oceans. (Part-1) Optical structure of the Kuroshio (Japan Current) from Lat. 20°N to Lat. 31°N along the meridian of 142°E. *J. Tokyo Univ. Fisheries*, **53**(1-2), 1-40.
- MATSUIKE, K. and Y. SASAKI (1968): The optical characteristic of the waters in the three oceans. (Part-2) Optical structure of the Antarctic Ocean from Lat. 45°S to Lat. 70°S and from the meridian of 132°E to 149°W including the Ross Sea. *J. Tokyo Univ. Fisheries*, **9**(1), (Special edition) 57-114.
- MATSUIKE, K. (1969): The optical characteristics of the water in the three oceans. (Part-3) The distribution of solar energy reached to and penetrated in the water of the Antarctic Ocean in the summer and its comparison to other oceans. *J. Oceanog. Soc. Japan*, **25**(2), 81-90.
- MATSUIKE, K., T. MORINAGA and T. SASAKI (1970): The optical characteristics of the water in the three oceans. (Part-4) An attempt to the approximate figures of seasonal solar energy reached to and penetrated in the water of the three oceans. *J. Oceanog. Soc. Japan*, **26**(1), 52-60.
- MOON, P. (1940): Proposed standard solar-radiation curves for engineering use. *J. Franklin Inst.*, **230**, 583-618.
- MOSBY, H. (1936): Verdunstung und Strahlung auf dem Meere. *Ann. Hydrogr. Berl.*, **64**, 282-286.
- NASU, K. (1964): Conditions hydrologiques dans la region sud-est de l'Océan Indian. *La mer*, **2**(1), 27-32. (In Japanese)
- Naval Weather Service Division (1956): *The U. S. Navy Marine Climatic Atlas of the World, 2*, North Pacific Ocean, Washington.
- Naval Weather Service Division (1957): *The U. S. Navy Marine Climatic Atlas of the World, 3*, Indian Ocean, Washington.
- Naval Weather Service Division (1965): *The U. S. Navy Marine Climatic Atlas of the World 7*, Antarctic Ocean, Washington.
- NEIBURGER, M. (1948): A note on the reflection of diffuse radiation by the sea surface. *Am. Geophys. Union, Trans.*, **29**, 647-652.
- NEUMANN, G. and R. HOLLMAN (1961): On the albedo of the sea surface. *Union Géod. Géophys. Intern., Monographie*, **10**, 72-83.
- NEUYMIN, H. G. (1970): Inhomogeneities of optical properties in deep-ocean waters. *J. Opt. Soc. Am.*, **60**, 690-693.
- PLATT, T. (1969): The concept of energy efficiency in primary production. *Limnol. Oceanog.*, **14**, 653-659.
- POOLE, H. H. and W. R. G. ATKINS (1929): Photoelectric measurements of submarine illumination through out year. *J. Mar. Biol. Ass. U. K.*, **16**, 297-324.
- POWELL, W. M. and G. L. CLARKE (1936): The reflection and absorption of daylight at the surface of the ocean. *J. Opt. Soc. Am.*, **26**, 111-120.
- PREISENDORFER, R. W. (1957): Exact reflectance under a cardioidal luminance distribution. *Quart. J. Roy. Meteorol. Soc.*, **83**, 540.
- PREISENDORFER, R. W. (1961): Application of radia-

- tive transfer theory to light measurements in the sea. Union Géod. Géophys. Inst., Monographie, **10**, 11-30.
- RYTHER, J.H. (1956): Photosynthesis in the ocean as a function of light intensity. *Limnol. Oceanog.*, **1**, 61-70.
- SAKAMOTO, I. and K. MATSUIKE (1965): A simplified method for estimating the sun's altitude from its meridian altitude at optional time. Report of Faculty of Fisheries, prefectural Univ. of Mie, **5**(2), 267-294.
- SAKAMOTO, I. and K. MATSUIKE (1966): A preliminary report on the primary productivity in the East Indian Ocean in winter. IIOE Report on productivity, 1963-1964, Umitaka-maru. Methods of experiments, Data and Outlines. *J. Tokyo Univ. Fisheries*, **8**(2), (Special edition) 173-226.
- SASAKI, T., N. OKAMI, G. OSHIBA and S. WATANABE (1958): Spectral energy distribution of submarine daylight off Kii peninsula. *Rec. Oceanog. Works Japan*, Spec. No. 2, 120-127.
- SASAKI, T., S. WATANABE, G. OSHIBA and N. OKAMI (1958): Measurements of angular distribution of submarine daylight by means of a new instrument. *J. Oceanog. Soc. Japan*, **14**(2), 47-52.
- SASAKI, T., N. OKAMI, M. KISHINO and G. OSHIBA (1968): Optical properties of the water in adjacent regions of the Kuroshio. *J. Oceanog. Soc. Japan*, **25**(2), 45-50.
- SHELFORD, V.E. and F.W. GAIL (1922): A Study of light-penetration into seawater made with the kunz photoelectric cell with particular reference to the distribution of plants. *Publ. Puget Sound. Biol. Stat.*, **3**, 141-176.
- Soviet Antarctic Expedition (1966): Atlas Antrktiki. *Izd. Post. Prezi., Akad. Nauk S. S. S. R.*
- STERN, M.E. (1970): Optical measurement of salt fingers. *Tellus*, **22**, 76-81.
- TABATA, S. (1964): Insolation in relation to cloud amount and sun's altitude. *Studies on Oceanography*. 202-210.
- TAKENOUTI, Y. (1940): Angular distribution of submarine solar radiations and the effect of altitude of the sun upon the vertical extinction coefficient. *Bull. Japan. Soc. Sci. Fisheries*, **8**, 213-219.
- TYLER, J.E. (1958): Comparison of light distribution above and below water. *J. Marine Res.*, **16**, 96-99.
- TYLER, J.E. (1960b): Radiance distribution as a function of depth in an underwater environment. *Bull. Scripps Inst. Oceanog. Univ. Calif.*, **7**, 363-412.
- TYLER, J.E. (1961b): Sun-altitude effect on the distribution of underwater light. *Limnol. Oceanog.*, **6**, 24-25.
- UKRAINTSEV, V.N. (1939): Approximate calculation of direct and diffuse radiation amounts. *Meteorol. i gidrol.*, **6**.
- WESTLAKE, D.F. (1965): Some problems in the measurement of radiation underwater: a review. *Photochem. Photobiol.*, **4**, 849-868.
- YAMAMOTO, G. (1956): Study of atmospheric radiation. *Lectureship of meteorology*. No. 4, Chizishokan Tokyo. 39 p. (In Japanese)

大洋における光学的性質に関する研究

松 生 治

要旨: 北太平洋, 東部インド洋および南極洋において行なった光学的観測に基づいて, 1. 各海域の海中の光学的構造ならびに特性, 2. 海洋上の可能日射量および海面到達日射量, 3. 海中太陽エネルギーフラックスの分布の研究を行なった。各海域では Blue, Green, および Amber のフィルターと表面コレクターを用いた水中照度計によって表層から 140 m 深までの upward および downward irradiance の測定を行なった。一方, 全航海期間にわたって Eppley 日射計による海面到達日射量の連続観測と WMO 規約に基づいて毎時の雲量, 雲形および太陽正面の雲の測定を行なった。

各海域での測定値から消散係数, 相対照度および Reflectance を求め, 東部インド洋, 黒潮とその南方海域, および南極洋の波長別光特性, ならびに波長間強度比の特性などを検討した。東部インド洋では, 各海流域と光学的性質に基づいた水塊の分類とがほとんど一致すること, 黒潮およびその南方海域では湧昇流域において, 特に Blue 光の Reflectance の著しい増大現象が存在する

こと、潮境や湧昇流域などは光学的面からも察知できること、南極洋では亜南極海域、南極海域および南極収束線海域は特に顕著に光学的性質の相違が存在することなどが見出された。さらに、各大洋の一般的性質の差が論じられ、各大洋はフィルター別のろ光特性、Reflectance および波長特性において、それぞれ異なった光学的性質をもっていることが判明した。一方、さきに述べた海面到達日射量の測定結果は、これまでおもに陸上の測定値に基づいて提出されている日射量の算出式による結果とは一致しない。著者は新たに光の大気透過率の太陽高度による変化を考慮して、可能日射量の算出式を導き、これを用いて南北両半球にわたる洋上の可能日射量を算出した。さらに、測定値に基づいて求めた雲量と日射量の減衰比との関係を用いて各海域における海面到達日射量を計算した。可能日射量の値は UKRAINTSEV (1939) の値より各緯度とも約 10% 小さく、BUDYKO (1956) の指摘を考慮すると、より reasonable であると考えられる。また、海面到達日射量は ASHBURN (1963) および Soviet Antarctic Expedition (1966) の結果とよく一致している。最後にこれらの結果を用いて海中太陽エネルギーフラックスについて各月ごとの分布状況と年間総量の分布とを COX and MUNK (1955) による海面反射量ならびに JERLOV (1964) による海水の光学的分類を考慮して計算した。深さ 10 m における海中太陽エネルギーフラックスはインド洋赤道海域で $33.4 \text{ kg}\cdot\text{cal}/\text{cm}^2\cdot\text{year}$ で、黒潮海域ではその 54%、亜南極海域では 44%、南極海域では 13%、南極収束線海域では 6% である。さらに、生産力範囲を $5 \text{ g}\cdot\text{cal}/\text{cm}^2\cdot\text{day}$ と仮定すると年間総計の大洋の生産力範囲の比は海面の単位面積について、インド洋赤道海域、北太平洋黒潮海域、亜南極海域および南極収束線以南の海域で約 100:75:50:20 である。

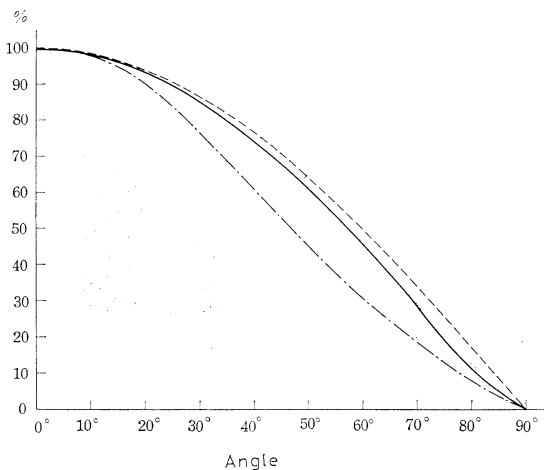


Fig. 1. Angular response of the underwater irradiance meter.

Remarks: Broken line, solid line, and broken-dot line exhibit the cosine value, response in air, and response in water, respectively.

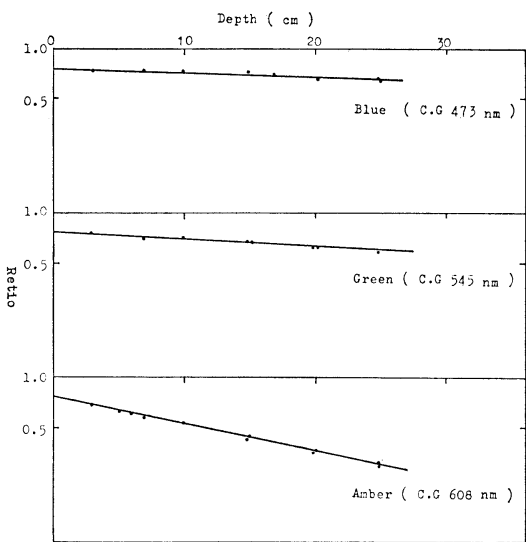


Fig. 2. Immersion effect of the underwater irradiance meter.

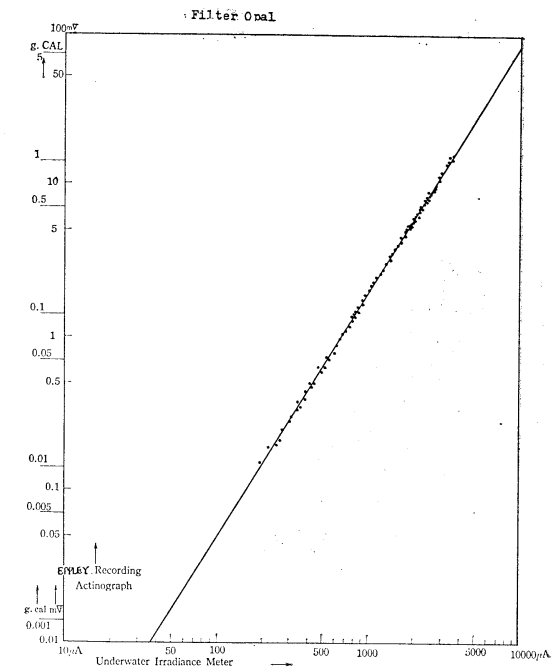
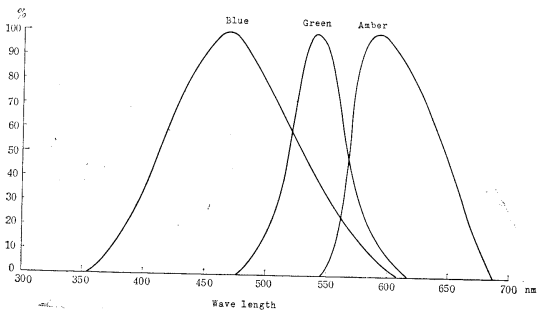


Fig. 4-(1). Calibration characteristics of the underwater irradiance meter.

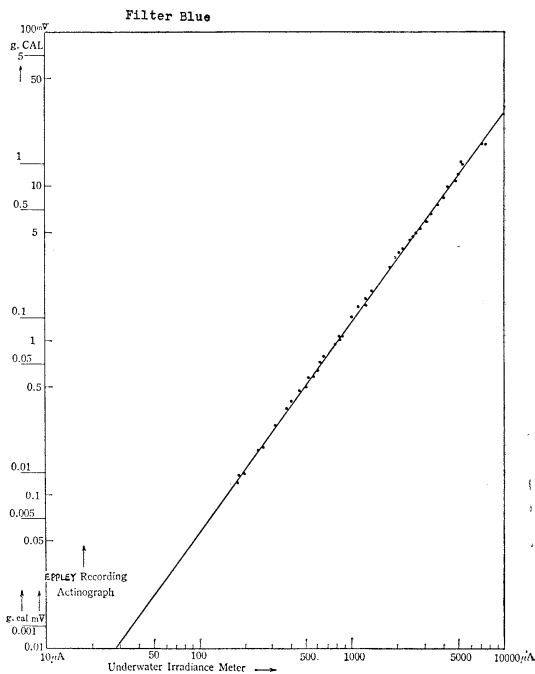


Fig. 4-(2). Calibration characteristics of the underwater irradiance meter.

← Fig. 3. Spectral sensitivity of the photocell with filter.

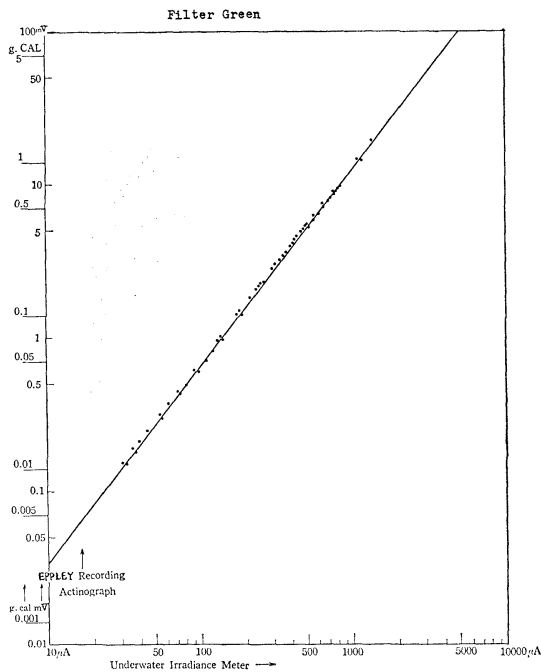


Fig. 4-(3). Calibration characteristics of the underwater irradiance meter.

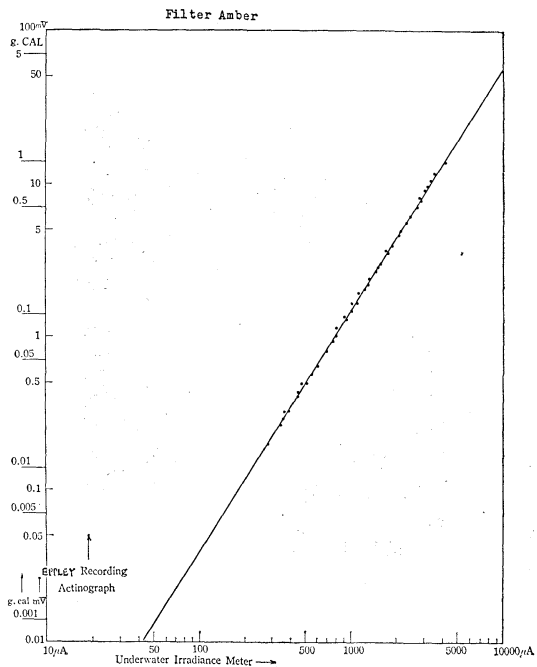


Fig. 4-(4). Calibration characteristics of the underwater irradiance meter.

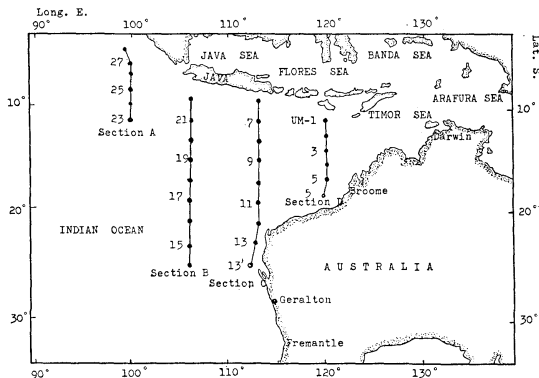


Fig. 5. Observation positions in the East Indian Ocean.

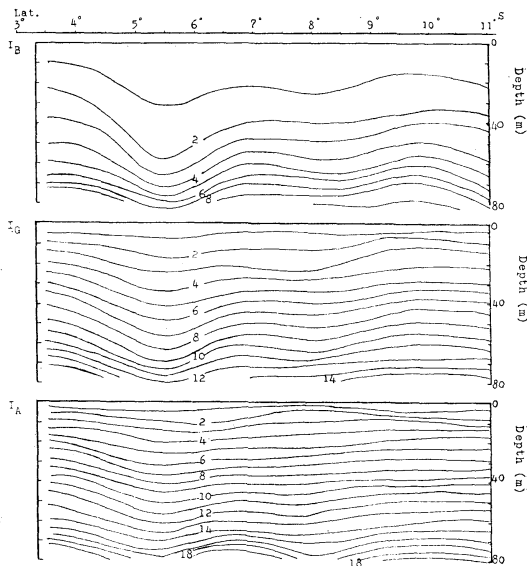


Fig. 6-(1). Vertical profiles of relative irradiance, *I*, in Section A of the East Indian Ocean.

Remarks: 1. Iso-lines show profiles of relative irradiance, *I*, which are vertically sectioned from Lat. 3°S to Lat. 11°S along a meridian of 100°E.

2. Signs B, G and A stand for blue, green and amber lights.

3. Figures on iso-lines denote as follows:

1 70.7 %	6 12.5 %
2 50.0	7 8.84
3 35.4	8 6.25
4 25.0	9 4.42
5 17.7	10 3.13

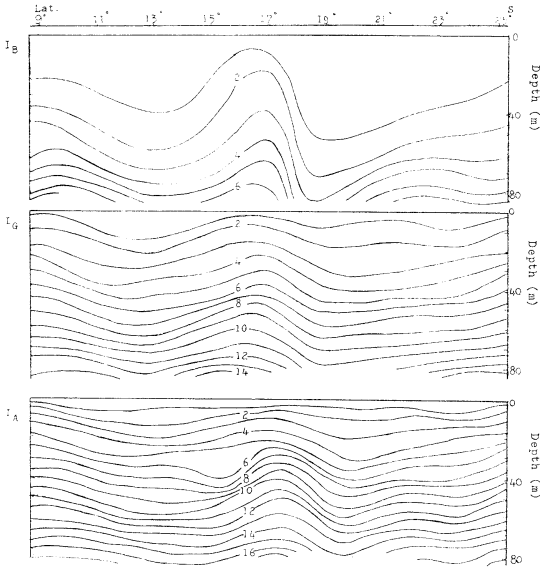


Fig. 6-(2). Vertical profiles of relative irradiance, *I*, in Section B of the East Indian Ocean.

- Remarks: 1. Iso-lines show profiles of relative irradiance, *I*, which are vertically sectioned from Lat. 9°S to Lat. 25°S along a meridian of 106°E.
2. Signs *B*, *G* and *A* stand for blue, green and amber lights.
3. Figures on iso-lines denote as follows:
- | | | | |
|---|--------|----|--------|
| 1 | 70.7 % | 6 | 12.5 % |
| 2 | 50.0 | 7 | 8.84 |
| 3 | 35.4 | 8 | 6.25 |
| 4 | 25.0 | 9 | 4.42 |
| 5 | 17.7 | 10 | 3.13 |

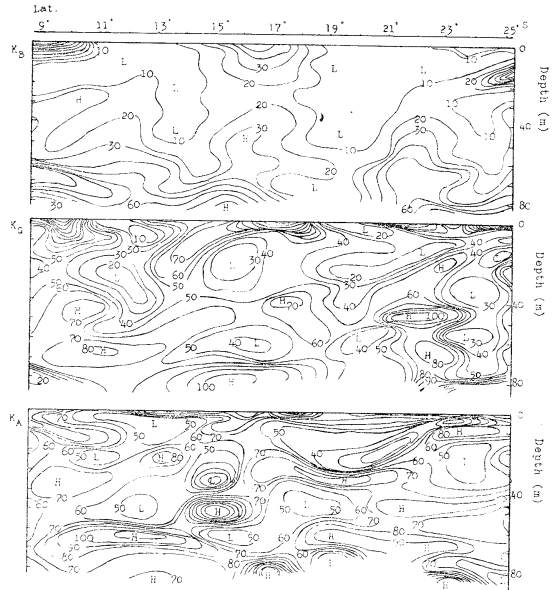
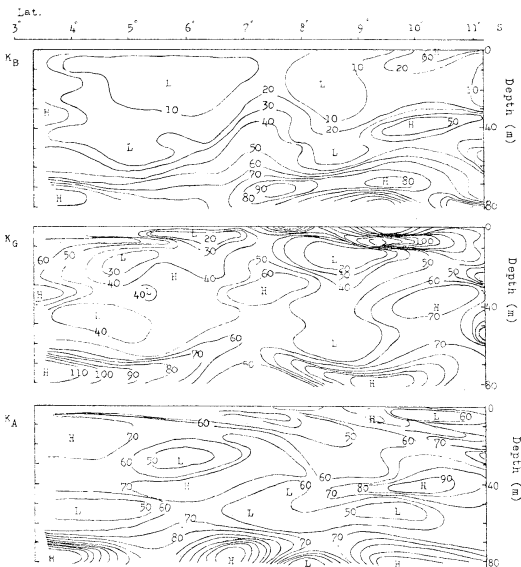


Fig. 7-(2). Vertical profiles of attenuation coefficient, *K*, in Section B of the East Indian Ocean.

- Remarks: 1. Iso-lines show profiles of attenuation coefficients, *K*, which are vertically sectioned from Lat. 9°S to Lat. 25°S along a meridian of 106°E.
2. Signs *B*, *G* and *A* stand for blue, green and amber lights.
3. Figures on iso-lines denote values of $K \times 10^3$.



← Fig. 7-(1). Vertical profiles of attenuation coefficients, *K*, in Section A of the East Indian Ocean.

- Remarks: 1. Iso-lines show profiles of attenuation coefficients, *K*, which are vertically sectioned from Lat. 3°S to Lat. 11°S along a meridian of 100°E.
2. Signs *B*, *G* and *A* stand for blue, green and amber lights.
3. Figures on iso-lines denote values of $K \times 10^3$.

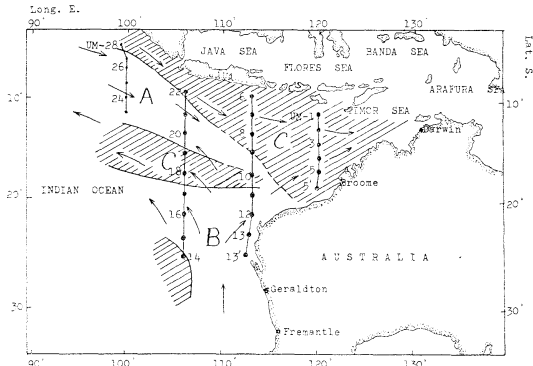


Fig. 8. Geographical distribution of three water-masses in view of spectral light transmittance in the surface layer of the East Indian Ocean. Remarks: 1. Signs A, B and C denote Water-mass A, Water-mass B and Water-mass C. 2. Arrow signs denote the direction of current.

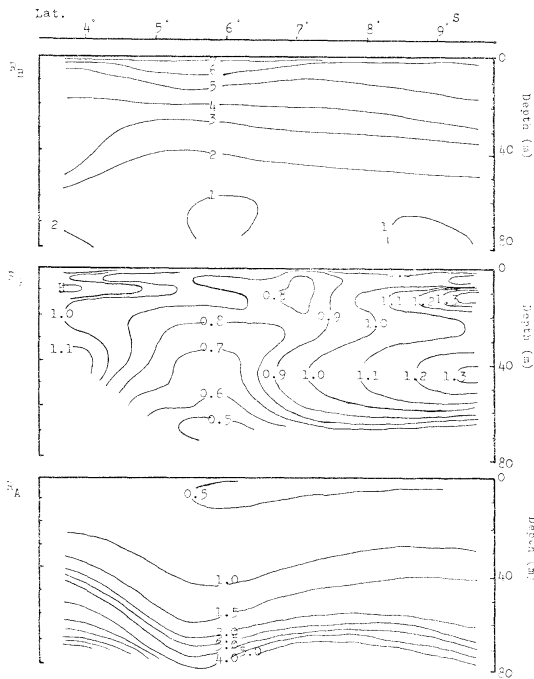


Fig. 9. Vertical profiles of reflectance, R , in Section A of the East Indian Ocean. Remarks: 1. Iso-lines show profiles of reflectance, R , which are vertically sectioned from Lat. 3°S to Lat. 11°S along a meridian of 100°E. 2. B , G and A stand for blue, green and amber lights. 3. Figures on iso-lines show values in %.

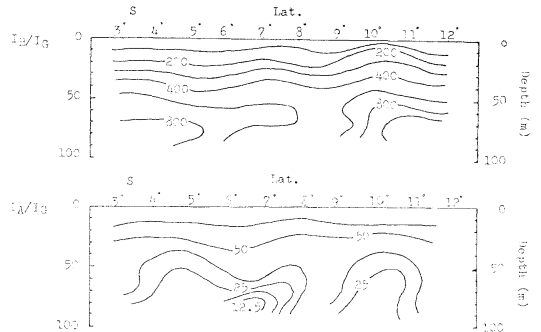


Fig. 10-(1). Vertical profiles of I_B/I_G and I_A/I_G in Section A of the East Indian Ocean. Remarks: Iso-lines show profiles of I_B/I_G and I_A/I_G which are vertically sectioned from Lat. 3°S to Lat. 11°S along a meridian of 100°E.

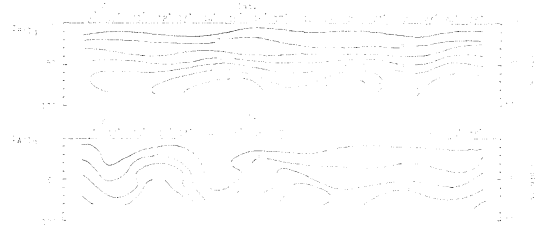


Fig. 10 (2). Vertical profiles of I_B/I_G and I_A/I_G in Section B of the East Indian Ocean. Remarks: Iso-lines show profiles of I_B/I_G and I_A/I_G which are vertically sectioned from Lat. 9°S to Lat. 25°S along a meridian of 106°E.

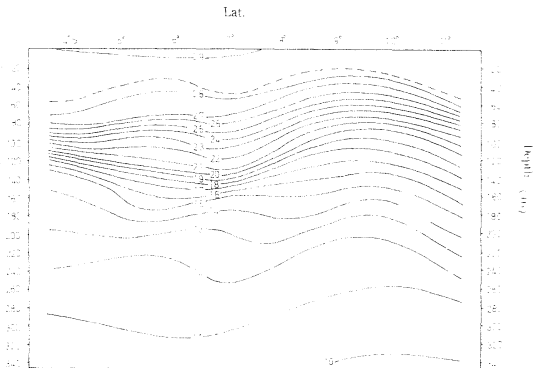


Fig. 11. Vertical profile of water temperature in Section A of the East Indian Ocean. Remarks: Iso-lines show a vertical distribution profile of water temperature (°C) sectioned across from Lat. 3°S to Lat. 11°S along a meridian of 100°E.

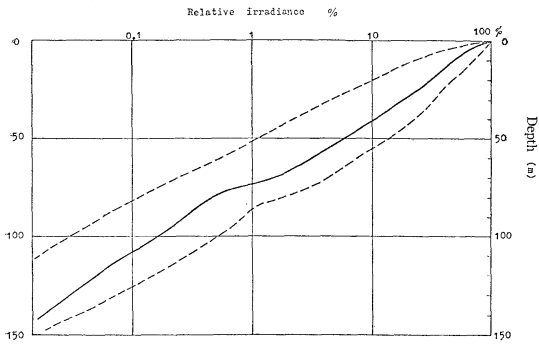


Fig. 12. The mean value of I_G with depth in the East Indian Ocean.
Remarks: Solid line exhibits mean value and both broken lines denote maximum and minimum values.

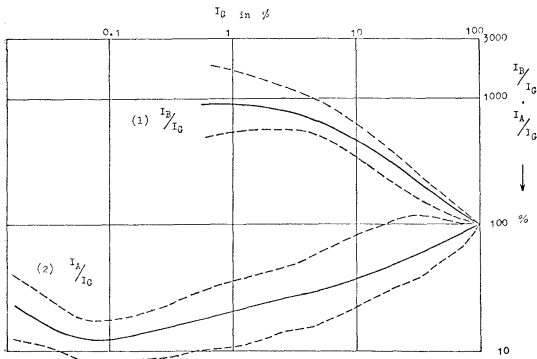


Fig. 13. The relation between I_G and I_B/I_G , and the relation between I_G and I_A/I_G in the East Indian Ocean.
Remarks: Solid lines exhibit mean values and both broken lines denote maximum and minimum values.

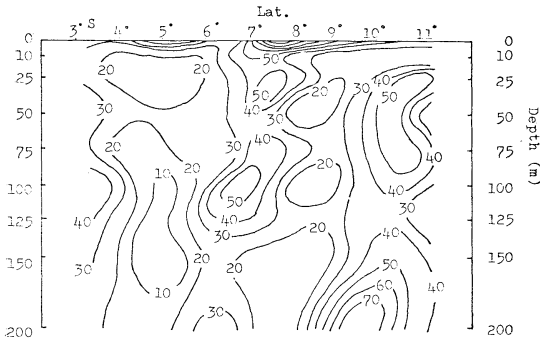


Fig. 14-(1). Vertical profile of seston quantity in Section A of the East Indian Ocean.
Remarks: 1. Diagram shows a vertical distribution profile of seston quantity sectioned across from Lat. 3°S to Lat. 11°S along a meridian of 100°E.
2. Figures in diagram denote values in mg/L.

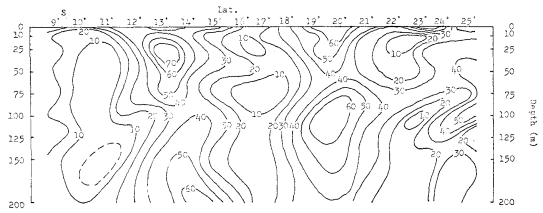


Fig. 14-(2). Vertical profile of seston quantity in Section B of the East Indian Ocean.
Remarks: 1. Diagram shows a vertical distribution profile of seston quantity sectioned across from Lat. 9°S to Lat. 25°S along a meridian of 106°E.
2. Figures in diagram denote values in mg/L.

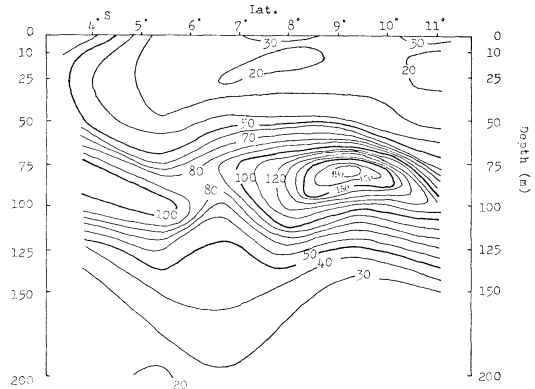


Fig. 15-(1). Vertical profiles of chlorophyll-a in Section A of the East Indian Ocean.
Remarks: 1. Diagram shows a vertical distribution profile of chlorophyll-a sectioned across from Lat. 3°S to Lat. 11°S along a meridian of 100°E.
2. Figures in diagram denote values in $\mu\text{g}/\text{m}^3$.



Fig. 15-(2). Vertical profile of chlorophyll-a in Section B of the East Indian Ocean.
Remarks: 1. Diagram shows a vertical distribution profile of chlorophyll-a sectioned across from Lat. 9°S to Lat. 25°S along a meridian of 106°E.
2. Figures in diagram denote in $\mu\text{g}/\text{m}^3$.

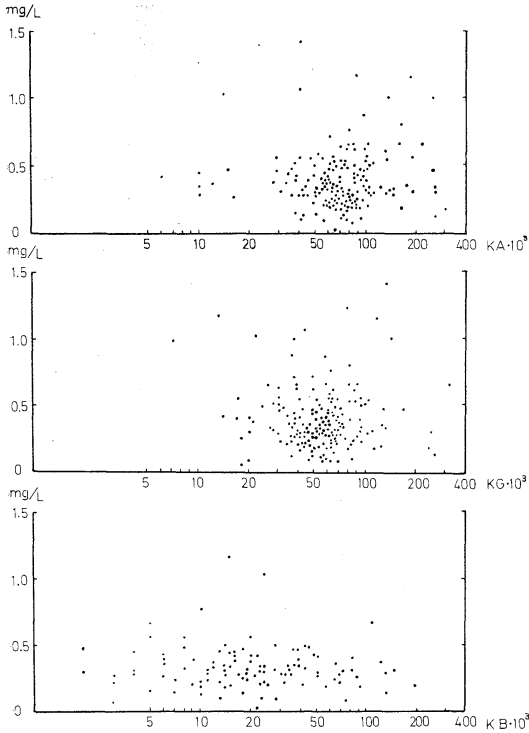


Fig. 16. Relation between attenuation coefficient, K , and seston quantity.
Remarks: B , G and A stand for blue, green and amber lights.

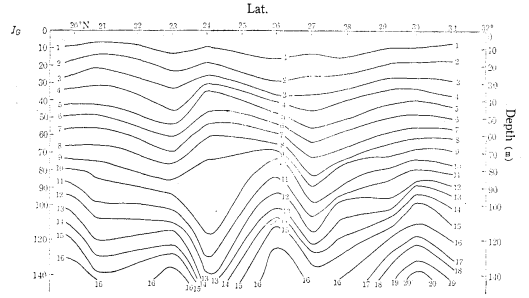


Fig. 17-(2). Vertical profile of relative irradiance, I , in the Kuroshio and its southern area.

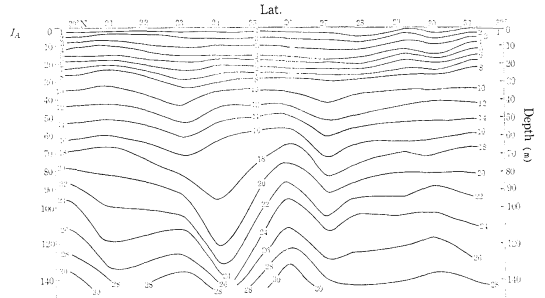


Fig. 17-(3). Vertical profile of relative irradiance, I , in the Kuroshio and its southern area.

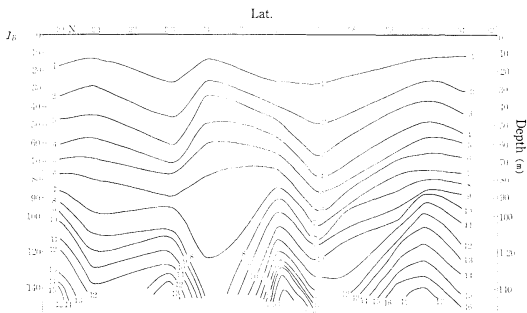


Fig. 17-(1). Vertical profile of relative irradiance, I , in the Kuroshio and its southern area.

Remarks: 1. Iso-lines show a profile of relative irradiance, I , which is vertically sectioned from Lat. 20°N to Lat. 31°N along a meridian of 142°E .

2. Signs B , G and A stand for blue, green and amber lights.

3. Figures on iso-lines denote as follows:

1	562%	5	56%	9	5.6%	13	0.56%
2	316	6	32	10	3.2	14	0.32
3	178	7	18	11	1.8	15	0.18
4	100	8	10	12	1.0	16	0.10

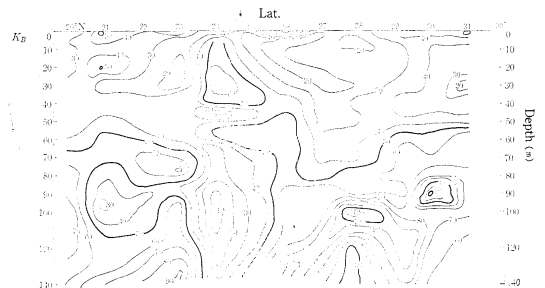


Fig. 18-(1). Vertical profile of attenuation coefficient, K , in the Kuroshio and its southern area.

Remarks: 1. Iso-lines show a profile of attenuation coefficient, K , which is vertically sectioned from Lat. 20°N to Lat. 31°N along a meridian of 142°E .

2. Signs B , G and A stand for blue, green and amber lights.

3. Figures on iso-lines denote values of $K \times 10^3$.

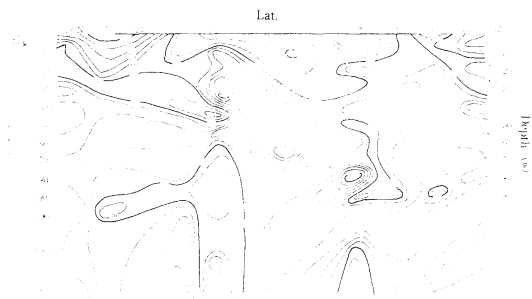


Fig. 18-(2). Vertical profile of attenuation coefficient, K , in the Kuroshio and its southern area.

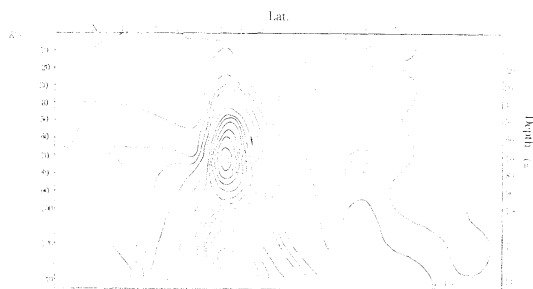


Fig. 19-(2). Vertical profile of reflectance, R , in the Kuroshio and its southern area.

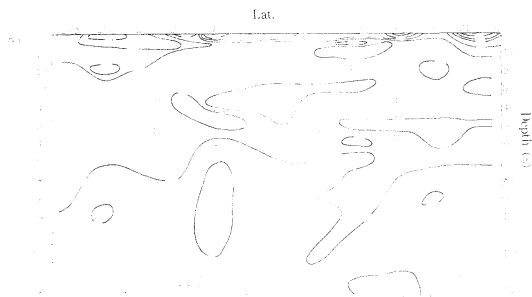


Fig. 18-(3). Vertical profile of attenuation coefficient, K , in the Kuroshio and its southern area.

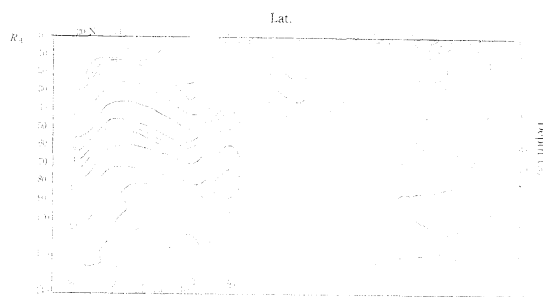


Fig. 19-(3). Vertical profile of reflectance, R , in the Kuroshio and its southern area.

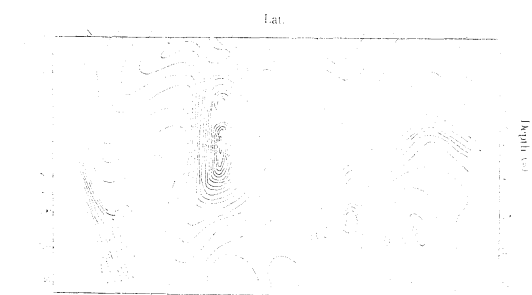


Fig. 19-(1). Vertical profile of reflectance, R , in the Kuroshio and its southern area.

Remarks: 1. Iso-lines show a profile of reflectance, R , which is vertically sectioned from Lat. 20°N to Lat. 31°N along a meridian of 142°E .

2. Signs B , G and A stand for blue, green and amber lights.

3. Figures on iso-lines denote reflectance, R , in value of $\%$.

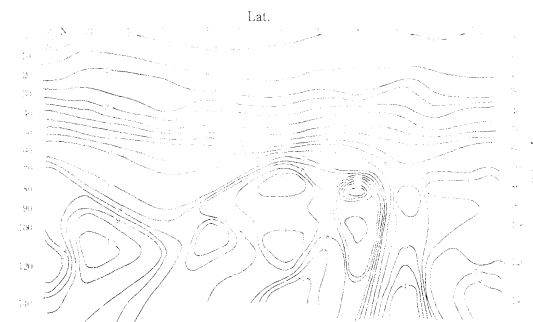


Fig. 20-(1). Vertical profile of I_B/I_G in the Kuroshio and its southern area.

Remarks: Iso-lines show a profile of I_B/I_G which is vertically sectioned from Lat. 20°N to Lat. 31°N along a meridian of 142°E .

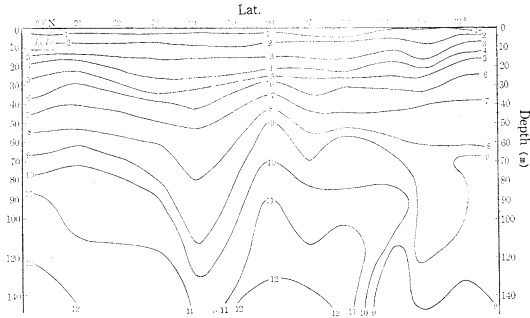


Fig. 20-(2). Vertical profile of I_A/I_G in the Kuroshio and its southern area.

Remarks: 1. Iso-lines show a profile of I_A/I_G which is vertically sectioned from Lat. 20°N to Lat. 31°N along a meridian of 142°E.

2. Figures on iso-lines denote as follows:

1	562 ‰	5	56 ‰	9	5.6 ‰	13	0.56 ‰
2	316	6	32	10	3.2	14	0.32
3	178	7	18	11	1.8	15	0.18
4	100	8	10	12	1.0	16	0.10

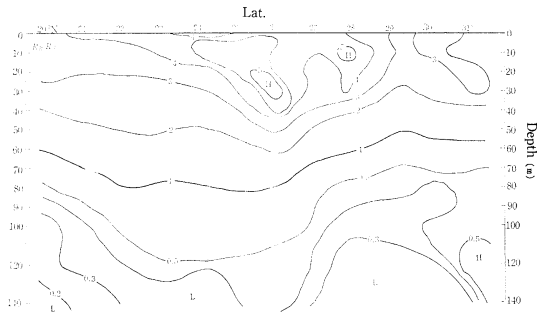
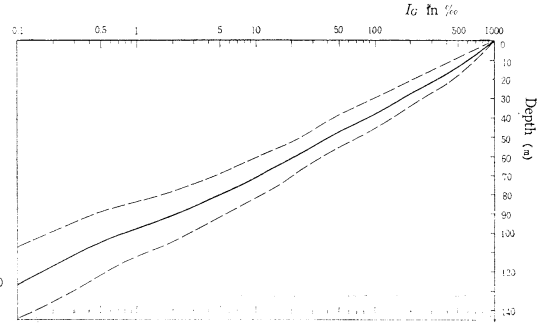
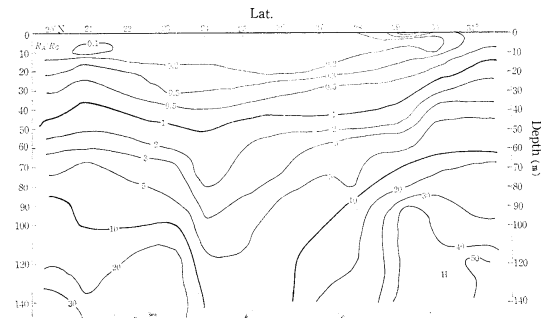
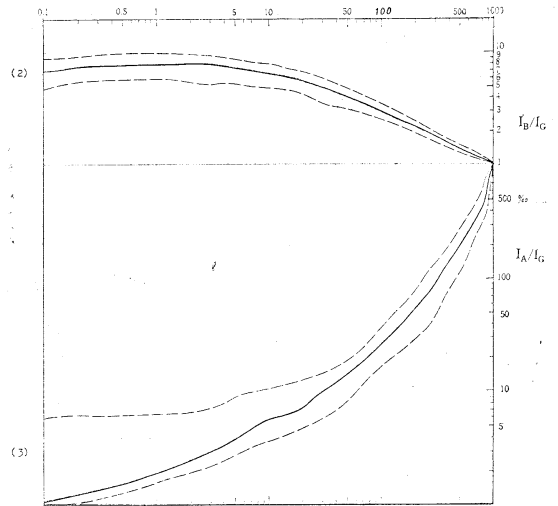


Fig. 21-(1). Vertical profile of R_B/R_G in the Kuroshio and its southern area.

Remarks: Iso-lines show a profile of R_B/R_G which is vertically sectioned from Lat. 20°N to Lat. 31°N along a meridian of 142°E.



(1)



(2)

(3)

Fig. 22-(1). The mean value of I_G with depth in the Kuroshio and its southern area.
22-(2). The relation between I_G and I_B/I_G in the Kuroshio and its southern area.
22-(3). The relation between I_G and I_A/I_G in the Kuroshio and its southern area.

Remarks: Solid line exhibits mean value and both broken lines denote maximum and minimum values.

←Fig. 21-(2). Vertical profile of R_A/R_G in the Kuroshio and its southern area.

Remarks: Iso-lines show a profile of R_A/R_G which is vertically sectioned from Lat. 20°N to Lat. 31°N along a meridian of 142°E.

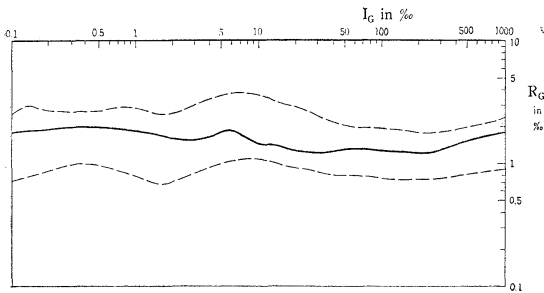


Fig. 23-(1). The relation between I_G and R_G in the Kuroshio and its southern area.

Remarks: Solid line exhibits mean value and both broken lines denote maximum and minimum values.

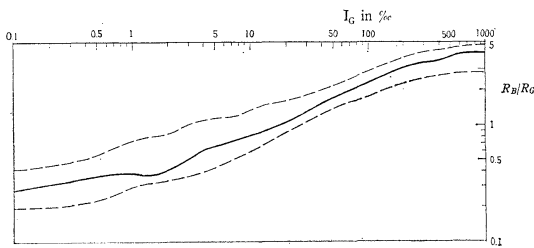


Fig. 23-(2). The relation between I_G and R_B/R_G in the Kuroshio and its southern area.

Remarks: Solid line exhibits mean value and both broken lines denote maximum and minimum values.

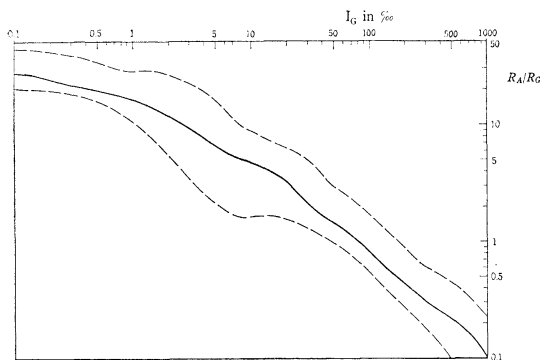


Fig. 23-(3). The relation between I_G and R_A/R_G in the Kuroshio and its southern area.

Remarks: Solid line exhibits mean value and both broken lines denote maximum and minimum values.

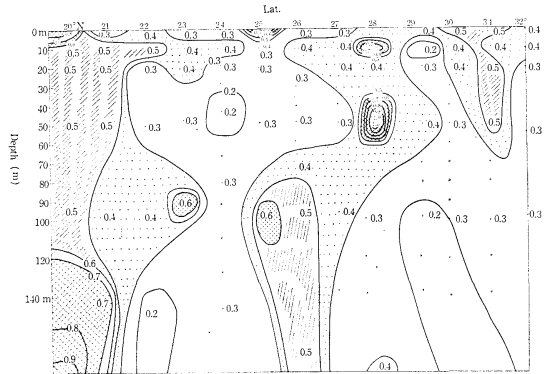


Fig. 24. Vertical profile of seston quantity in the Kuroshio and its southern area.

Remarks: 1. Iso-lines show profile of seston quantity which is vertically sectioned from Lat. 20°N to Lat. 31°N along a meridian of 142°E.

2. Figures in diagram denote values in mg/l.

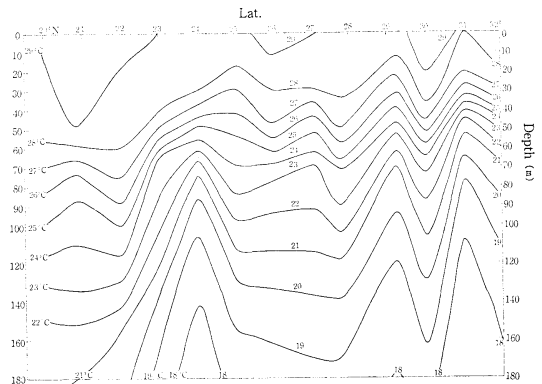


Fig. 25. Vertical profile of water temperature in the Kuroshio and its southern area.

Remarks: Iso-lines show profile of water temperature (°C) which is vertically sectioned from Lat. 20°N to Lat. 31°N along a meridian of 142°E.

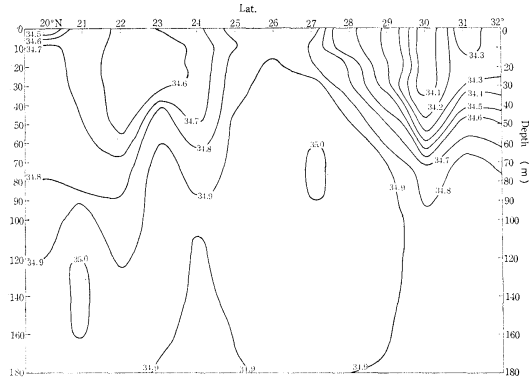


Fig. 26. Vertical profile of salinity in the Kuroshio and its southern area.

- Remarks: 1. Iso-lines show profile of salinity which is vertically sectioned from Lat. 20°N to Lat. 31°N along a meridian of 142°E.
 2. Figures on iso-lines indicate values in ‰.

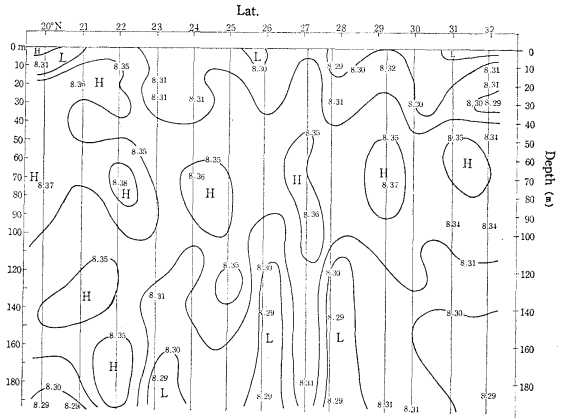


Fig. 28. Vertical profile of pH in the Kuroshio and its southern area.

- Remarks: Iso-lines show profile of pH which are vertically sectioned from Lat. 20°N to Lat. 31°N along a meridian of 142°E.

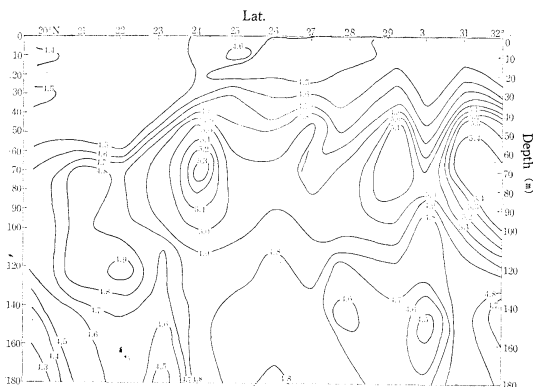


Fig. 27. Vertical profile of oxygen in the Kuroshio and its southern area.

- Remarks: 1. Iso-lines show profile of oxygen which is vertically sectioned from Lat. 20°N to Lat. 31°N along a meridian of 142°E.
 2. Figures on iso-lines indicate values in ml/l.

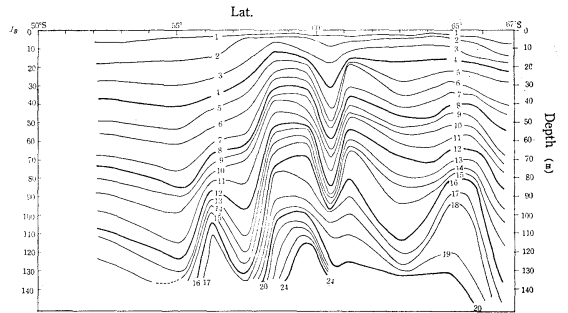


Fig. 29-(1). Vertical profile of relative irradiance, *I*, in the Antarctic Ocean.

- Remarks: 1. Iso-lines show a profile of relative irradiance, *I*, which is vertically sectioned between the positions of Lat. 50°S, Long. 180° and Lat. 67°S, Long. 149°W.
 2. Signs *B*, *G* and *A* stand for blue, green and amber light, respectively.

3. Figures on iso-lines denote as follows:
- | | | | | | | | |
|---|-------|---|------|----|-------|----|--------|
| 1 | 562 ‰ | 5 | 56 ‰ | 9 | 5.6 ‰ | 13 | 0.56 ‰ |
| 2 | 316 | 6 | 32 | 10 | 3.2 | 14 | 0.32 |
| 3 | 178 | 7 | 18 | 11 | 1.8 | 15 | 0.18 |
| 4 | 100 | 8 | 10 | 12 | 1.0 | 16 | 0.10 |

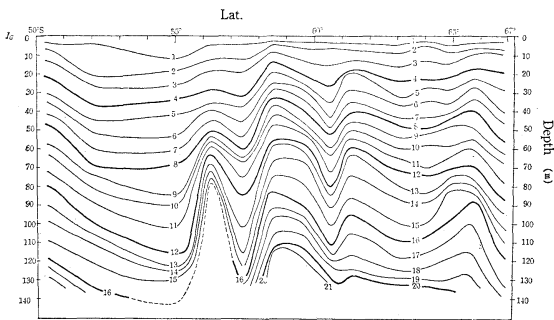


Fig. 29-(2). Vertical profile of relative irradiance, I , in the Antarctic Ocean.

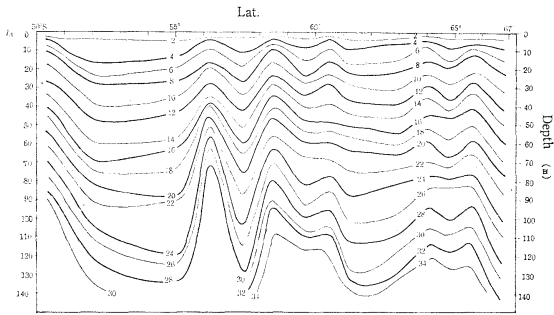


Fig. 29-(3). Vertical profile of relative irradiance, I , in the Antarctic Ocean.

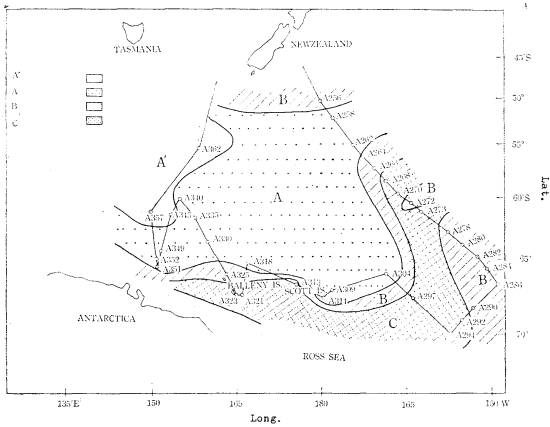


Fig. 30. Geographical distribution of different waters in view of spectral light transmittance of the surface layer in the Antarctic Ocean. Remarks: Signs A, A', B and C denote Water A, Water A', Water B and Water C.

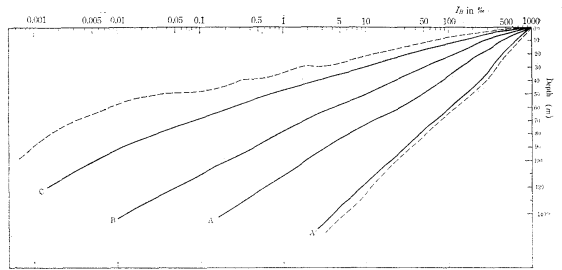


Fig. 31-(1). The mean value of I_B with depth in Water A, Water A', Water B and Water C of the Antarctic Ocean.

Remarks: Water A and A' Water B and Water C correspond to the Sub-Antarctic area, the Antarctic area and the Antarctic Convergence area.

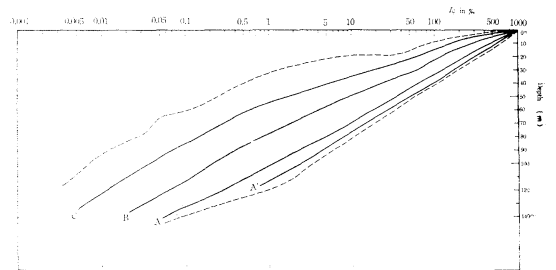


Fig. 31-(2). The mean value of I_G with depth in Water A, Water A', Water B and Water C of the Antarctic Ocean.

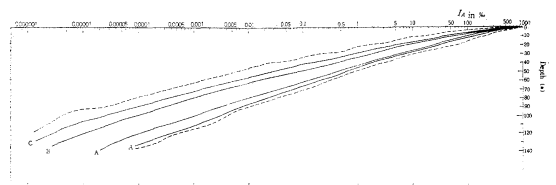


Fig. 31-(3). The mean value of I_A with depth in Water A, Water A', Water B and Water C of the Antarctic Ocean.

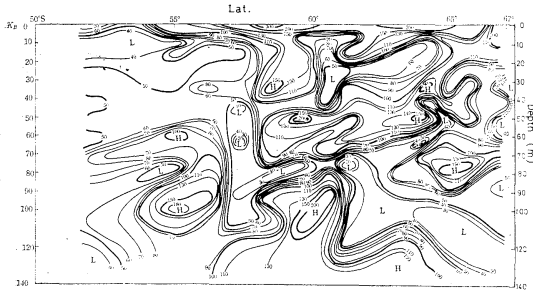


Fig. 32-(1). Vertical profile of attenuation coefficient, K , in the Antarctic Ocean.

- Remarks: 1. Iso-lines show a profile of attenuation coefficient, K , which is vertically sectioned between the positions of Lat. 50°S , Long. 180° and Lat. 67°S , Long. 149°W .
2. Signs B , G and A stand for blue, green and amber light, respectively.
3. Figures on iso-lines indicate values of $K \times 10^3$.

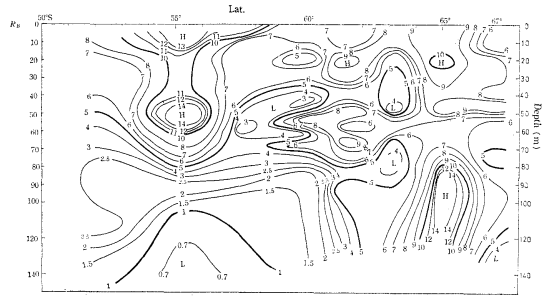


Fig. 33-(1). Vertical profile of reflectance, R , in the Antarctic Ocean.

- Remarks: 1. Iso-lines show a profile of reflectance, R , which is vertically sectioned between the positions of Lat. 50°S , Long. 180° and Lat. 67°S , Long. 149°W .
2. Signs B , G and A stand for blue, green and amber light, respectively.
3. Figures on iso-lines denote reflectance in value of $\%$.

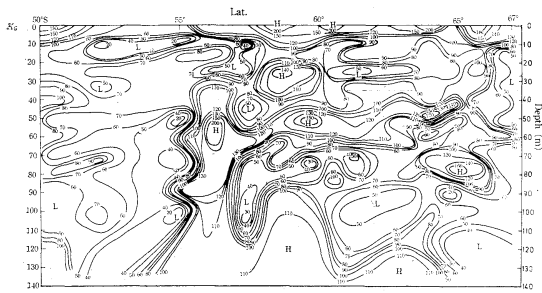


Fig. 32-(2). Vertical profile of attenuation coefficient, K , in the Antarctic Ocean.

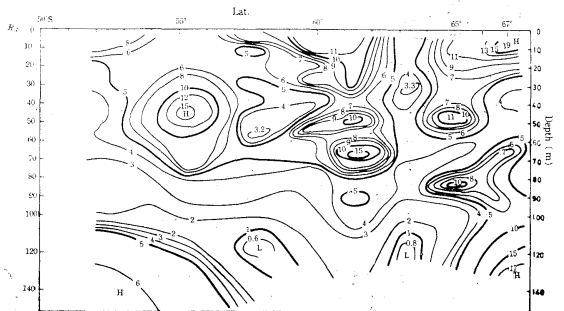


Fig. 33-(2). Vertical profile of reflectance, R , in the Antarctic Ocean.

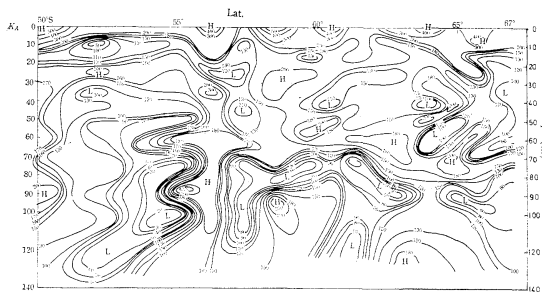


Fig. 32-(3). Vertical profile of attenuation coefficient, K , in the Antarctic Ocean.

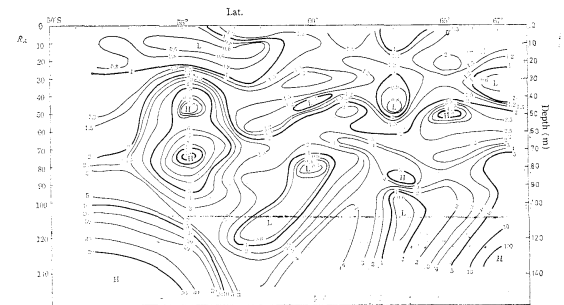


Fig. 33-(3). Vertical profile of reflectance, R , in the Antarctic Ocean.

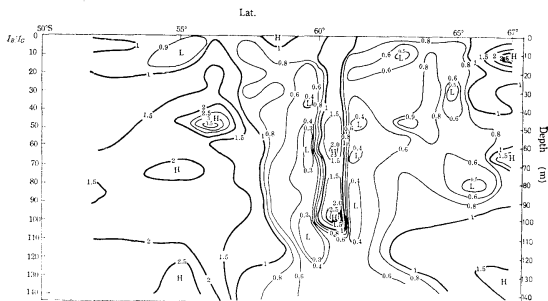


Fig. 34-(1). Vertical profile of I_B/I_G in the Antarctic Ocean.

Remarks: Iso-lines show a profile of I_B/I_G , which is vertically sectioned between the positions of Lat. 50°S , Long. 180° and Lat. 67°S , Long. 149°W .

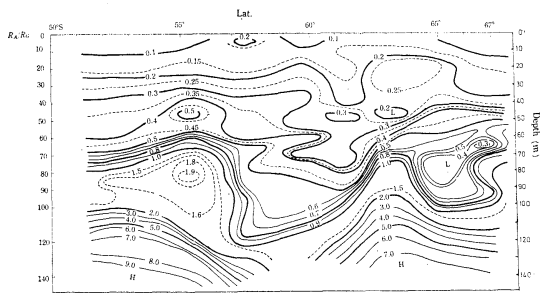


Fig. 35-(2). Vertical profile of R_A/R_G in the Antarctic Ocean.

Remarks: Iso-lines show a profile of R_A/R_G , which is vertically sectioned between the positions of Lat. 50°S , Long. 180° and Lat. 67°S , Long. 149°W .

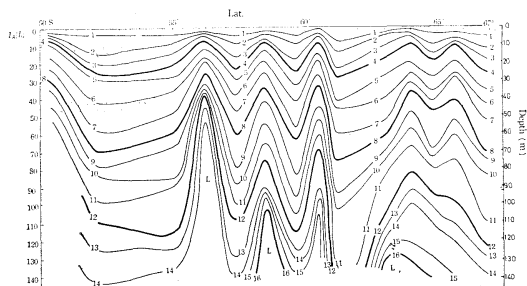


Fig. 34-(2). Vertical profile of I_A/I_G in the Antarctic Ocean.

Remarks: 1. Iso-lines show a profile of I_A/I_G , which is vertically sectioned between the positions of Lat. 50°S , Long. 180° and Lat. 67°S , Long. 149°W .

2. Figures on iso-lines denote as follows:

1	563 ‰	5	56 ‰	9	5.6 ‰	13	0.56 ‰
2	316	6	32	10	3.2	14	0.32
3	178	7	18	11	1.8	15	0.18
4	100	8	10	12	1.0	16	0.10

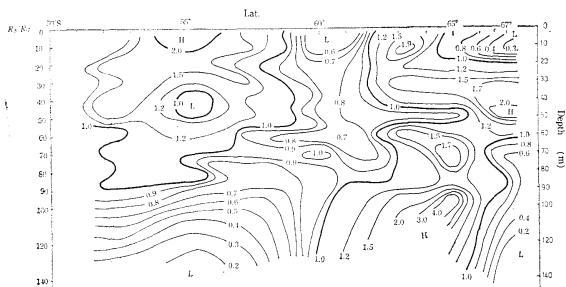


Fig. 35-(1). Vertical profile of R_B/R_G in the Antarctic Ocean.

Remarks: Iso-lines show a profile of R_B/R_G , which is vertically sectioned between the positions of Lat. 50°S , Long. 180° and Lat. 67°S , Long. 149°W .

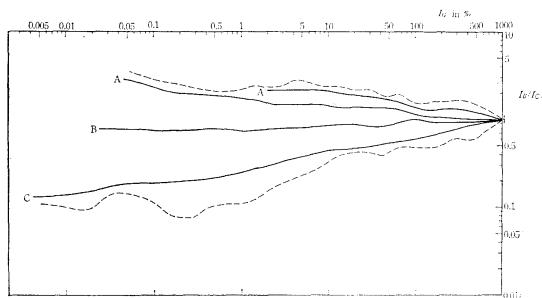


Fig. 36-(1). The relation between I_G and I_B/I_G in the Antarctic Ocean.

Remarks: Signs A, A', B and C denote Water A, Water A', Water B, and Water C.

2. Water A and A', Water B and Water C correspond to the Sub-Antarctic area, the Antarctic area and the Antarctic Convergence area.

3. Solid lines exhibit mean values.

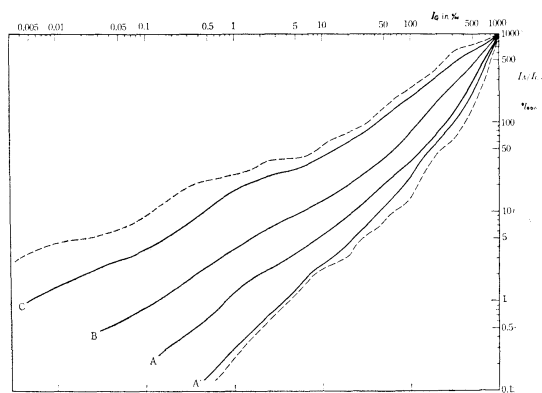


Fig. 36-(2). The relation between I_G and I_A/I_G in the Antarctic Ocean.

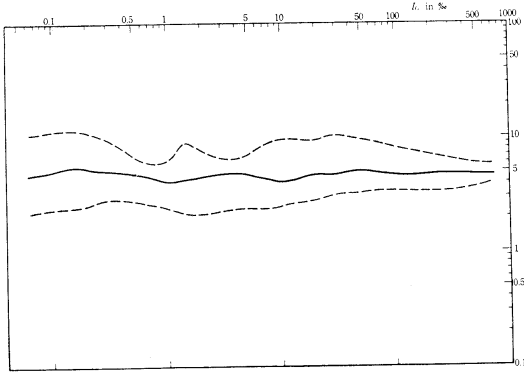


Fig. 37-(1). The relation between I_G and R_G in the Antarctic Ocean.
Remarks: Solid line exhibits mean value.

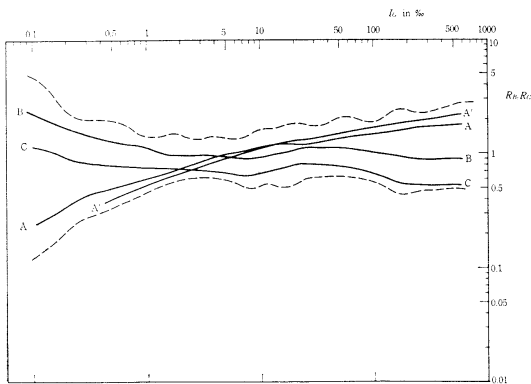


Fig. 37-(2). The relation between I_G and R_B/R_G in the Antarctic Ocean.
Remarks: 1. Signs A, A', B and C denote Water A, Water A', Water B and Water C.
2. Solid lines exhibit mean values.

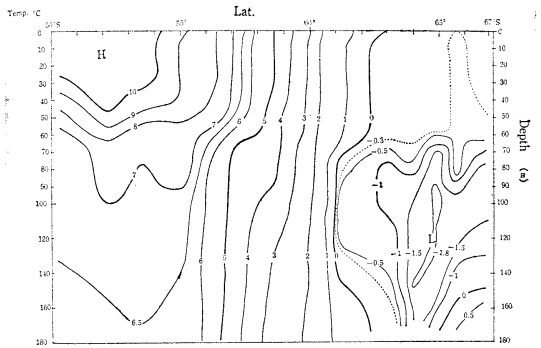
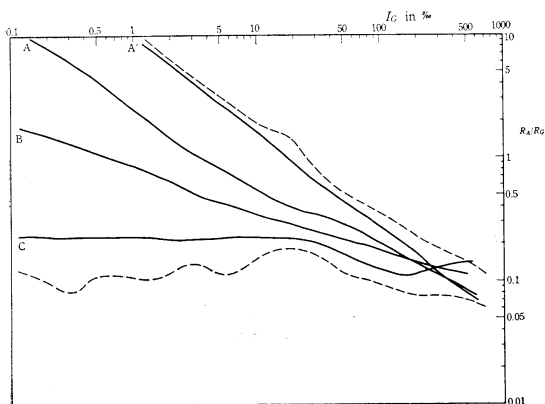


Fig. 38. Vertical profile of water temperature in the Antarctic Ocean.
Remarks: Iso-lines show a vertical distribution profile of water temperature ($^{\circ}\text{C}$) sectioned across between the positions of Lat. 50°S , Long. 180° and Lat. 67°S , Long. 149°W .

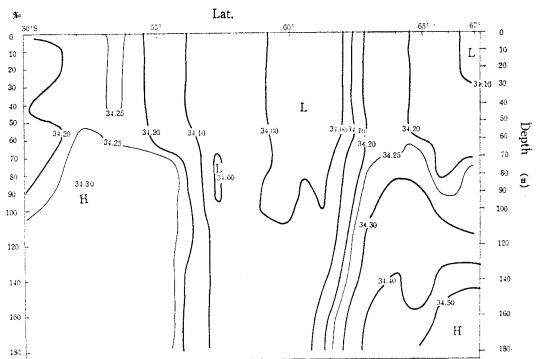


Fig. 39. Vertical profile of salinity in the Antarctic Ocean.
Remarks: 1. Iso-lines show a vertical distribution profile of salinity sectioned across between the positions of Lat. 50°S , Long. 180° and Lat. 67°S , Long. 149°W .
2. Figures on iso-lines indicate values in ‰.

← Fig. 37-(3). The relation between I_G and R_A/R_G in the Antarctic Ocean.
Remarks: 1. Signs A, A', B and C denote Water A, Water A', Water B and Water C.
2. Solid lines exhibit mean values.

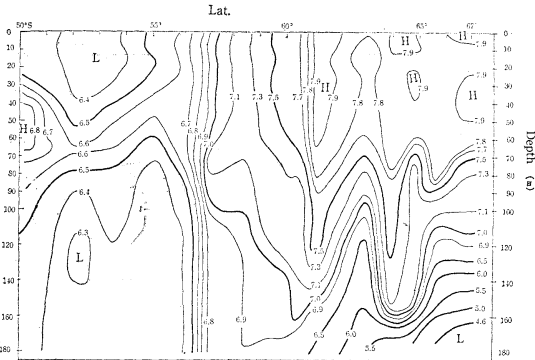


Fig. 40. Vertical profile of oxygen in the Antarctic Ocean.

- Remarks: 1. Iso-lines show a vertical distribution profile of oxygen sectioned across between the positions of Lat. 50°S, Long. 180° and Lat. 67°S, Long. 149°W.
2. Figures on iso-lines indicate values in ml/l.

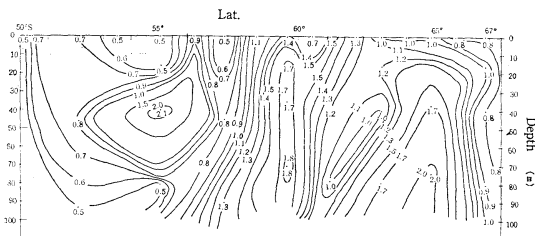


Fig. 41. Vertical profile of seston quantity in the Antarctic Ocean.

- Remarks: 1. Iso-lines show a vertical distribution profile of seston quantity sectioned across between the positions of Lat. 50°S, Long. 180° and Lat. 67°S, Long. 149°W.
2. Figures on iso-lines denote values in mg/l.

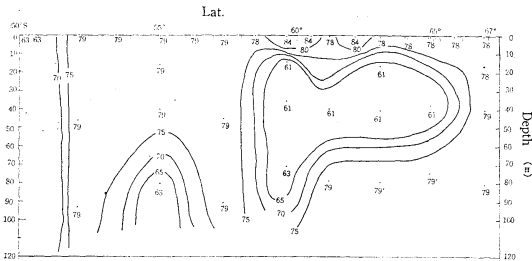


Fig. 42-(1). Vertical profile of wet seston colours in the Antarctic Ocean.

- Remarks: 1. Figures on iso-lines denote following colour Nos. of wet seston.
61 apricot yellow 72 ivory
63 maple 77 malmaison
68 drab 78 mustard
69 maple sugar 79 crach

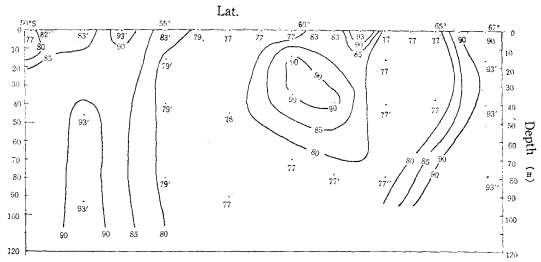
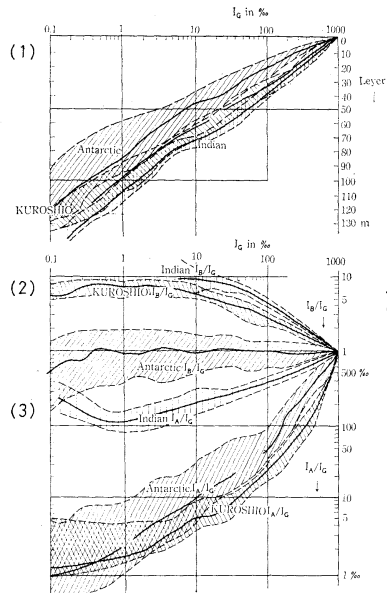


Fig. 42-(2). Vertical profile of dry seston colours.



- Fig. 43-(1). The mean value of I_G in the three oceans.
43-(2). The relation between I_G and I_B/I_G in the three oceans.
43-(3). The relation between I_G and I_A/I_G in the three oceans.

Remarks: 1. Symbols , and denote Antarctic Ocean, Indian Ocean, and Kuroshio and its southern area, respectively.

2. Solid lines exhibit mean values and both broken lines denote maximum and minimum values.

- ← 81 light stone 85 old gold
82 olive drab 89 citrus yellow
83 dust 90 oyster white
84 bronze 93 old moss
2. Symbol (') put on colour Nos. represents the same sort of colours which are slightly lighter.

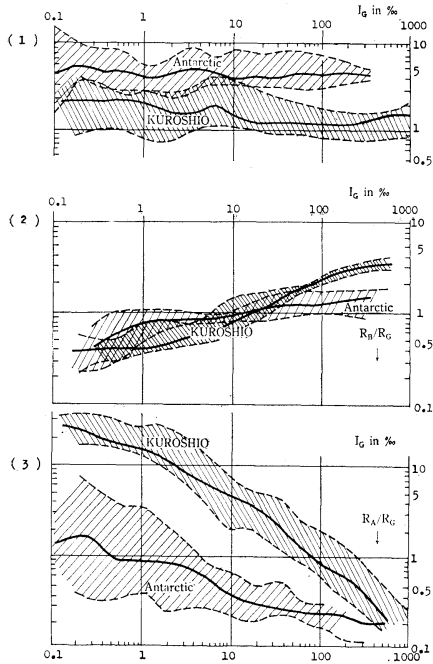


Fig. 44-(1). The relation between I_G and R_B/R_G in the two oceans.
 44-(2). The relation between I_G and R_B/R_G in the two oceans.
 44-(3). The relation between I_G and R_A/R_G in the two oceans.

Remarks: 1. Symbols and denote Antarctic Ocean, and Kuroshio and its southern area, respectively.

2. Solid lines exhibit mean values and both broken lines denote maximum and minimum values.

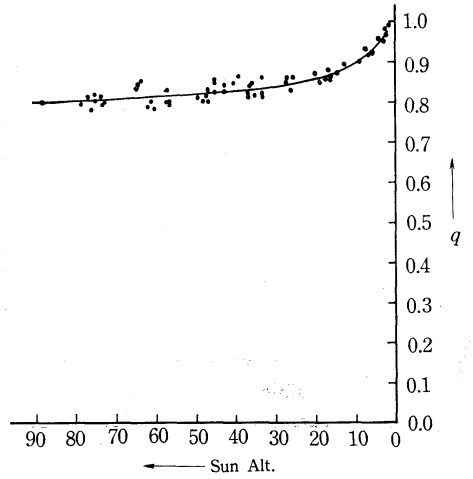


Fig. 46. Relation between light transmittance in air, q , and sun's altitude in clear sky.

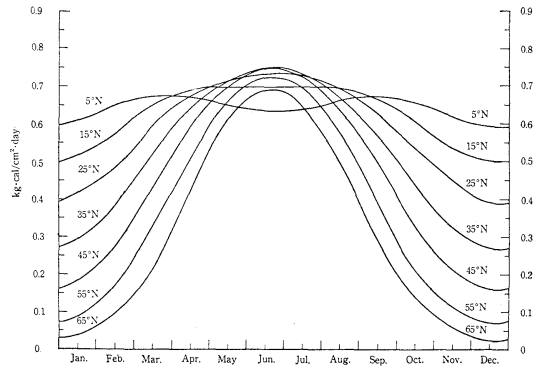


Fig. 47-(1). Possible insolation attained on the sea surface. (the Northern Hemisphere)

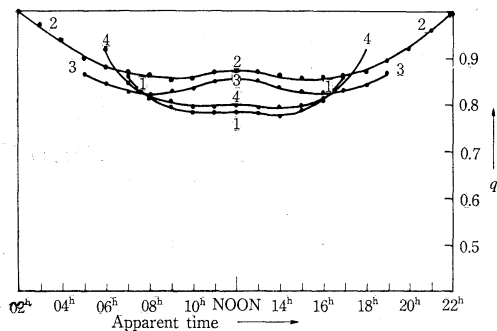


Fig. 45. Daily changes of light transmittance in air, q , in clear sky.

Remarks: Figures on curves denote as follows:

Figure	Region	Month and date	Meridian altitude of the sun
1	North Pacific Ocean	Oct. 31, 1964	60.3°
2	Antarctic Ocean	Dec. 14, 1964	49.6°
3	Antarctic Ocean	Dec. 25, 1964	67.7°
4	South Pacific Ocean	Nov. 13, 1964	88.7°

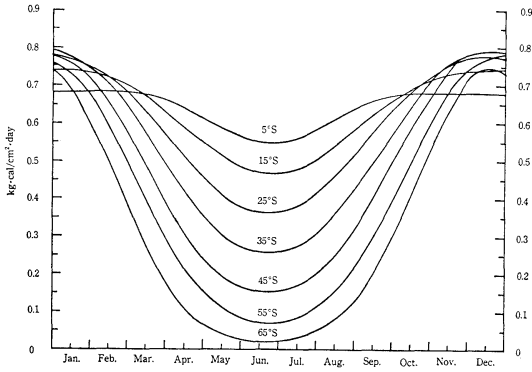


Fig. 47-(2). Possible insolation attained on the sea surface. (the Southern Hemisphere)

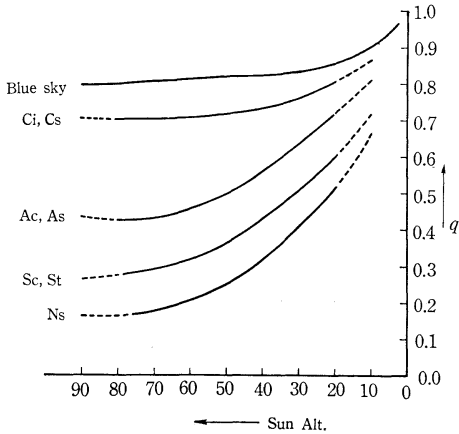


Fig. 48. Relation between light transmittance in air, q , and sun's altitude in each clouds form.

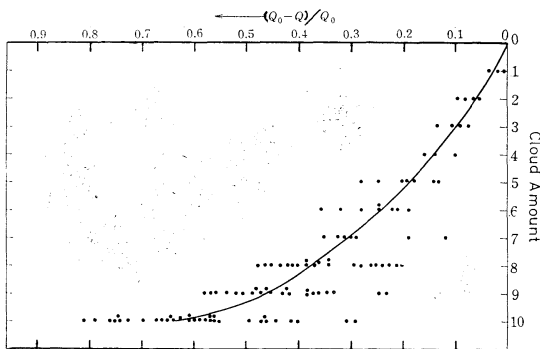


Fig. 49. Relation between the reduction ratio of insolation, $(Q_0 - Q)/Q_0$, and cloud amount.
 Q_0 : Possible insolation
 Q : Actual insolation

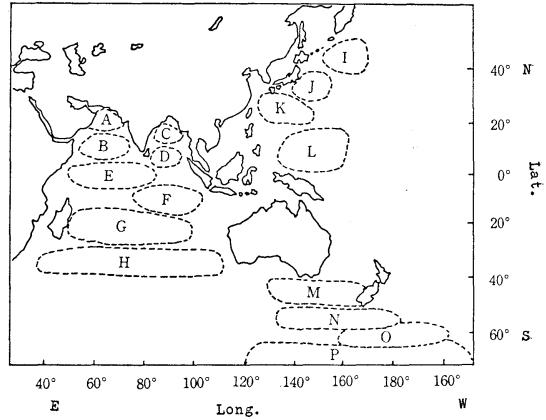


Fig. 50. Index chart of seas areas A to P.

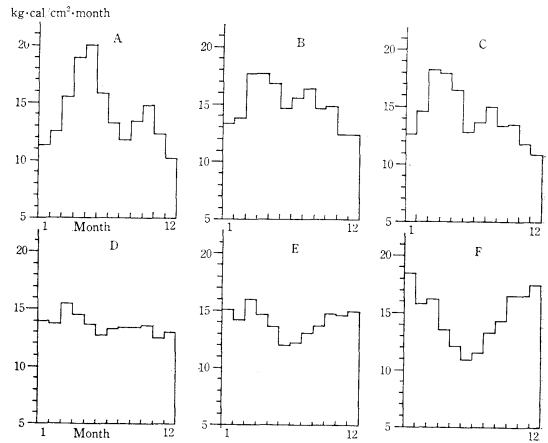


Fig. 51-(A)~(F). Actual insolation attained on the sea surface.
 Remarks: Alphabetical letters from A to F stand for different areas corresponding to index chart shown in Fig. 50.

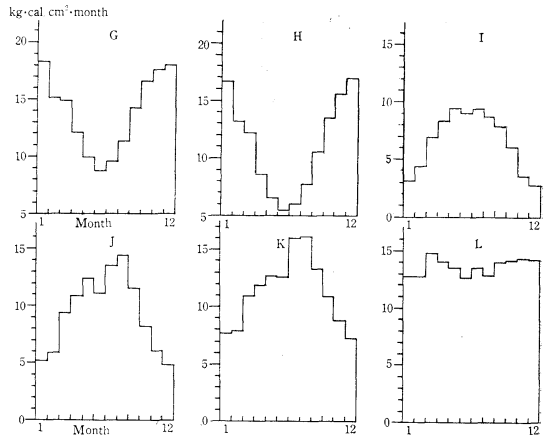


Fig. 51-(G)~(L). Actual insolation attained on the sea surface.
 Remarks: Alphabetical letters from G to L stand for different areas corresponding to index chart shown in Fig. 50.

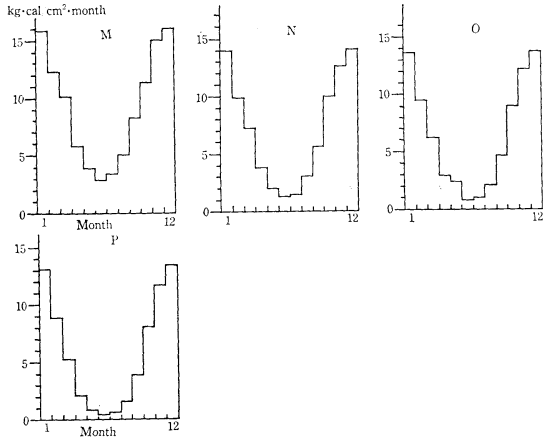


Fig. 51-(M)~(P). Actual insolation attained on the sea surface.

Remarks: Alphabetical letters from M to P stand for different areas corresponding to index chart shown in Fig. 50.

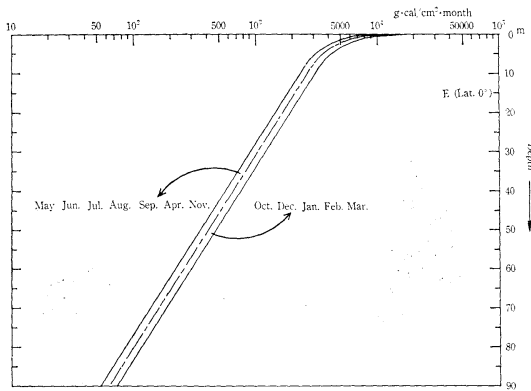


Fig. 52-(1). Distribution of underwater solar energy in E area of the Indian Ocean.

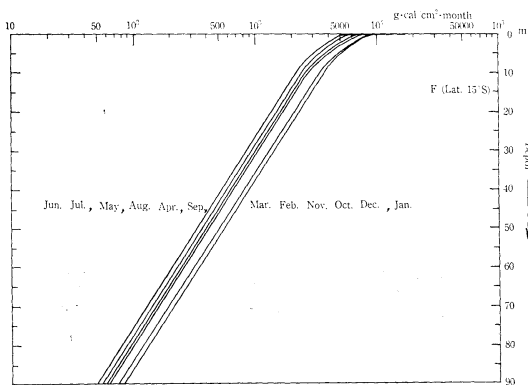


Fig. 52-(2). Distribution of underwater solar energy in F area of the Indian Ocean.

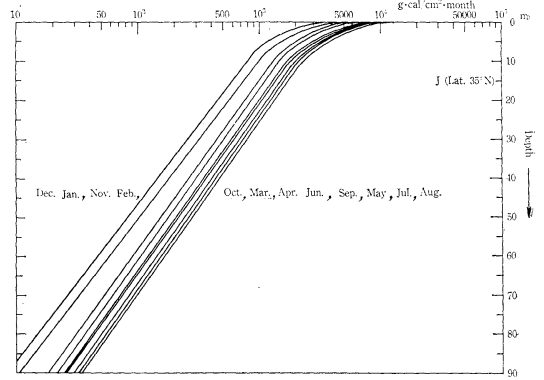


Fig. 52-(3). Distribution of underwater solar energy in J area of the North Pacific Ocean.

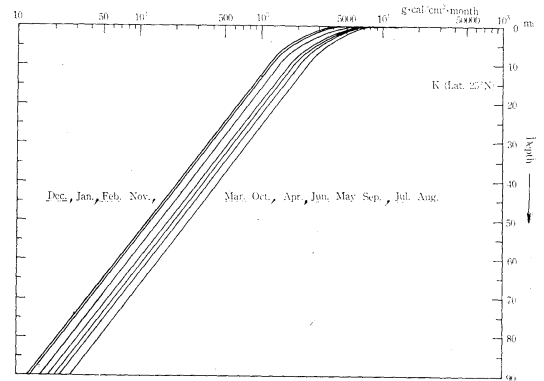


Fig. 52-(4). Distribution of underwater solar energy in K area of the North Pacific Ocean.

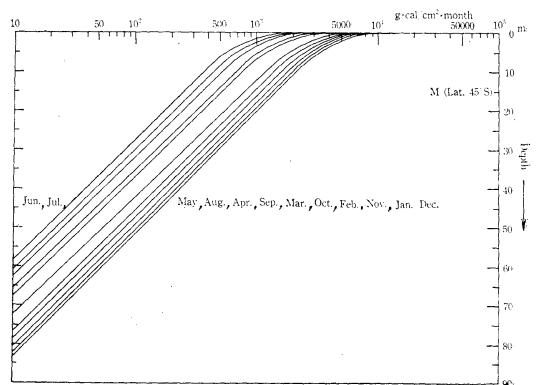


Fig. 52-(5). Distribution of underwater solar energy in M area of the South Pacific Ocean.

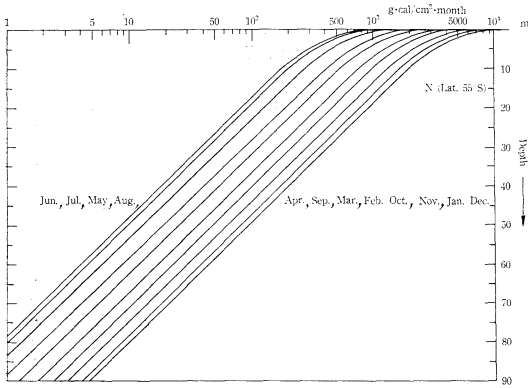


Fig. 52-(6). Distribution of underwater solar energy in N area of the Sub-Antarctic Water.

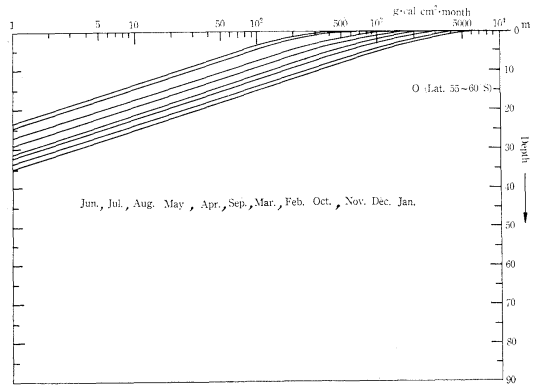


Fig. 52-(8). Distribution of underwater solar energy in O area of the Antarctic Convergence Water.

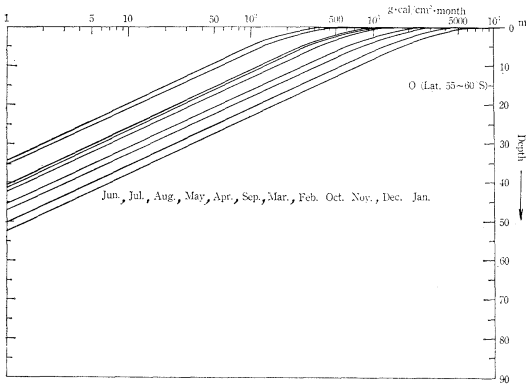


Fig. 52-(7). Distribution of underwater solar energy in O area of the Antarctic Water.

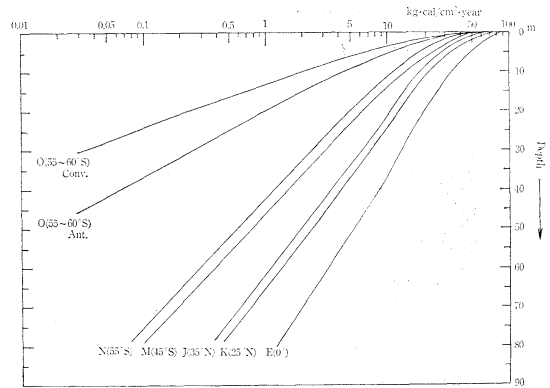


Fig. 53. Annual amount of underwater solar energy.

Remarks: 1. Alphabetical letters of E, K, J, M, N, O (Ant) and O (Conv) stand for different areas corresponding to index chart shown in Fig. 50.

2. Signs of Ant and Conv stand for the Antarctic Water and the Antarctic Convergence Water.

カタクチイワシの灯下におけるむれ形成について*

井上 実** 笹倉 邦夫**

Schooling Mechanism of Anchovy Under a Lamp

Makoto INOUE and Kunio SASAKURA

Abstract: It might be beyond doubt that phototropic fish such as anchovy, sardine, mackerel and saury are also schooling species. Some studies have shown that vision is the most important sensory system for schooling behaviour, and the schools break down at night in low intensity of illumination. Therefore, it is expected that when the dispersed fish are exposed by the artificial light, they will reform into a school again in the illuminated area. However, in a few cases, it is clear that schooling may still occur without light and this is suggested schooling behaviour is depended on other senses in addition to vision.

In the present paper, the schooling mechanism of anchovy, *Engraulis japonica*, under a lamp was studied by experiments on the following problems;

- 1) Whether each individual has gathered under a lamp with the same behaviour in response to light or not?
- 2) Whether the schooling behaviour is reinforced by visual orientation to other individuals when they have entered the illuminated area or not?

Considering the experimental results that each fish shows quite different selective response to light and don't form a group in the partly illuminated area, but form a close group in a current, we obtained the following conclusion. The maintaining school of anchovy under a lamp is due to the positive phototaxis of individuals to the lamp, and at the same time the mutual attraction of individual fish depending on either visual contact in the illuminated area, or swimming movements of fish, engendering water current, or pressure wave which could be detected by fish.

1. 緒言

カタクチイワシを始めとして、マイワシ・アジ・サバ・サンマのように走光性の発達した魚類は、また、むれ作りの性質も発達している。魚のむれ作りの機構のなかで視覚が重要な要素であることは、いくつかの研究¹⁾²⁾によって明らかにされている。したがって、夜間むれが分散しても、人工光線の光野に入れば視覚が働き、むれは再編することが考えられる。

魚が光に反応する明るさの閾値から推定した仲間を認め得る照度の閾値は、 10^{-2} lux あるいはそれ以下であり³⁾、また、BLAXTER and HOLLIDAY⁴⁾

によれば、カタクチイワシがむれを維持する最低の明るさは 10^{-2} lux である。しかし、実験室内の狭い水槽のなかでは、カタクチイワシに対し 10^{-2} lux をはるかに上回る照明を与えても、むれを作らない場合があり、むれ作りの感覚要素は視覚だけではないことを推定せしめる。

一方、WOODHEAD⁵⁾ はニシン目の魚種が光源のもとでむれとして滞留する統一的行動は、その魚のもつ走光性、好適照度選択性、光域内での仲間に対する視覚的指向性によるものと考えている。しかし、個体あるいはむれがその好む絶対照度を有するかどうか明らかでなく、また、かならずしも各個体が同一の好適照度をもっていなくとも、仲間相互の誘引度が強ければ一定の光野に集まることが推察される。

* 1973年1月26日受理

** 東京水産大学 Tokyo University of Fisheries

本研究では灯下に集まるカタクチイワシのむれが、どのような機構によって作られるのか、すなわち、各個体の光に対する反応の同一性によるのか、個体間の相互誘引性によるのか、さらに相互誘引性とすれば視覚以外の他の感覚が働いているかどうかについて調べた。

なお、ここでいう“むれ”とは BREDER⁴⁾, SHAW⁶⁾らの定義するように個体間の間隔、方向性、追従性の点で統一的行動をとるまとまり (school) とは限定せず、相互誘引を基礎とした単なるまとまり (aggregation) として考えるものである。

2. 実験装置

カタクチイワシ (以下、イワシと称する) の灯下におけるむれ形成の機構を調べるため、次の4種の実験を行なった。

- 実験 1) 円形水路のなかで、実験魚の光に対する反応に個体差があるか。
- 実験 2) 円形水路の局部光野のなかで、むれを作るかどうか。
- 実験 3) 円形水路のなかで、むれが分散し始める照度はどのくらいか。
- 実験 4) 直線水路のなかで、観測個体が局部光野の刺激個体に視覚的に誘引されるかどうか。

実験 1)~3)を行なった円形水路は著者が今迄に、ハヤ・イワシなどを用いて種々の実験を行ない、すでにいくつかの論文⁷⁾⁸⁾にその装置の機構を示しているため、ここでは詳細な説明は省くが簡単に示すと次の通りである。

透明なアクリル製のドーナツ型の円形水路 (外周の直径 112 cm, 内周の直径 92 cm, 水路の幅 10 cm, 水路の高さ 15 cm) に海水を 7.5 cm まで入れ、水路をモーターで回転させ 25 cm/sec の流れを作る。実験魚は流れにさかのぼって泳ぐ。また、円形水路の外側を透明なアクリル板でかこいスクリーンとし、白・黒のしま模様をスクリーン上に張り、スクリーンをモーターで回転させると、しま模様は定速で移動するため、魚は視覚運動反応を起し、流れがなくともしま模様を追従して遊

泳する。さらに水路の上に水面上 10 cm の高さに、対称の位置 2ヶ所に乾電池 3 V を電源とした笠つき豆電球 (2 W) を吊す。この電球による光野は Fig. 1 に示されるようで、照度計 (東芝 9 号型) による測定では、上限は 20 lux, 下限 (測定可能下限) は 0.1 lux で、下限は光源下の最も明るいところから直線距離で 10 cm のところにある。この装置を暗室に入れ、さらに完全な暗黒状態に保つため、装置全体をケージに入れ、ケージは暗幕で蔽った。ケージには明順応用の照明 (蛍光灯デライト, 40 W 2本) がついている。

実験 4)を行なった木製水槽 (Fig. 2) は 200×17.5×16.5 cm, 内面は灰色のペンキ塗りで、実験の際は水深を 8 cm とした。本水槽は暗室におかれ、水槽中央、1.5 m の高さに 60 W の白熱灯がある。また、20 cm の間隔で水槽を 10 区画に等分し、その一端に 10 W の電球に笠をつけ、水面上 15 cm から吊した際の水槽内の照度分布は Fig. 2 のよ

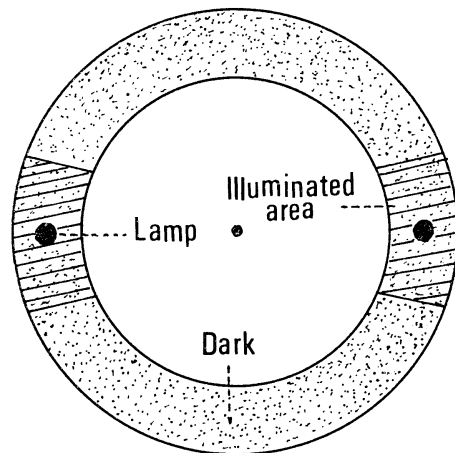


Fig. 1. Illuminated areas by 2 W lamps in an annular trough. A current is streamed in the trough by rounding the trough.

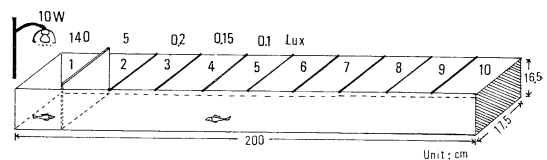


Fig. 2. Wooden trough in which the effect of light or visual stimulative fish to attract fish is observed.

うである。水槽の上縁にマークをつけ、各区画の目印とし、区画1と区画2との間に透明アクリル板を入れ仕切り板とした。区画1には魚を1ないし3尾入れ、視覚刺激による誘引効果を全光野（水槽全体の照明）の場合と、局部光野（区画1だけを照明）の場合について調べた。

3. 実験魚

一連の実験は次の期間と水温で行なわれた。

実験 1) 1968年11月 7~10日。水温16~17°C,

実験魚体長 9.0~10.5 cm。

実験 2) 1972年11月13~18日。水温17~18°C,

体長 7.0~8.5 cm。

実験 3), 4) 1972年12月12~17日。水温15~16°C,

体長 7.5~9.0 cm。

これらの実験に使用したイワシは、東京湾で漁獲した直後いけす網に収容し、館山湾で蓄養したものである。これらの一部を直径 1.0 m の竹籠に移し、本学館山実習場の棧橋沖に浮べておき、その中から約 100 尾ずつ、1~2 日目ごとに同場コンクリート水槽 (3×1×0.8 m) に移す。実験ごとに必要尾数の 4~5 倍の魚を飼育水槽からとり出し、外傷がなく、鱗の剥離が少なく、体色が鮮やかなものを選び実験装置に入れた。

4. 実験方法と結果

実験 1)

本実験ではイワシの光に対する反応の個体差がどの程度であるかを、局部光野内における滞留時間の長短によって調べた。

円形水路に入れた実験魚 1 尾が十分落ちついてから照明を消し、暗順応時間として 5 分とり、続いて水路上の豆球を点灯し局部光野を 2 ケ所に作り、局部光野に留まる時間を測定した。この場合、魚が一つの光野に入った時点から観測を始め、その光野を離れると計時を止め、別の光野に入るか、元の光野に戻ると再び計時を行ない、その集計を滞留時間とした。各実験個体に対する測定時間は 5 分である。同一の実験魚に対して、最初は固定光源下における滞留時間を測定し、次いで光源を 12.0 cm/sec で回転し、移動光源下における滞留時間を測る。両者の測定の間、暗順応で 5 分間

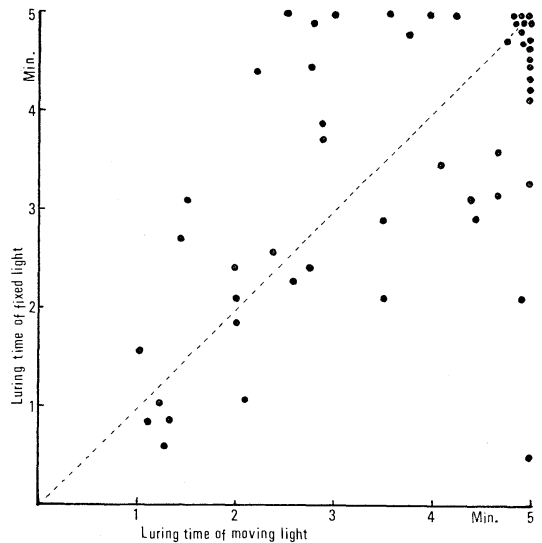


Fig. 3. Relation between the response of fish to fixed lamps and moving lamps.

休息させる。二つの測定が終わった後、実験魚を交換し、52 尾の魚について実験を行なった。この測定結果は Fig. 3 に示される。

Fig. 3 からうかがわれることは、固定光源に対しても移動光源に対しても個体ごとの滞留時間はまちまちで、光に対する反応に著しい個体差のあることである。なお、固定光源に長時間滞留する個体は移動光源にも長時間滞留し、反対に固定光源に短時間しか滞留しない個体は移動光源にも短時間しか滞留しない傾向がうかがわれ、両者の相関度を滞留時間 1 分単位に区分して計算すると 0.46 であり、固定光源と移動光源とに対する個体ごとの反応に多少の相関があるとみられる。

滞留時間の短い個体が、光源の明るさを変えることにより滞留時間が増加するかどうかは調べなかったが、もしイワシが好適照度を持ち、さらに好適照度が 20~0.1 lux にあれば、この水路の光野のなかで滞留時間の短い個体はその好む明るさの位置で長時間滞留することが考えられる。しかし、実際は滞留時間の短い個体をふくめ各個体は、光源直下のもっとも明るい位置に定位置していた。これらのことから、イワシの人工光線に対する反応には個体差が著しく、その反応の強弱は与えられた光の照度とは関係なく、個体自体の

保有するものであろうと考えられる。

実験 2)

円形水路のなかで5尾のイワシのまとまり程度(以下、むれのまとまりと称する)を調べるため、水路の条件を次の通りに変え、どのような条件のもとでむれはよくまとまるかを調べた。実験魚は水路内で1時間明順応させるが、この間、5尾の動きはまとまりがなく、ばらばらであった。

条件 1) 全光野 A (水路全体を照明。水面上の照度 40 lux。)

条件 2) 全光野 B (同上、ただし水路の内壁に黒い紙を張る。)

条件 3) 局部光野 (2 W 光源による水路の局部照明, 2ヶ所。)

条件 4) 移動局部光野 (2 W 光源の回転, 回転速度 12 cm/sec。)

条件 5) 全光野+水流 (流速 20 cm/sec。)

条件 6) 暗光野 (水路全体を暗くする。)

条件 7) 全光野+しま模様 (しま模様回転速度 20 cm/sec。)

条件 2) で水路の内壁に黒い紙を張ったのは次の理由による。水路は内壁, 外壁ともに透明であるが, 外壁の外周には条件 7) を除き黒い紙を張り実験魚が水路の外壁を通しては何も見ることができないようにした。同様に内壁にも紙を張ることが望ましいが, それでは水路内の魚の位置の観測は真上からでないと行なわれないが, 上方にはケージがあるので観測は困難である。しかし, 水路内の魚は内壁を通して反対側の水路にいる魚を見ることがあり得ると思われるので, その影響を調べるため条件 2) では水路の内壁に黒い紙を張り, 視覚的にも完全にドーナツ型水槽になるようにした。しかし, 結果的には条件 1), 2) において魚の分布状態やむれのまとまり程度には変わらなかったため, 条件 3)~7) の実験では水路全体の魚の分布が一見して判断できるように, 水路の内壁には黒い紙を張っていない。

また, 水路の底に砂を敷くと, 条件 1) の場合, むれのまとまりはよくなったので砂を敷いた場合の観察も行なった。ただし, 砂を敷いた場合には

流れを起すことはできないので, 条件 5) の実験は行なっていない。これらの結果を Table 1 にまとめて示す。また, 条件 1)~7) における魚の分布状態の 1 例は Fig. 4 に, および条件 1) の 1 分おき 5 分間観測の 1 例 (Table 1, test 1, Light) は Fig. 5 に示す。

むれのまとまり程度は各個体の頭位方向を考慮に入れ, 個体相互間の接近度により量的に評価する。水路の回転軸を中心にして45度の範囲内で同じ方向に頭を向けているものが2尾おれば5点, 3尾おれば個体相互に誘引性が働くものとして15点, 90度の範囲内で同じ方向に頭位を向けているもの2尾に2点, 3尾に6点を与える。2尾間の体の向きが90度までは頭位方向は同じとみなした。しかし, 頭位方向および個体間の接近度の測定は写真ではなく, 瞬間的な目視によったもので多少の誤差は免れない。この評価の方法を例を用いて示すと次のようである。Fig. 6-A の90度の区域内に2尾いるので2点, 45度の区域内に3尾いるので15点, 合計17点となる。図中, 2尾のグループと3尾のグループは相互誘引性はないとする。

Table 1. Degree of schooling of five fish under seven or six conditions of the annular trough in the cases that the bottom is covered with sand or not. Degree of schooling is shown with mark calculating based on the method of Fig. 6.

Condition of trough	Trough		No sand				
	No. of test		1	2	3	4	5
1. Light	20	15	18	15	18		
2. Ditto. Inside wall is covered with black paper	20	15	18	21	18		
3. Part illuminated	13	13	12	14	13		
4. Moving part illuminated	12	12	9	8	9		
5. Current	27	26	26	28	24		
6. Dark	7	8	11	8	10		
7. Visual screen	10	11	10	14	12		
	Trough		Sand				
1. Light	29	30	26				
2. Ditto. with black paper	25	26	30				
3. Part illuminated	11	13	12				
4. Moving part illuminated	14	8	9				
6. Dark	7	12	10				
7. Visual screen	12	10	10				

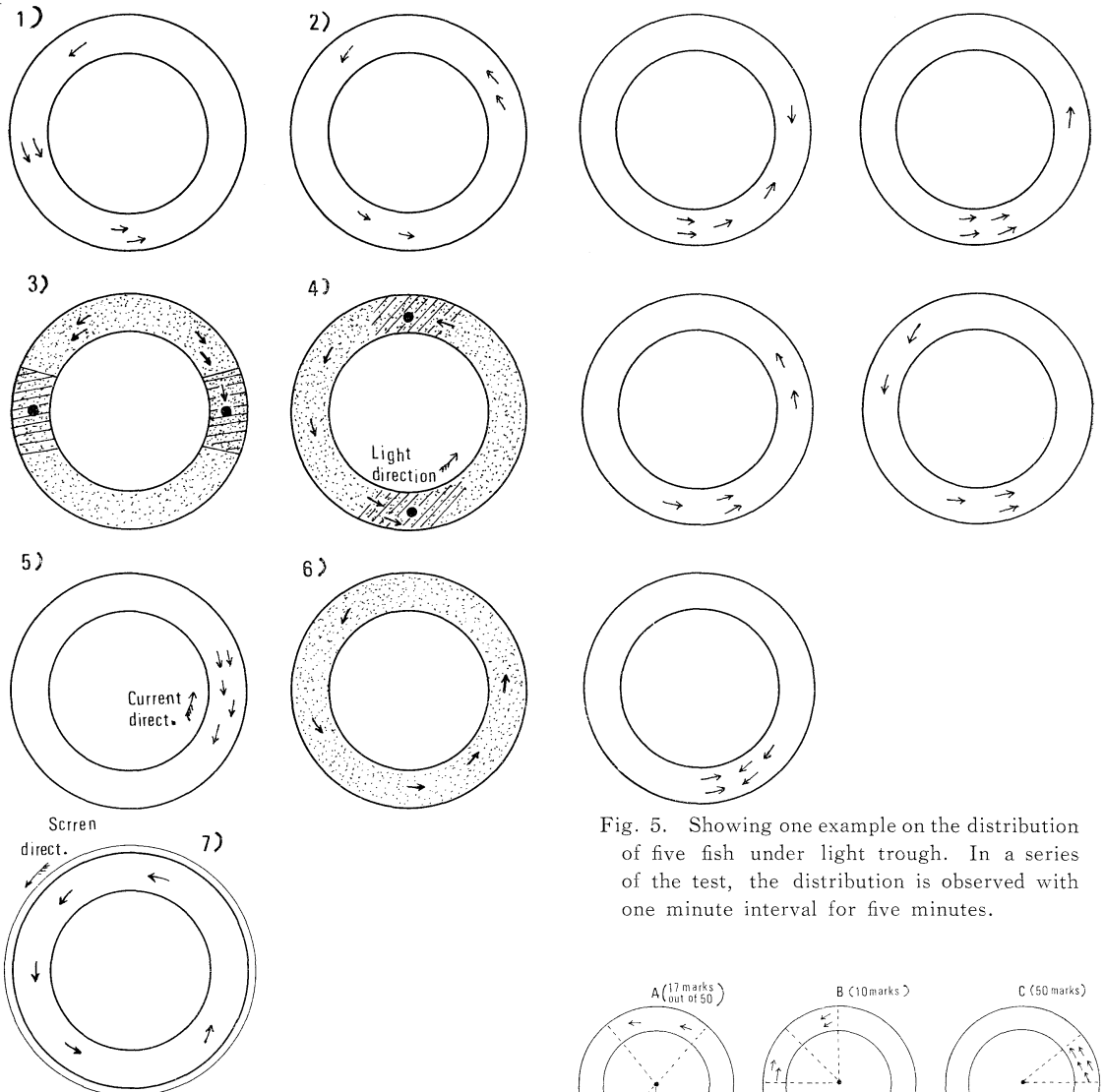


Fig. 4. Showing one example on the distribution of five fish under seven conditions (see Table 1) of the annular trough.

Fig. 5. Showing one example on the distribution of five fish under light trough. In a series of the test, the distribution is observed with one minute interval for five minutes.

Fig. 6-B では 45 度の区域外に 1 尾いるが、これは評価の対象にはならない。また、2 グループは 90 度以内にいるが、頭位方向が反対なので評価せず、合計 10 点となる。Fig. 6-C では 5 尾とも 45 度以内で、同方向に泳いでいるので満点の 50 点を与える。

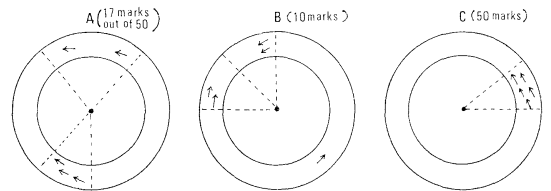


Fig. 6. Calculation on marks of schooling of five fish. When there are two fish in the V-shaped sections of 45 and 90 degrees, the marks of schooling are 2 and 10, respectively. When there are three fish in the V-shaped sections of 45 and 90 degrees, the marks are 6 and 15, respectively.

実験魚 5 尾を水路に入れ、1 時間水路に順応させ、条件 1) について実験を行なった後、条件 3), 4), 6) について実験する際は暗順応、その他は明

順応をそれぞれ 5 分行なう。観測は 1 条件について 5 分間行ない、1 分ごとに魚の水路内の分布を記録する。条件 6) の場合は水路が暗黒状態にな

っており、そのままでは魚の分布が分らないので、懐中電灯で水面を瞬間的に照射して調べた。Table 1 の結果は1分ごとの点数を集計して平均したものである。

Table 1 の結果によると、底面に砂を敷かない場合、水路に流れがある条件 5) の場合がもっともまとまりがよく、その他は明瞭な差がないが、その中でも条件 6) の暗光野の中ではまとまりが最も悪い。これは魚が視覚を失ったためと解釈できる。条件 1), 2) は対照実験で、全光野で刺激を与えない場合であるが、むれのまとまりは悪く、また条件 1) と 2) では前述のように相違はほとんどみられなかった。条件 3), 4) の局部光野では視覚が働くと思われる光野のなかでも、むれを作る傾向はほとんどみられなかった。また、条件 7) の全光野にしま模様が回転する場合は、個体間の相互誘引より個体各自が受けるしま模様刺激の方が大きく、個体各自が任意の目標をとったため分散するように考えられる。

一方、底面に砂を敷くと、流れがなくとも条件 1), 2) の全光野のなかでよくむれを作って泳ぐが、砂を敷いた場合、流れを流すことはできないので、条件 5) との比較はできない。その他の条件ではむれのまとまりは、砂を敷かない場合と大差がない。砂を敷くことによって、むれのまとまりのよくなる理由については明らかでないが、底面からの光の反射が減ずること、および、環境が自然条件に多少とも近づくことが、むれ作りの効果により影響を与えているかもしれない。

条件 3) の場合、局部光野のなかに各個体が集合する傾向は少なく、むしろ水路全体に分散する傾向がみられるが、局部光野を移動させた条件 4) の場合はさらにまとまりは悪くなった。条件 3) の場合、光野には常に1尾以上の魚が存在しており、最も明るい位置で完全に静止状態ではなく、体を左右に小さく振動させながら滞留している。その他、1尾が光野に出たり入ったりしている場合もある。滞留時間は前者は30秒以上、後者は10~20秒で光野を離れる。観測を開始した直後には同時に一つの光野に3尾くらい入るが、10~15秒の滞留で1尾だけ残り、他は光野を離れる。この1尾

もやがて他の魚と入れ換る。

光を移動すると、魚は光へ追従する。しかし、2尾以上の個体がまとまって光野のなかに入り、そのまま光野の移動と共にむれが移動することは極めて稀で、多くは単体で灯下を泳いでゆく。魚が30秒以上光について泳いでいることは少なく、一旦光から離れた魚は次に回ってくる光源について泳ぐか、あるいは光につかないか何れかである。条件 3) でも 4) の場合でも、特に顕著に光につく個体が見受けられ、光に対する反応に個体差があることが分り、このことは実験 1) の結果と同じである。砂のある場合、ない場合でも局部光野での行動はほぼ同じで、砂が敷いてあるから光によく反応するとはいえない。

この局部光野における魚の行動からみて、灯下に留まっている魚は他の魚を誘引する作用があるとは考えられないし、あるとしても極めて微弱であろう。また、5尾の魚が同じ好適照度をもってゐるなら、20-0.1 lux の局部光野に入り、その結果、この狭い光野のなかにまとまりを作るように考えられる。しかし、局部光野におけるむれのまとまりの悪いことはこの考えを否定している。

実験 3)

本実験では、水路内の魚はどの程度の明るさまでむれを維持できるかを調べ、灯下におけるイワシのむれ形成の基礎資料とした。

100 W 電球 1 個の照明で電圧 100 V の場合、水路の明るさは 450 lux であり、これを電圧調整器により電圧を次第に減じてゆき、また、50 lux からは 10 W の電球にかえ、照度計の測定限界 0.1 lux まで減光した。本実験の魚は実験 2) で使用した魚と違い、全光野の水路のなかを5尾がまとまって泳ぎ、5分間に19回回転した。観測は水路に流れがある場合とない場合について行ない、その結果は Table 2 に示す。表中の数字は Table 1 と同じ方法で計算したもので、実験魚のまとまりを示す。

同表によれば、流れのある場合はない場合にくらべ実験魚のまとまりははるかによく、そのことは実験 2) の結果と同じである。また、1 lux ま

Table 2. Light intensity at which five anchovies stopped schooling in the cases of streaming a current in the trough or not. Figures in the Table show the degree of schooling.

Condition trough	Light intensity (lux)										
	450	400	300	139	50	30	15	10	5	1	0.1
Current	31	42	46	50	48	50	37	46	48	41	5
No current	16	22	11	21	39	34	29	19	38	27	5

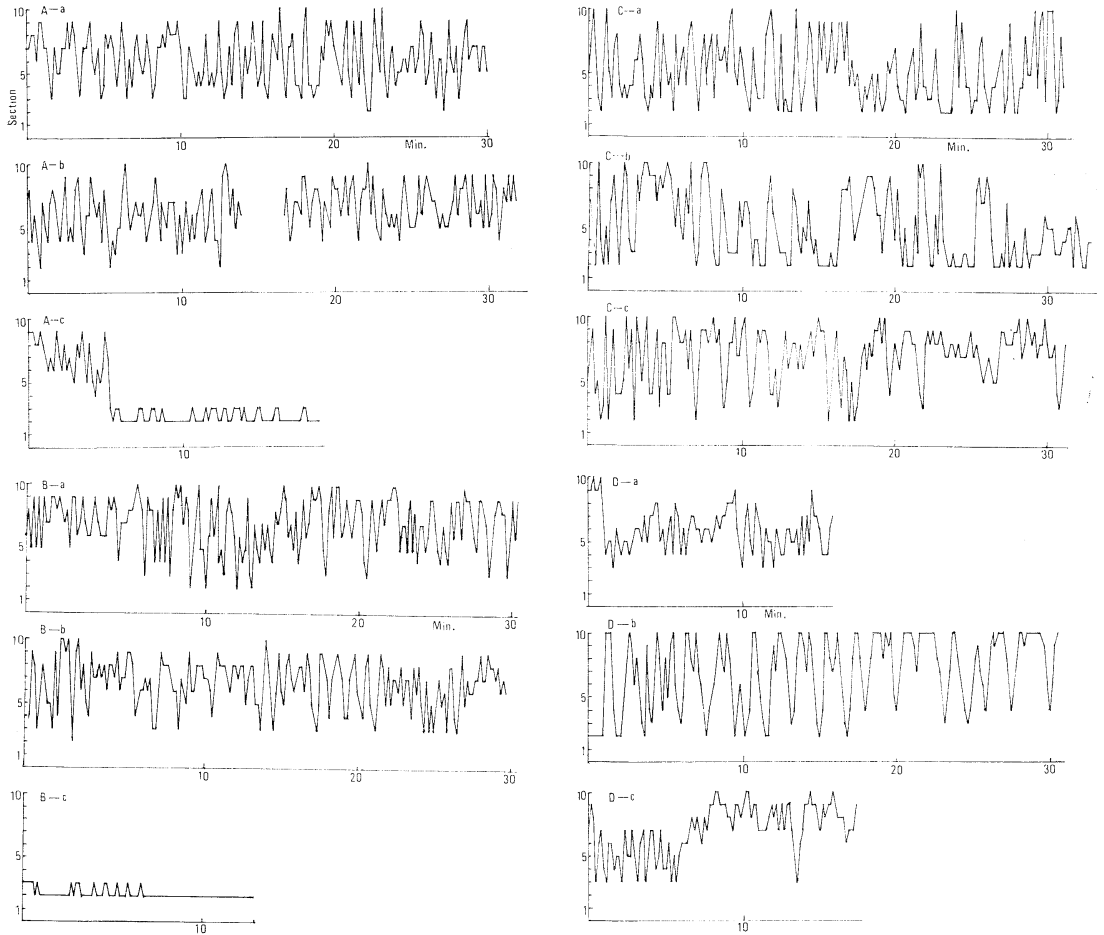


Fig. 7. Locomotion of one fish in the trough (see Fig. 2), when light and, or visual stimulative fish in section 1 are attractive.

A.B.C.D—a: Light trough, one stimulative fish in section 1.

A.B.C—b: Light trough, three fish in illuminated section 1.

A.B.C—c: Dark trough, three fish in illuminated section 1.

D—b: Dark trough, one fish in illuminated section 1.

D—c: Dark trough, three fish in illuminated section 1.

では照度の変化に関係なく、同じ程度にむれはまとまっていたが、0.1 lux で流れのあるなしに関係なくむれは分散した。したがって、この円形水

路のなかでは 0.1 lux が視覚的にむれを維持できる閾値であり、実験 2) の局部光野 20-0.1 lux では照明域の末端では、むれ作りのため十分の明

るさとはいえないかもしれない。しかし、前述のようにこの光野のもとでは、魚はもっとも明るい部分に定位しているのだから、他の魚が光野のなかの魚を認める十分の明るさである。

なお、表には示していないが、本実験の魚は前述のように実験 2) で使用した魚より、明順応のなかでまとまりがよいので、照明を消し 2W の電球を点灯し、その局部光野のなかでのむれのまとまり程度を調べたが、実験 2) の場合と同様、各個体がむれを作ることはなかった。

実験 4)

視覚刺激魚の誘引効果を調べるため、直線水路の一端、区画 1 に刺激魚を入れた場合と入れない場合について、10 秒ごとに観察個体の位置を区画番号 (Fig. 2) によって調べ、15~30 分連続観測を行なった。その結果は、Fig. 7A~D に示される。Fig. 7-A では全光野において区画 1 に魚 3 尾を拘束し、視覚刺激魚とした場合と (A-a), 区画 1 に魚を入れない場合 (A-b) について観察個体の行動を調べているが、何れの場合も観察個体は区画 2-10 をほぼ等速度で移動する行動をとり、視覚魚の誘引効果はみられない。次に室内の照明を消し、区画 1 に魚 3 尾を入れ、区画 1 を局部照明した場合は (A-c), 観察魚は区画 2, 3 に長時間滞留し誘引効果はうかがわれた。

このことは Fig. 7-B でも同様であり、魚は刺激個体群には反応せず、局部光野の光刺激に誘引されたことを示す。しかし、Fig. 7-C では刺激個体群には勿論、局部光野にも誘引されなかった。Fig. 7-D は刺激魚の尾数の変化による誘引度を調べたもので、その結果、局部光野における刺激魚の増加は誘引効果を増加するとはいえないことが明らかになった。また、Fig. 7-C, D の観察魚は局部光野にも誘引されなかったことから、走光性がないか、あるいは微弱なものといえる。

5. 考 察

海洋を遊泳するイワシが人工光線のもとで、むれを形成するかどうかは、むれの構造の概念を緒言で述べたように幅広く規定すれば、明らかにむ

れを作るといえよう。このむれ形成の機構としては、次のことを仮説として挙げるができる。

- 1) 各個体の走光性により各個体が光野に入ったとしても、見掛け上のむれはできる。この場合、各個体が相互誘引性をもっておれば、密度の高いむれができる。
- 2) 相互誘引性がなくとも、各個体の光に対する反応 (選択照度×反応時間) が同じであれば、同一光野を占有しむれができる。

2) の場合、各個体の選択照度が同一であれば、各個体は一定空間にまとまるが、選択照度とは照度の範囲の決め方で変る概念である。したがって、ここでは一定照度 S に対する反応時間 T を調べ、T が個体によって違うかどうかにより光に対する反応 R の相違を調べた。実験 1) では 52 尾の実験魚は S に対し、T は個体によりかなり差があり、R の個体差は著しいと考えられ、むれ作り機構は仮説 2) では十分に説明できないように思える。また、イワシが選択照度あるいは好適照度を絶対値として持ってないことは、IMAMURA and TAKEUCHI⁹⁾ の光源の明るさを変えた水槽実験により示されており、魚がよく集まる明るさは環境の変化に伴う可変的なものとも考えられる。また、黒木・中馬¹⁰⁾ の集魚灯に集まるイワシの行動を魚探機で調べた実験では、灯に集まったイワシ群は相当な遊泳速度で集合離散し、活発な運動を行なったとみられるので、灯下のイワシは一定照度域に静止的に滞留するものではないように考えられる。これらのことも仮説 2) の不十分なことを示唆している。

日中、魚がむれを作るのは個体間の相互誘引によるものであろう。むれの相互誘引性のなかで視覚が重要な感覚であることは緒言で述べた通りである。イワシに相互誘引性が絶えず働いておれば、夜間、視覚が失われ、むれが分散しても、たまたま集魚灯の光野のなかで仲間が認められれば視覚に基づく相互誘引性によりむれを再編することがあろう。

実験 2) では、円形水路の 5 尾の魚は全光野の場合より、局部光野の場合の方がまとまりが悪かったことは、灯下によるむれ作り効果はそれ程顕著

でないことを意味している。一方、飼育水槽のなかのイワシに局部照明を与えた場合、光源下の明るい区域を中心に円を画いて比較的好くまとまって泳いでおり、また同じ水槽を用いて実験を行なった IMAMURA and TAKEUCHI⁹⁾ の報告でも、灯下にむれをつくることを述べている。相互誘引性は視覚の他、聴覚ないし側線感覚（以下、両者を振動感覚と呼ぶ。遊泳によって生ずる渦は振動感覚とは別に水力学的効果をもつ⁶⁾が、ここでは渦の効果も振動感覚にふくめる。）、あるいは臭覚などの感覚に基づいているものである⁶⁾。実験 2) で、流れがあるとむれのまとまりがよくなり、また、円形水路より遊泳範囲の広い飼育水槽のなかでよくまとまることは、個体相互の運動がむれ形成のために必要なことを推察せしめる。すなわち、個体の運動は視覚に対しては視覚運動反応を解発し、振動感覚に対しては水流による振動・渦・遊泳音により影響を与えるであろう。

むれ形成における視覚運動反応の効果については、SHAW¹¹⁾ が述べており、イワシの視覚運動反応の強さについては著者⁹⁾ によって確かめられており、また、円形水路の流れのなかのむれは決して一点に定位することなく、絶えず動き続けているので、この間、個体相互は仲間の動きに対し視覚運動反応を生じ、それが視覚の面でむれ形成に強く影響しているであろう。一方、遊泳によって生ずる遊泳音・渦・水の振動により振動感覚が刺激され、視覚、振動感覚両面からむれ形成が補償されているものと考えられる。このことはまた、むれ形成のためには、仲間に対する形態視覚だけではその効果が薄いことを意味している。

MOULTON¹²⁾ は *Carnax latus* と *Anchoviella choerostoma* が夜も昼も密なむれを維持していること、そして盲目の *Anchoviella* はむれが統一性のある行動をしているときは正常な魚とむれを作ることを調べ、このことから彼は魚の遊泳音および遊泳の際に生ずる水の流れと圧力がむれ形成に有効な刺激となることを示唆し、同じ考えを BREYDER¹⁾ も示している。

円形水路の光野のなかのイワシは、光源下で身体を左右に振動させているが、遊泳運動はなく、

また直線水路のなかでは視覚刺激魚はアクリル板で仕切られ、水の振動は観察個体まで伝達されないで、振動感覚に作用する効果はない。また、振動感覚だけではむれを形成することが困難であることは、しま模様刺激により仲間に対する保目標性を失わせた場合、各個体がそれぞれ任意の位置で遊泳していることから考えられる。それに対し、大型水槽の光野のなかでは遊泳範囲は広く、イワシは自由に泳ぎ回るので、仲間に対して視覚運動反応を生じさせ易く、同時に振動感覚にも働きかけるのでむれを作り易いものと考えられる。

海洋では集魚灯下に集まる個体数は多く、遊泳範囲は広く、視覚的にも振動感覚的にも相互誘引効果は一層高まるのであろう。実験 3) の円形水路の観測、および大型水槽における観測⁹⁾ では、イワシのむれの分散する明るさは 10^{-1} lux で、海洋では 10^{-2} lux (BLAXTER and HOLLIDAY) であるが、この数値の違いは水槽と海洋とでのむれ内部の相互誘引の強弱を示しているとも解釈できる。

以上の考察から、イワシの灯下におけるむれ形成は、各個体の同一照度選択のような光に対する反応の同一性によるものではなく、個体相互の誘引の結果であり、その相互誘引性は視覚としては視覚運動反応に依存することが大きく、また、遊泳によって生ずる水の振動・遊泳音・渦が振動感覚に作用し、あるいは水力学的効果として作用するものと考えられる。

6. 要 約

1) カタクチイワシの灯下におけるむれ形成の機構を調べるため、円形水路・直線水路を用いて実験を行なった。

2) カタクチイワシの光反応には個体差が著しいこと、流れを与えるとむれを形成すること、20-0.1 lux の局部照明域ではむれを作らないこと、局部照明域にいる視覚刺激個体には誘引されることが明らかになった。

3) 以上の実験結果から、灯下におけるむれ形成は、光に対する反応の同一性によるのではなく、

個体相互の誘引の結果であり、誘引効果は個体群の運動によって高まることを考察した。

文 献

- 1) BREDER, C. M. (1959): Studies on social grouping in fishes. Bull. Mus. Nat. Hist., **117**(6), 399-481.
- 2) WHITNEY, R. R. (1960): Schooling of fish relative to available light. Trans. Am. Fish. Soc., **98**(3), 497-507.
- 3) 田村 保 (1970): 魚類生理(川本信之編), 427-428, 恒星社厚生閣, 東京.
- 4) BLAXTER, J. H. S. and F. C. T. HOLLIDAY (1964): The behaviour and physiology of herring and other clupeids. Advances in Marine Biology, **1**, 261-393, Academic Press, New York and London.
- 5) WOODHEAD, P. M. J. (1966): The behaviour of fish in relation to light in the sea. Oceanog. Mar. Biol. Ann. Rev., **4**, 337-403.
- 6) SHAW, E. (1967): Some new thought on the schooling of fishes. FAO Fish. Reports, **62**(2).
- 7) INOUE, M. (1967): Observation on the swimming speed of fish in an annular trough-I. Effect of visual screen on goldfish. La mer (Bulletin de la Société franco-japonaise d'océanographie), **5**(4), 238-243.
- 8) INOUE, M. and K. MIYASAKA (1968): Observation on the swimming speed of fish in an annular trough-II. Swimming performance of anchovy by its rounding direction. La mer, **6**(4), 237-242.
- 9) IMAMURA, Y. and S. TAKEUCHI (1960): Study of the disposition of fish toward light-V. The strength of illumination comfortable to *Engraulis japonicas*. J. Tokyo Univ. Fish., **46**(1-2), 133-148.
- 10) 黒木敏郎・中馬三千雄 (1968): 灯に集まる魚群の立体的記録例について. 鹿大水紀, **6**, 77-81.
- 11) SHAW, E. (1965): The optomotor response and the schooling of fish. Spec. Pubs. int. Commn. NW. Atlant. Fish., **6**, 753-755.
- 12) MOULTON, J. M. (1964): In acoustic behaviour of animals. edited by P. M. J. WOODHEAD. Oceanog., Mar., Biol., **4**, 337-403.

The Visibility of Underwater Objects to the Human Eye*

Ryohei TSUDA**

Abstract: The visual range of each netting was measured with Research Submarine Kuroshio-II and colour nettings which closely matched the underwater surroundings were examined. The red and yellow twines were more visible near sea bed than sea surface. This result suggests that though one perceives the objects as colour contrast near sea surface, as it becomes deeper, with a consequent absorption of a long wave length, these are depended upon brightness contrast. It is apparent from the results of our experiment that the standards of between 10 % and 20 % reflectance are the least visible. It is at once seen that twines and bars of meshes which matched the standards of between 10 % and 20 % reflectance are best camouflaged and therefore most closely match the water background.

1. Introduction

Sighting ranges depend on the distribution of the light field underwater, the clarity of the water, the nature or type of object we wish to sight, its position in relation to the observer, the ability of the observer to see and of the diver. Even in the clear water it is rare for a diver to see any object farther than 40 m away and in turbid water it is often within 1 m. Generally speaking, underwater objects are illuminated from above but seen from the side, thus the study of the direction of underwater light is very important an investigation of visibility. The picture is made more complicated because light from above has a rather different spectral intensity curve than light from the side.

The aim of this investigation was to find the effect of colour on the nettings with Research Submarine Kuroshio-II. It should be made to make them inconspicuous underwater. Further aims are to study the light conditions underwater and the visual function, the behaviours of fishes to them.

2. Apparatus and procedure

In the past, the measurements of the visual range in the sea waters were observed with SCUBA diving (HEMMINGS *et al.*, 1965; LYTHGOE, 1968; KINNEY *et al.*, 1967, 1969), how-

ever, the diving works depended on the limited air and the occurrence of the submarine sickness caused by deep diving were hindering the sufficient process, so we measured the underwater visibility of the nettings and the twines with Research Submarine Kuroshio-II. An outline of Kuroshio-II and the arrangement of apparatus to measure the visual range are shown in Fig. 1. Aluminium stairs, 6 m in length and 0.5 m in width were fixed to her front and a wire frame of about 0.4 m squares was attached to the edge of it. The net samples were rigged on it. By using the handle inside the submarine, the wire frame could be moved back and forth. The N-point of the visibility of each netting and cord can be determined by the reading marked on the meter board attached to the handle. The measurements (off Muroran where we made two dives on Aug. 30, 1969, depth 22 m and 36 m, location; 42°19'N, 140°55'E) were made as near to noon as possible. During all the experiments, the water was calm and there was no perceptible ground swell. The netting samples used in the experiments

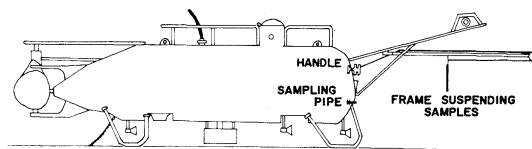


Fig. 1. Outline of the research submarine "Kuroshio-II" and the apparatus for measuring visual range.

* Received January 30, 1973

** Faculty of Agriculture, Kinki University

and all synthetic fibres were as shown in Table 1. The spectral reflectances for the seven basic colours are given in Fig. 2.

Table 1. Sample of twines.

	Material	d*
Yellow	Dyed 'Nylon'	0.95
Blue	Dyed 'Nylon'	0.95
Green	Dyed 'Nylon'	0.95
Red	Dyed 'Nylon'	0.95
Black	Melt dyed 'Nylon'	0.91
Grey	Melt dyed 'Nylon'	0.60
White	'Nylon'	1.05

* Diameter (mm)

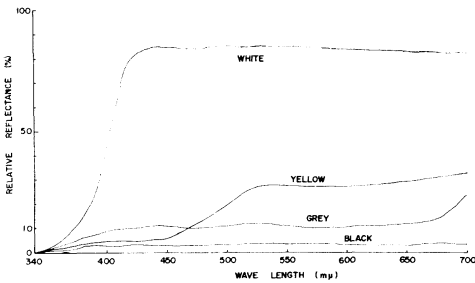
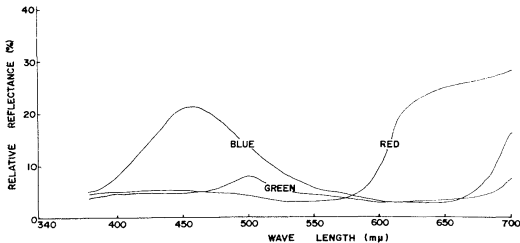


Fig. 2. Spectral reflectance of nettings.

3. Results and discussion

Experiments were made on 2 sets of depth-ness, one for measurement of 4, 10, 23 and 36 m and the other for measurement of 7, 15 and 22 m below the sea surface. As an example, the results are represented in Fig. 3. The colours that are easiest to see underwater at the limit of visibility with natural illumination and a water background are white, yellow, orange and red in the turbid bodies of water and the most difficult colours to see at the limits of visibility under natural illumination and a water background are grey, black, blue

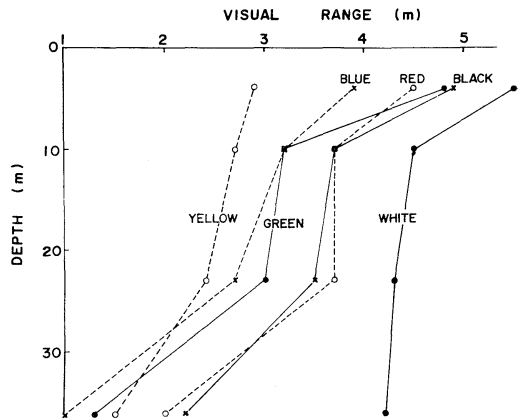


Fig. 3. Sighting range at each depth.

and green, whose major spectral components are absorbed in murky water (KINNEY *et al.*, 1967, 1969). For the surface, yellow is the most visible. It means that not only brightness contrast, but also colour contrast are depended on the underwater visibility. Measured values of the visual range of a bar of mesh and a knot of it are plotted against the depth in Fig. 4. The visual range of knots is more visible than a bar of mesh near the surface, but those become similar with increasing depth. As it becomes deeper, both yellow and red twine are found to have increased in viewing distance. The results with twines seen against a water

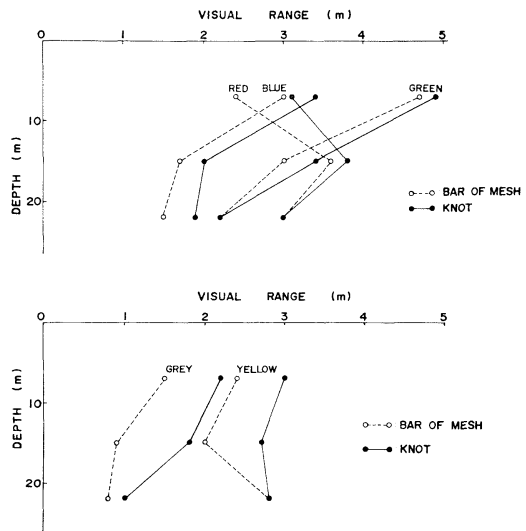


Fig. 4. Sighting range at each depth.

background suggest that though one perceives the objects as colour contrast near the surface, as it becomes deeper, with a consequent absorption of a long wave length, both red and yellow object are darkly and those are depended upon brightness contrast.

When the contrast between the brightness of object and that of its background falls below the threshold of brightness, we can not recognize the object but when the former falls below the latter over some extent, we can do it. In this case, as the background is brighter than the object, we observe it as a silhouette. As above-mentioned, it must be proved through the examination of relationship between the reflectance of the dyed netting and its visual range. The results so obtained are plotted in Fig. 5. It is at once seen that twines and nettings which matched the standards of between 10% and 20% reflectance are best camouflaged and therefore most closely match the water background. The results agree with the experiment in laboratory (TSUDA *et al.*, 1973).

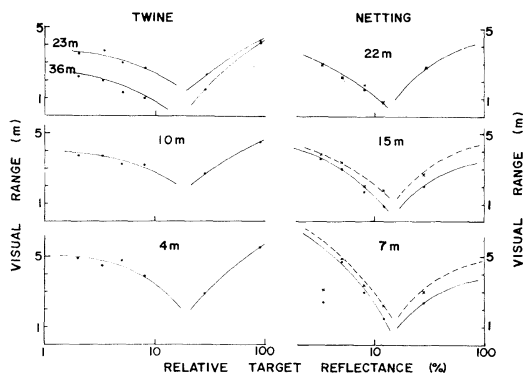


Fig. 5. Results of two experiments sighting dyed twines and nettings different reflectance at each depth: bar of mesh....., knot.... (right).

So far as uniformly dyed fishing nets concerned, perfect camouflage can not, even in theory, be achieved cylindrical twines and the upper surface of each twine will always be brighter than the lower because light coming from above is always brighter than light from below. Therefore, whatever net colour, part of it must always fall to match the water background. Even so it is of such practical importance to know how to make well camouflaged nettings that it is worth trying to find the best colour even though the perfect solution is impossible.

Acknowledgements

The author wishes to thank Professor Naoichi INOUE, University of Hokkaido for his kindness and suggestion and to Mr. Hitoshi TAKEDA, technician of Kuroshio-II for his co-operation. Thanks are also to Dr. Masahiro KAJIHARA for his kind advice.

References

- DUNTLEY, S. Q. (1960): Improved nomographs for calculating visibility by swimmers, (natural light). Bureau of Ships Contract NObs-72039. Rep. 5-3' Feb.
- HEMMINGS, C. C. and J. N. LYTHGOE (1965): The visibility of underwater objects. Symposium of the underwater association for Malta, 23-30.
- KINNEY, J. A., S. M. LURIA and D. O. WEITZMAN (1967): Visibility of colours underwater. *J. Opt. Soc. Amer.*, **57**, 802-809.
- KINNEY, J. A., S. M. LURIA and D. O. WEITZMAN (1969): Visibility of underwater using artificial illumination. *J. Opt. Soc. Amer.*, **59**, 624-628.
- LYTHGOE, J. N. (1968): Visual pigments and visual range underwater. *Vision Res.*, **38**, 997-1011.
- TSUDA, R. and N. INOUE (1973): Study on the underwater visibility of net twines by the human eye-III. Estimation of threshold of brightness contrast. *Bull. Jap. Soc. Fish.* (in contribution)

人間の目に対する物体の水中視程

津 田 良 平

要旨: 各種着色網糸の視程を, “くろしおII号” を使って測定し, 背景の明るさと良くマッチした網糸の色を調べた。赤色や黄色の網糸は, 表面近くより深い方が良く見える。この現象は, 表面近くで色のコントラストとして識別されていたものが, 深くなるにつれて波長の選択吸収により, 色として識別されず, 明るさのコントラストとして識別されるものと考えられる。着色網糸の明るさと視程の関係を見ると, 10~20% の反射率辺りで, 視程の減少が見られる。その結果, 10~20% の反射率をもつ物体は, 水中の背景の明るさと良くマッチして, 見えにくくなるものと考えられる。

学 会 記 事

1. 昭和47年12月11日、東京水産大学において第1回日仏海洋学会賞受賞候補者推薦委員会を開き、互選の結果、齋藤泰一氏が委員長となり、評議員全員に往復葉書によって受賞候補1件ずつを12月26日までに推薦してもらおうよう依頼することに決定した。
2. 昭和47年12月14日、東京水産大学において編集委員会を開き、第10巻第3号の編集を行なった。
3. 昭和47年12月27日、東京水産大学において第2回学会賞受賞候補者推薦委員会を開き、受賞候補者推薦依頼の結果を検討して、48年度の受賞候補者として草下孝也氏を推すことにした。

4. 下記の諸氏が入会された。(正会員)

氏 名	所 属	紹介者
出 雲 義 朗	国立公衆衛生院	佐々木忠義
ソワッソン・パトリック	東京水産大学	〃

5. 退 会: 加曾利元博, 田中満佐人, 本間琢也

6. 死 亡

名誉会員鈴木章之氏は、昭和48年1月19日逝去された。謹んで御冥福を祈る。

7. 会員の住所、所属の変更。

氏 名	郵便番号	新住所又は新所属
浦 純二	280	千葉市新港146 (株)日本港湾コンサルタント水理研究所
棚橋善克	980	仙台市国見4-13-11
多田利義	100	千代田区大手町 気象庁予報課

8. 交換及び寄贈図書。

- 1) 海洋機器開発, 4(12), 1972
- 2) 国立科学博物館専報, 第5号, 1972
- 3) 国立科学博物館研究報告, 15(4), 1972
- 4) 水路研究論文集, 1972
- 5) 海洋博ニュース, No. 2, 1972, No. 3, 1973
- 6) 沖繩国際海洋博覧会の概要
- 7) 航海, 第38号, 昭47
- 8) 鯨研通信, 254号, 255号, 1972
- 9) 宇佐臨海実験所研究報告, 18(1), 1971
- 10) 宇佐臨海実験所, 1971
- 11) CSK NEWS LETTER, No. 39, 1972
- 12) Ocean Age, 4(12), 1972, 5(1), 1973
- 13) Revue des Travaux de l'Institut des Pêches Maritimes, Tome XXXVI Fasc 3, 1972

日仏海洋学会役員

顧 問 ユベール・ブロッシェ ジャン・デルサルト
ジャック・ロベール アレクシス・ドランデール

名誉会長 ベルナル・フランク

会 長 佐々木忠義

常任幹事 永田 正, 大柴五八郎

幹 事 阿部友三郎, 石野 誠, 井上 実, 今村 豊
岩下光男, 宇野 寛, 川原田 裕, 神田献二
菊地真一, 鬼頭正隆, 草下孝也, 齋藤泰一,
佐々木幸康, 杉浦吉雄, 高木和徳, 高野健三
辻田時美, 富永政英, 奈須敬二, 西村 実,
根本敬久, 半沢正男, 松生 洽, 松尾邦之助,
丸茂隆三, 森田良美, 山中鷹之助 (50音順)

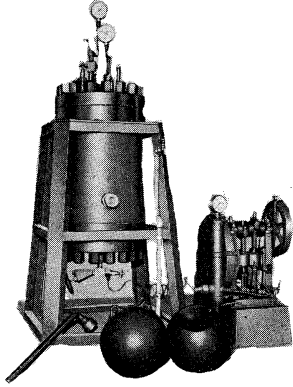
監 事 久保田 穰, 岩崎秀人

評 議員 赤松英雄, 秋山 勉, 阿部宗明, 阿部友三郎,
新崎盛敏, 有賀祐勝, 石野 誠, 市村俊英,
井上直一, 井上 実, 今村 豊, 入江春彦,
岩崎秀人, 岩下光男, 岩田憲幸, 上野福三,
宇田道隆, 宇野 寛, 大内正夫, 大柴五八郎,
大村秀雄, 岡部史郎, 梶浦欣二郎, 金谷太郎,
川合英夫, 川上太左英, 川口守一, 川村輝良,
川村文三郎, 川原田 裕, 神田献二, 菊地真一,
鬼頭正隆, 木村喜之助, 草下孝也, 楠 宏,
国司秀明, 久保田 穰, 黒木敏郎, 小林 博,
小牧勇蔵, 近藤 仁, 西条八束, 齋藤泰一,
齋藤行正, 坂本市太郎, 佐々木忠義, 佐々木幸
康, 猿橋勝子, 椎野秀雄, 柴田恵司, 下村敏正,
庄司大太郎, 末広恭雄, 杉浦吉雄, 多賀信六,
高木和徳, 高野健三, 高橋淳雄, 田畑忠司,
田村 保, 千葉卓夫, 土屋靖彦, 辻田時美,
寺本俊彦, 富永政英, 鳥居鉄也, 中井甚二郎,
中野猿人, 永田 正, 永田 豊, 奈須敬二,
奈須紀幸, 新野 弘, 西村 実, 新田忠雄,
根本敬久, 野村 正, 花岡 資, 半沢正男,
半谷高久, 菱田耕造, 日比谷 京, 桧山義夫,
平野敏行, 深沢文雄, 福島久雄, 淵 秀隆,
星野通平, 増沢譲太郎, 松井 魁, 松生 洽,
松尾邦之助, 松崎卓一, 松平康男, 丸茂隆三,
溝口哲夫, 三宅泰雄, 宮崎千博, 宮崎正衛,
元田 茂, 森田良美, 森安茂雄, 安井 正,
矢部 博, 山路 勇, 山中鷹之助, 山中 一,
依田啓二, 渡辺貫太郎, 渡辺精一 (50音順)
マルセル・ジュクラリウス, ジャン・アング
ティル, ロジェ・ペリカ

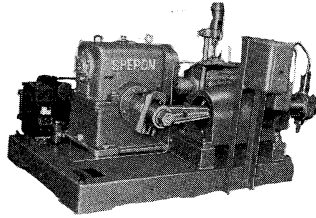
賛 助 会 員

旭化成工業株式会社	東京都千代田区有楽町 1-12-1
井出利明	釧路市白金町 11
株式会社内田老鶴園新社	東京都千代田区九段北 1-4
梅林弘直	東京都千代田区大手町 2-2-1 新大手町ビル7階 極東貿易株式会社
小樽船用電機株式会社	小樽市色内町 1-20
株式会社オルガノ	東京都文京区本郷 5-5-16
株式会社オーシャンエージ	東京都豊島区南池袋 1-18-21
海上電機株式会社	東京都千代田区神田錦町 1-19
社団法人海洋開発産業技術協会	東京都港区六本木 4-1-13
株式会社海洋開発センター	東京都港区赤坂 1-9-1
協同低温工業株式会社	東京都千代田区神田佐久間町 1-21 山伝ビル
協和商工株式会社	東京都新宿区下落合 1-513 第二正明ビル
栗山ゴム株式会社	大阪市東淀川区西中島町 1-195
小松川化工機株式会社	東京都江戸川区小松川 1-2645
小山川康三	東京都文京区本駒込 6-15-10 英和印刷社
三信船舶電具株式会社	東京都千代田区内神田 1-15
三洋水路測量株式会社	東京都港区新橋 5-23-7 三栄ビル
シュナイダー財団極東駐在事務所	東京都港区芝琴平町 38 日本ガス協会ビル
昭和電装株式会社	高松市福岡町 467
大洋電機株式会社	東京都千代田区神田錦町 3-16
株式会社高瀬鉄工所	東京都江戸川区松江 1-11-15
株式会社鶴見精機工作所	横浜市鶴見区鶴見町 1506
帝国酸素株式会社	神戸市兵庫区高松町 22-1
東京木材株式会社	東京都中央区築地 4-2 築三ビル
株式会社東京久栄	東京都中央区八重洲 3-3 八重洲口会館
東京急行電鉄株式会社	東京都渋谷区桜丘町 26-20
東京製網繊維ロープ株式会社	東京都中央区日本橋室町 2-8 古河ビル
東京レブ株式会社	東京都豊島区池袋 2-1120 ローズマンション 302号
株式会社東邦電探	東京都杉並区上高井戸 5-327
東洋海洋開発株式会社	東京都中央区宝町 3-4
中川防蝕工業株式会社	東京都千代田区神田鍛冶町 2-1 東京建物ビル
株式会社ナック	東京都中央区銀座 1-5-6
日本アクアラング株式会社	東京都豊島区北大塚 1-16-6 大塚ビル
日本海事広報協会海の世界編集部	東京都港区琴平町 35 船舶振興ビル
日本海洋産業株式会社	東京都千代田区神田美土代町 1
日本テトラポッド株式会社	東京都港区新橋 2-1-13 新橋富士ビル9階
日本テレスコム株式会社	東京都港区六本木 4-11-10 六本木富士ビル
社団法人日本能率協会	東京都港区芝公園25号地
日本無線株式会社	東京都港区芝桜川町 25 第五森ビル
船用電球株式会社	東京都目黒区下目黒 1-6-21
有限会社ハラダ電機製作所	東京都豊島区池袋 8-3292
ヒエン電工株式会社	堺市松屋町 1-3
深田多満男	東京都港区芝虎ノ門8 虎ノ門実業会館 深田サルベージ株式会社
藤田潔雄	東京都中央区銀座西 7-6 株式会社ビデオプロモーション
藤田峯	東京都江東区南砂 1-3-25 株式会社 中村鉄工所
フランス物産株式会社	東京都千代田区神田小川町 3-20-2 増淵ビル
古野電気株式会社	東京都中央区八重洲 4-5 藤和ビル
丸文株式会社	東京都中央区日本橋大伝馬町 2-1-1
三井海洋開発株式会社	東京都千代田区霞ヶ関 3-2-5 霞ヶ関ビル3002号室
三菱重工株式会社	東京都千代田区丸の内 2-5-1
株式会社吉田製作所	東京都台東区上野 3-13-9
吉野計器製作所	東京都北区西ヶ原 1-14
株式会社離合	東京都千代田区神田鍛冶町 1-2 丸石ビル
株式会社渡部計器製作所	東京都文京区向丘 1-7-17

ヨシダの海洋試験機



(高圧テスト容器)

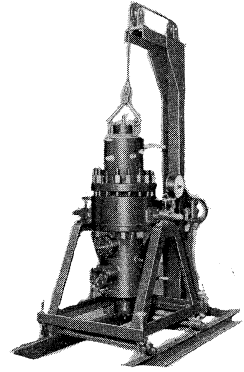


(高圧ポンプ)

水圧試験装置
 高圧水圧ポンプ
 透水試験装置
 流水実験装置
 恒温水槽
 回流水槽

衝撃、抗張力、摩耗試験機

☆ その他各種試験機装置設計製作



(透水試験装置)



株式
 会社

吉田製作所

東京都台東区上野3丁目13番9号 電話 (832) 4351~5

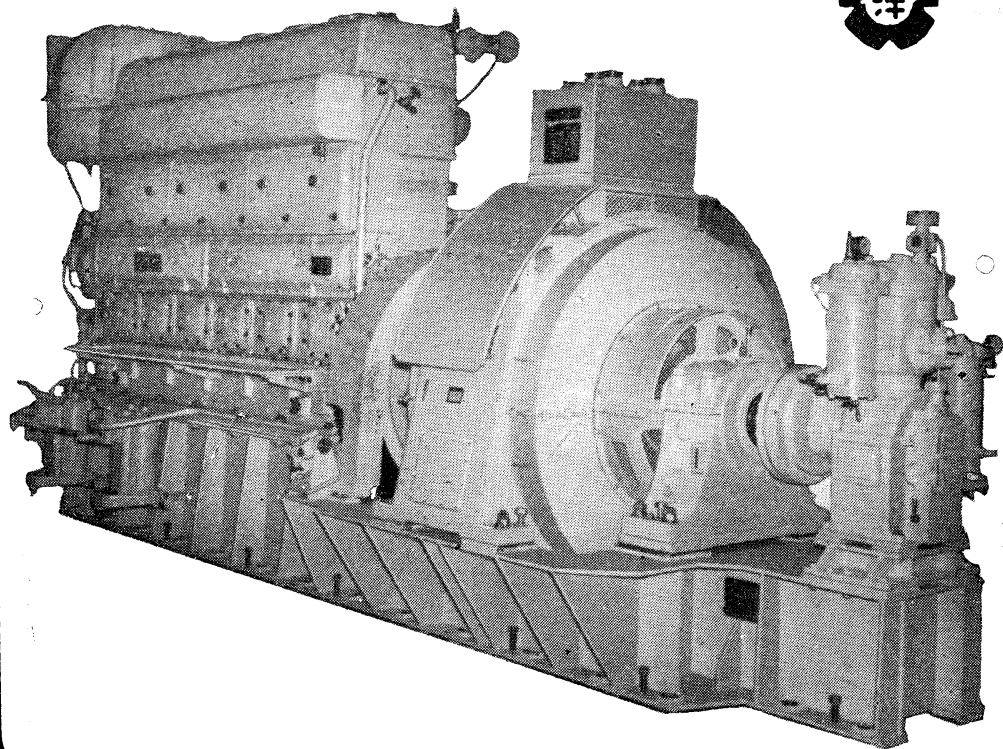
7IL は無限の可能性に挑戦する

- ◆ 漁撈電子機器
- ◆ 航海計器
- ◆ 海洋開発機器
- ◆ 航空機用電子機器
- ◆ 各種制御機器
- ◆ コンピュータ端末機器
- ◆ 各種情報システム



本社 / 西宮市芦原町9-52 ☎0798(65)2111(大代) 支社 / 東京都中央区八重洲4-5-5 和ビル ☎03(272)8491(代) ほか37ヶ所

ながい経験と最新の技術を誇る！
大洋の船舶用電気機器



主要生産品目

自励・他励交流発電機
 直流発電機
 各種電動機及制御装置
 船舶自動化装置
 配電盤

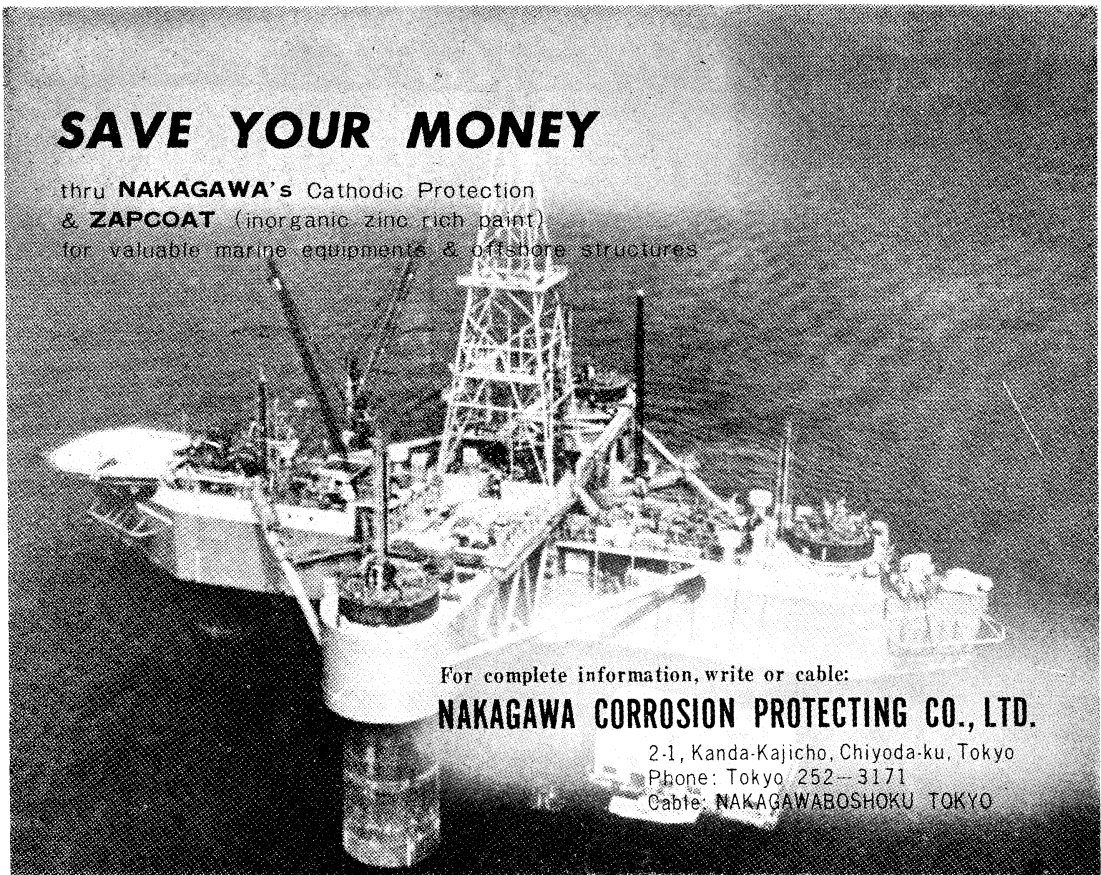
大洋電機株式会社

取締役社長 山田沢三

本社 東京都千代田区神田錦町3の16
 電話 東京 (293) 3061~8
 岐阜工場 岐阜県羽島郡笠松町如月町18
 電話 笠松 4111~5
 伊勢崎工場 群馬県伊勢崎市八斗島町726
 電話 伊勢崎 1815・1816・1835・816
 下関出張所 下関市竹崎町3-9-9
 電話 下関 (22) 2820・3704
 北海道出張所 札幌市北二条東二丁目 浜建ビル
 電話 札幌 (25) 6347(23)8061・8261

SAVE YOUR MONEY

thru **NAKAGAWA's** Cathodic Protection
& **ZAPCOAT** (inorganic zinc rich paint)
for valuable marine equipments & offshore structures



For complete information, write or cable:

NAKAGAWA CORROSION PROTECTING CO., LTD.

2-1, Kanda-Kajicho, Chiyoda-ku, Tokyo

Phone: Tokyo 252-3171

Cable: NAKAGAWABOSHOKU TOKYO

水路測量と土質調査

Hydrographic Survey and Marine Geological Survey

SANYO Hydrographic Survey Co., LTD.

業 務 深浅測量, 底質土質調査, 国土保全測量調査, 海洋資源開発測量調査

防災工事測量調査, マイルポストの測量, 航海保安に必要な調査, 海底ケーブル沈設測量調査, 潮汐, 潮流, 海流, 波浪の観測

一般海洋観測調査, その他一般海事関係の観測調査および関係業務の技術, 科学的研究

特 色 高性能の精密計測機の整備拡充

元海上保安庁職員をもつて組織する優秀なる我国唯一の技術陣

総代理店(連絡先)は全国的組織網を持つ三井物産 K. K の本, 支店出張所

三 洋 水 路 測 量 株 式 会 社

東京都港区新橋5丁目23番7号

電話 (432) 2971~4

Murayama

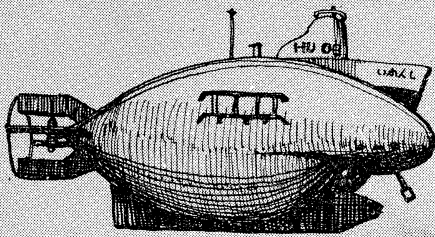
水中濁度計
水中照度計
電導度計



株式会社 村山電機製作所

本社 東京都目黒区五本木2-13-1
出張所 名古屋・大阪・北九州

海底資源の開発に活躍—潜水調査船“しんかい”



陸・海・空 世界に伸びる 本社

川崎重工

神戸市生田区中町通2-16-1
日生川崎ビル3~7階
東京支社 東京都港区芝浜松町3-5
世界貿易センタービル

Exploiting the Ocean by...

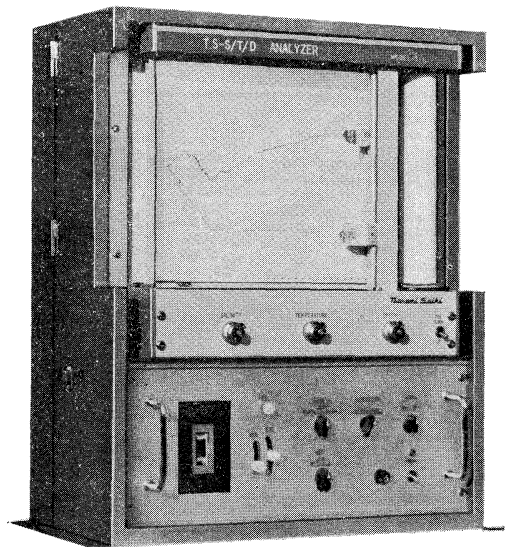
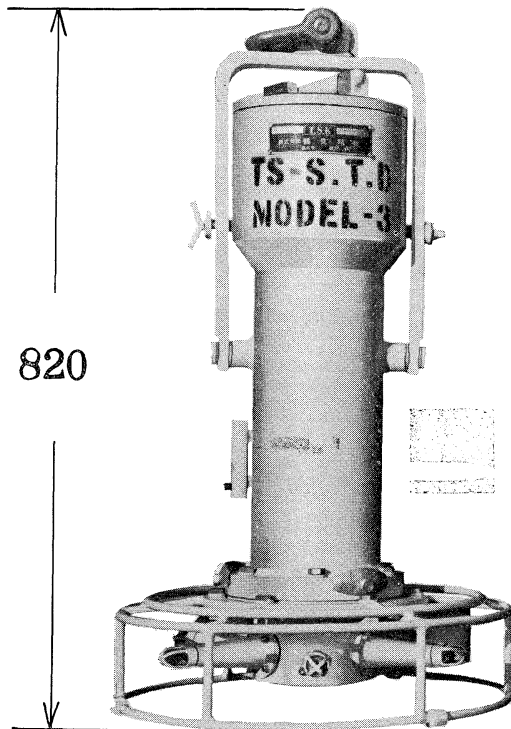
T.S.K. OCEANOGRAPHIC INSTRUMENTS

REPRESENTATIVE GROUPS OF INSTRUMENTS AND SYSTEMS

新製品!

T.S.-磁気テープ記録式 S.T.D. システム Model 3-1

本器は各方面で御使用いただいております T.S.-S.T.D. M3 の電気回路部を I.C 化したもので、従来の大きさの約 2/3 になっています。従って取扱い容易、小型ウインチによる投入、揚収が可能な利点がありますので小型観測船による御使用にも適しております。



	測定範囲	精 度
塩 分	31~36 ‰S	±0.04‰S
水 温	-2~35°C	±0.1°C
深 度	0~1000 m	±5 m

	水中センサー	船上アナライザー
寸 法	450 (最大) × 820 l	530 × 250 × 660
重 量	30 kg (空中)	43 kg

THE TSURUMI SEIKI CO., LTD.

1506 Tsurumi-cho Tsurumi-ku, Yokohama, 230 Japan

TSK. USA.

CABLE ADDRESS
TSURUMISEIKI Yokohama

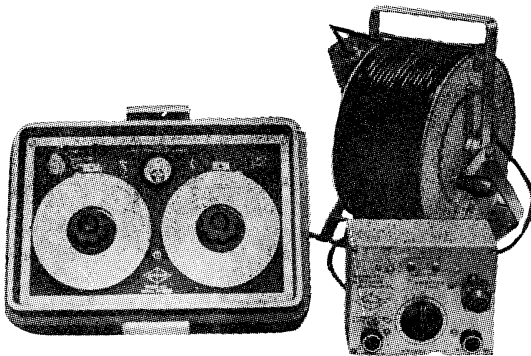
TELEPHONE
Yokohama 521-5252~5

3446 Kurtz St.,
San Diego, Calif. 92110, U.S.A

IWAMIYA INSTRUMENTATION LABORATORY

AUTO-LAB PORTABLE S-T BRIDGE

Model 602



オート・ラブ誘導起電式精密塩分計に引続いて、開発された温度と塩分の現場測定用の可搬型海洋測器です。温度、塩分ともダイヤルで直読出来、簡便で堅牢しかも高精度なソリッドステートのユニット結合構造の最新鋭計器です。

温度：0~35°C 1/2 確度 ±0.1°C

塩分：Scale 1. 0~32‰S 確度 ±0.1‰S
Scale 2. 32~42‰S 確度 ±0.03‰S

電源：電池 9V, 200時間使用可能

追加附属品

ステンレス製ケーブルリール
半自動式電極プラチナイザー

製造品目

転倒温度計 各種
電気式水温計 各種
採水器・海洋観測機器
気象用・理化学用温度計
サーモレンジャー 温度調節器
ミグスター

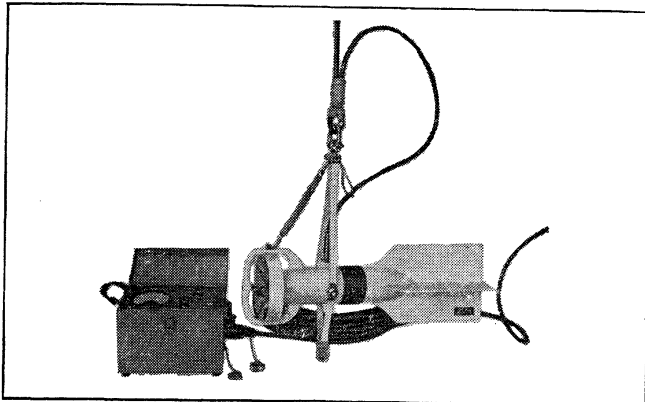
日本およびアジア総代理店



株式会社 渡部計器製作所

東京都文京区向丘1の7の17
TEL (811) 0044 (代表) ☎ 113

(カタログ御希望の方は誌名御記入の上御請求下さい)



Direct-Reading Current & Direction Meter

Model

CM-2

Catalogues are to be sent immediately upon receipt of your order products

Products

KM-2: Direct Reading Knot-Meter for Trawl-Boats to Control Adequate Speed

EI-5: Electric Meter of Water Temperature

ECT-5: Electric Conduction and Temperature Meter for Chlorine

TOHO DENTAN CO., LTD.

Office: 1-8-9, Miyamae, Suginami-Ku, Tokyo. Tel. Tokyo (03) 334-3451~3

メルタック

熱溶融型接着剤ですから、溶剤や水を含まないの乾燥の必要がなく、瞬間的に接着します。

ポリエチレン、アルミ箔等にも良く接着します。

ポリロック

含浸、注型、充填用として使用される接着性と作業性の良好なシーリング材です。

ポリワックス

ワックスを主成分とし、各種ポリマーをブレンドした防湿、密封用のシーリングワックスです。

東京工材株式会社

東京都中央区築地 4-7-1 TEL (542) 3361 (代)

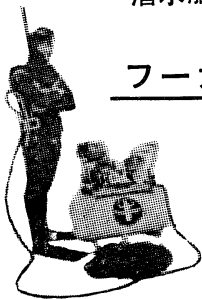
アクアラング

aqua-lung



◎ カタログ 進呈 ◎
潜水服採寸表

フーカ-潜水具



- 最新式アクアラング器具一式
- フーカ-潜水具
沿岸工事、水中調査、養魚、養殖、漁業、救難作業等の水中作業に画期的な高能率を示す潜水器具
- ナイロンジャージ付スポンジゴム潜水服
軽くて強く……保温性がよく……着心地快適
- アクアラング事業部併設
水中作業のご依頼に応じますのでご照会下さい
- アクアラング講習会常設
東京にアクアラング訓練用プールを設置

仏国・スピロテック社 日本総代理店
米国・U.S. ダイバーズ社

日本アクアラング株式会社

九州営業所 福岡市島飼1の5の33
電話 福岡(74)8907
名古屋営業所 名古屋市中川区東出町3の1
電話 名古屋(331)5016

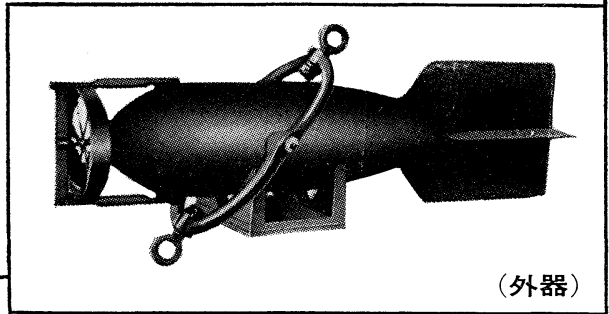
東京支社 東京都豊島区北大塚1丁目16の6
(国電大塚駅前大塚ビル一階)
電話 東京(918)6526(代表)

本社 神戸市兵庫区高松町22の1
神戸営業所 (帝國酸素株式会社内)
電話 神戸(67)5501(大代表)

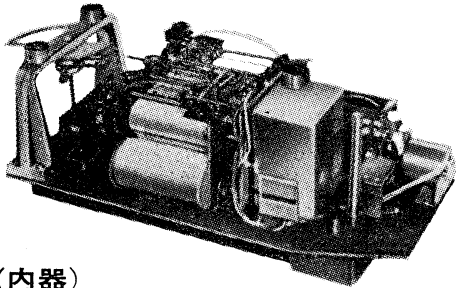
長期捲自記流速計

(NC-II)

本流速計は海中に設置し、内蔵した記録器に流速流向を同時に記録するプロペラ型の流速計で約20日間の記録を取る事が出来ます。但し流速は20分毎に3分間の平均流速を又流向は20分毎に一回、共に棒グラフ状に記録しますから読取が非常に簡単なのが特徴となっております。



(外器)



(内器)

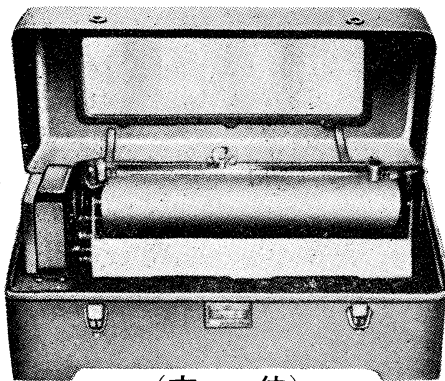
プロペラはA, B, C三枚一組になって居り

A(弱流用).....1m/sec	} 迄で一枚毎に検定 してあります。
B(中流用).....2m/sec	
C(強流用).....3m/sec	

弱流ペラーに依る最低速度は約4cm/secです。

フース型長期捲自記検潮器

(LFT-III)



(本 体)

営業品目

階段抵抗式波高計
ケーブル式波高計
フース型検潮器
小野式自記流速計
自記水位計
港施型土圧計
理研式水中カメラ
その他海洋観測諸計器

協和商工株式会社

東京都豊島区目白4丁目24番地1号
TEL (952) 1376代表 〒171

昭和 48 年 2 月 25 日 印刷
昭和 48 年 2 月 28 日 発行

う み 第 11 卷
第 1 号

定価 400

編集者 今 村 豊
発行者 佐 々 木 忠 義
発行所 日 仏 海 洋 学 会
財団法人 日仏会館内
東京都千代田区神田駿河台2-3
郵便番号:101
電話 (291) 1141
振替番号:東京96503

印刷者 小 山 康 三
印刷所 英 和 印 刷 社
東京都文京区本駒込6-15-10
郵便番号:113
電話 (941) 6500

第 11 卷 第 1 号

目 次

原 著

大洋における光学的性質に関する研究 (英文).....	松生 治	1
カタクチイワシの灯下におけるむれ形成について	井上 実・笹倉邦夫	45
人間の目に対する物体の水中視程 (英文).....	津田良平	55
学会記事		59

Tome 11 N° 1

SOMMAIRE

Notes originales

A Study on Optical Nature in Oceanic Waters.....	Kanau MATSUIKE	1
Schooling Mechanism of Anchovy Under a Lamp (in Japanese)	Makoto INOUE and Kunio SASAKURA	45
The Visibility of Underwater Objects to the Human Eye	Ryohei TSUDA	55
Procès-Vergaux.....		59